UCSF
UC San Francisco Electronic Theses and Dissertations

Title
Functionally graded bioactive coatings

Permalink
https://escholarship.org/uc/item/8gh7p49v

Author
Foppiano, Silvia

Publication Date
2004

Peer reviewed|Thesis/dissertation

eScholarship.org Powered by the California Digital Library
University of California

Functionally Graded Bioactive Coatings: from Fabrication to Testing

by

Silvia Foppiano

DISSERTATION

Submitted in partial satisfaction of the requirements for the degree of

DOCTOR OF PHILOSOPHY

in

Oral and Craniofacial Sciences

in the

GRADUATE DIVISION

of the

UNIVERSITY OF CALIFORNIA, SAN FRANCISCO

Acknoweledgements

I would like to give my deepest thanks to Dr. Dorothy Price for setting the wheels in motion, to Dr. Antoni P. Tomsia for giving me a priceless opportunity, and to my dear friends Dr. Jose Gomez-Vega and Dr. Nesrin Basoz for pushing me to take this opportunity.
I will always be grateful to you.

Every year spent at UCSF has been better than the previous one, I can not measure the personal and professional growth, but it could not have been possible without the patience and support of my numerous mentors and friends:
Grace Nonomura, Larry Watanabe, Dr. Eduardo Saiz, Dr. Tamara Alliston, Dr. Wu Li, his lovely wife Dr. Chen Li, and Dr. Michael Depew.
Thank you.

Last but not least I would like to thank the NIH/NIDCR, my advisor and the dissertation committee: Dr. Sally J.Marshall, Dr. Grayson W. Marshall, Dr. Caroline Damsky, Dr. Pamela DenBesten, and once again Dr. Antoni P. Tomsia.

There are more people to thank that this page can contain, I apologize for not mentioning everyone.

I dedicate this work to my friends, my family, Jeremy and Mario.

"Lorrique, il 23 luglio del 1988 pensavo che fosse finito tutto li'. Guarda dove sono arrivata".

"In bocca al lupo"
"Crepi il lupo"
"E che Dio ti benedica" ☺

X-Mailer: QUALCOMM Windows Eudora Version 6.0.3.0
Date: Thu, 28 Oct 2004 09:10:33 -0700
To: "James M. Anderson" <jma6@po.cwru.edu>
From: "Grayson Marshall, DDS, MPH, PhD" <graymar@itsa.ucsf.edu>
Subject: Re: request for permission to reproduce

Thank you.

At 08:40 AM 10/28/2004, you wrote:

Dear Dr. Marshall:

We have no problem with reproducing the article for Ms. Foppiano's thesis and only request that appropriate acknowledgment of it's appearance in JBMR-A be made in the thesis.

With kindest regards,

Bonnie Lou Berry
Assistant to Dr. Anderson

At 01:07 PM 10/27/2004 -0700, you wrote:

Dear Dr. Anderson,

we would like the written permission from the journal to reproduce the article "The influence of novel bioactive glasses on in vitro osteoblast behavior " by Foppiano S, Marshall SJ, Marshall GW and Tomsia AP published in: J Biomed Mater Res. 2004 Nov 1;71A(2):242-9.

Silvia Foppiano needs to include the article in her Ph.D dissertation.

If you could fax the document to the attention of Dr. Grayson W Marshall at 415 476 0858 we would greatly appreciate it.

Sincerely,

Grayson

Grayson Marshall, DDS, MPH, PhD
Professor and Chair, Div. of Biomaterials and Bioengineering

Dept. of Preventive and Restorative Dental Sciences
Director, COHORT and DDS PhD Programs
Chair, Graduate Group in Oral and Craniofacial Sciences
University of California San Francisco
707 Parnassus Ave Box 0758
San Francisco, CA 94143-0758
415-476-9119 415-476-0858 (fax)
Bio : www.ucsf.edu/ocsci/gwm.html
Lab: www.ucsf.edu/marshall/

Functionally Graded Bioactive Coatings: from Fabrication to testing

By Silvia Foppiano

Abstract

Every year about half a million Americans undergo total joint replacement surgery of some kind. This number is expected to steadily increase in the future. About 20% of these patients will need a revision surgery because of implant failure, with a significant increase in health care cost.

Current implant materials for load bearing applications must be strong enough to support the loads involved in daily activities, and bioinert, to limit reactivity in the body that may cause inflammatory and other adverse reactions. Metal alloys are typically used as materials for load bearing implants and rely on mechanical interlocking to achieve fixation which can be improved by using bone cements.

To improve implant osteointegration, metal implants have been coated with a bone-like mineral: hydroxyapatite (HA). The plasma spray technique is commonly used to apply the HA coating. Such implants do not require the use of bone cement. Plasma sprayed HA coated implants are FDA approved and currently on the market, but their properties are not reproducible or reliable. Thus, coating delamination can occur.

Our research group developed a novel family of bioactive glasses which were enameled onto titanium alloy using a functionally graded approach. We stratified the coating with different glass compositions to fulfill different functions. We coupled a first glass layer, with a good CTE match to the alloy, with a second layer of bioactive glass obtaining a functionally graded bioactive coating (FGC).

In this thesis for the first time the cytocompatibility of novel bioactive glasses, and their functionally graded coatings on Ti6Al4V, was studied with an *in vitro* bone model (MC3T3-E1.4 mouse preosteblast cells). The novel bioactive glasses are cytocompatible and no compositional change is required. The fabrication process is reproducible, introduces a small (average 6 vol%) amount of crystallization, which does not significantly affect bioactivity in SBF as tested. The coatings are cytocompatible, but should be preconditioned in SBF prior to their use. Preconditioning stabilizes the coatings, eliminates possible contaminants introduced during processing and handling, and yields dissolution products capable of inducing specific gene expression (e.g. Runx-2). Future research will involve identification of such dissolution products as well as *in vivo* testing.

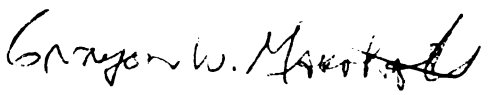

Dr. Grayson W. Marshall (Dissertation Committee Chair)

Table of Contents

		Page
Chapter 1.	Introduction	**1**
Chapter 2.	The influence of novel bioactive glasses on *in vitro* osteoblast behavior	**26**
Chapter 3.	Functionally graded bioactive coatings: the effect of fabrication process on glass bioactivity in simulated body fluid	**51**
Chapter 4.	Functionally graded bioactive coatings: Reproducibility of fabrication process and stability of the coating under cell culture conditions	**68**
Chapter 5.	Incompletely Resolved Issues	**95**
Chapter 6.	Bioactive glass coatings affect osteoblast-like cells behavior	**116**
Chapter 7.	Summary, Discussion, Conclusions and Future Work	**138**

List of Tables

		Page
Chapter 2.	Table 1.	**44**
Chapter 3.	Table 1.	**61**
	Table 2.	**62**
Chapter 4.	Table 1.	**84**
	Table 2.	**85**
Chapter 5.	Table 1.	**107**
	Table 2.	**108**
	Table 3.	**109**
Chapter 6	Table 1.	**131**
	Table 2.	**132**

List of Figures

		Page
Chapter 2	Figure 1.	**45**
	Figure 2.	**46**
	Figure 3.	**47**
	Figure 4.	**48**
	Figure 5.	**49**
	Figure 6.	**50**
Chapter 3	Figure 1.	**63**
	Figure 2.	**64**
	Figure 3.	**65**
	Figure 4.	**66**
	Figure 5.	**67**
Chapter 4	Figure 1.	**86**
	Figure 2.	**87**
	Figure 3.	**88**
	Figure 4.	**89**
	Figure 5.	**90**
	Figure 6.	**91**
	Figure 7.	**93**
	Figure 8.	**94**

Chapter 5 Figure 1 **111**

Figure 2. **112**

Figure 3. **113**

Figure 4. **114**

Figure 5. **115**

Chapter 6 Figure 1. **133**

Figure 2. **134**

Figure 3. **135**

Figure 4. **136**

Figure 5. **137**

Chapter 1

Introduction

Preface

This introductory chapter provides an overview of common problems related to the failure of load bearing implants for both orthopedics and dental applications.

It illustrates what characteristics guide the choice of materials for implants, and attempts that have been made to improve the bone-bonding interface and provide bioactivity. One such attempt resulted in the fabrication of novel functionally graded coatings of bioactive glasses on titanium alloy (Ti6Al4V) which are the center of this thesis.

The hypothesis and goal of this research are then illustrated together with an outline of the rationale behind the tests conducted and reported in each following chapter. Last, a general background is provided and an historical perspective.

Introduction

In this work different aspects of the fabrication process and *in vitro* osteoblastic response to novel composite materials are investigated. These novel materials are functionally graded enameled coatings (FGC) of bioactive glasses on titanium alloy (Ti6Al4V) and their ultimate use may be as implant materials for orthopedic or dental applications. A cross-disciplinary approach is key to understanding and improving the relationship between materials and tissues. Critical input from materials scientists, biomechanics engineers, cell and molecular biologists, orthopedic and oral surgeons is required to design, develop and study biomaterials for these particular applications. Effective communication between these areas of science is necessary but complicated by the fact that the language and methodology of one is very different from the others. Success in this field cannot be obtained without a constant dialogue communicating methods and

results. Only when these different disciplines crossed paths, mostly in the last century, substantial progress was achieved.

Success rate of load bearing implants

How to design implants to replace teeth and bone damaged or lost because of trauma or disease is an important scientific and clinical question. From 1994 to 1999 the number of hip and knee joint replacement performed in the U.S. steadily increased to reach a combined total of about 500,000 surgeries.[1] Because of the extended life expectancy of the Western world population and the increasingly younger age of patients, we can predict that this number is destined to increase in the future. An estimated 20% of implants fail within 15 years, and will require a second, usually less successful, revision surgery.[2] The success rate of dental implants is higher but also more difficult to estimate because of lack of standardized implant placement techniques, and success criteria. In general, the quality of bone is a crucial factor. Implants in bone classified as type IV, with low density trabecular bone and a thin layer of cortical bone, fail at a much higher rate than those in bone of type III, II and I, that have increasingly higher density and amount of cortical bone.[3]. Location is another variable, for example dental implants of the Branemark type are more successful in the mandible (90%) than in the maxilla (80%).[4] A number of factors can contribute to implant failure including: infection, poor quality of the bone (e.g. osteoporotic bone), stress shielding due to modulus of elasticity mismatch, and operator error.[5] Bioinert materials with inappropriate tribological properties can result in loosening of the implant, and release of particulate debris in the surrounding tissue, often with cytotoxic effects.[6-14] Furthermore, if the implant is not well-fitting and/or is loaded at an inappropriate time it will be encapsulated by fibrous

tissue. Bone is highly responsive to mechanical stress such as gravity,[15] when improper transfer of stresses across the bone-biomaterial interface occurs, (caused by either a too stiff material or the presence of a fibrous tissue surrounding the implant),[16,17] bone resorption or osteolysis, leading to loosening and ultimately implant failure often occurs.[2,5,18] The heat developed by the reaming procedure during surgery (as well as the heat developed by the setting reaction of bone cements)[19] should be controlled to avoid formation of necrotic bone, which further complicates the bone remodeling as does infection.[20-23] Among the relevant factors underlying implant success is the formation of a bond between implant and bone. Failure to establish this "bond" and to maintain it during implant function is the main cause of failure in dental and orthopedic implants.

Materials for load bearing implants

Similarly to other organs such as liver and kidney, bone has parenchymal and stromal components. The stroma provides the scaffold that supports the physiologically competent parenchyma. Remarkably, the ability of an organ to heal, regaining function, is highly dependent on the preservation of the stroma. Many approaches to bone regeneration are based on the fabrication of scaffolds that mimic the natural bone stroma and involve the fabrication of hydroxyapatite frameworks with interconnected porosity of specific size that attempt to recreate the harvesian system of cortical bone or the trabecular network of cancellous bone. Such scaffolds have found limited use, and because of poor biomechanical properties they are unsuitable for load bearing applications.[24] The choice of materials suitable for dental and orthopedic implants is limited by a combination of factors, including biocompatibility and mechanical properties. Bioinert materials with suitable mechanical properties, such as stainless steel,

titanium and cobalt chromium alloys (i.e. 316L, Ti6Al4V and Co-Cr-Mo), are commonly used for making implants. Their retention relies on mechanical interaction due to the presence of either a synthetic bone cement or a mesh-like modified surface to allow bone ingrowth.[5,25] Several approaches have been used to modify implant surfaces in order to increase contact with bone, generating true osteointegration, i.e. without intervening layers of fibrous tissue of any thickness.[4] The most common approach is implant coating with plasma sprayed hydroxyapatite (HA), a mineral closely related to bone apatite, or a similar calcium phosphate. *In vivo* animal models showed that bone bonds readily to plasma sprayed HA coatings.[26-31] A major problem of this coating method is that it requires high temperatures and yields non-homogeneous coatings with large amounts of amorphous calcium phosphates.[32-34] The unpredictable solubility of the amorphous phases and the lack of reliable bonding between metal and coating might cause coating delamination under tensile loads, resulting in unreliable implants.[31,35-37] Other coating techniques, such as magnetron sputtered deposition,[38] ion beam assisted deposition,[39] sol-gel coating,[40] surface induced mineralization[41] and others[42] have been investigated. All these techniques yield coatings with similar drawbacks to the plasma sprayed ones such as unreliable adhesion, continuous coating dissolution, variability in surface topography and phase formation.

Bioactive glasses

In 1969 Hench and his colleagues developed glasses termed "bioactive" according to this definition: "a bioactive material is one that elicits a specific biological response at the interface of the material which results in the formation of a bond between the tissues and the material".[43] Biomaterials used for bone implants can be classified as bioinert or

bioactive depending on their surface reactivity. Bioinert materials do not form direct strong "bonds" with bone, while bioactive ones do.[43,44] There is some controversy about the nature of this bond. Transmission electron microscopy (TEM) studies indicated that collagen fibers are interdigitating with a bioactive material's surface,[45,46] but what anchors collagen molecules to the implant? Other studies indicated the presence of mineral in direct apposition to implanted bioactive glass-ceramics.[18,47] Is there also a chemical bond involved, and between what molecules or atoms? These are still unanswered questions. In the environment of the body a bioactive glass undergoes surface reactions that lead to the formation of apatite-like mineral, resulting in the "direct bond" to bone.[31,48,49] The reaction rates should also be appropriate; glasses that react too slowly can show reduced bioactivity.[50] Immersion of bioactive glasses in simulated body fluid, an electrolyte solution similar to blood plasma, is widely accepted as the *in vitro* test to predict *in vivo* bioactivity.[50-57] In such solution bioactive glasses show a dynamic chemical behavior which can be summarized as follows: 1) ion leaching, 2) loss of soluble silica and alkalinization of the environment, 3) re-polymerization of the Si-rich surface (formation of silica gel film), 4) migration of calcium and phosphates from the subsurface through the silica gel layer with concomitant incorporation of soluble calcium and phosphates from the solution into an amorphous layer and 5) crystallization of a calcium phosphate layer by incorporation of hydroxyl groups from the solution to form apatite-like mineral.[18]

Leaching of alkali, or alkaline earth elements, occurs rapidly because they are modifiers and not part of the glass network. Dissolution is due to breaking of the silica network and release of silica in solution. This leads to the formation of a silica-rich gel layer on the

glass surface whose formation is an inverse function of the initial silica content of the glass. SiO_2 content seems to be the primary limiting factor affecting glass bioactivity. About 59 wt% has been reported as the compositional upper limit for bioactivity of melt derived glasses.[50] There is almost no limit for sol-gel derived glasses because of their high-surface area silica-rich layer formation.[53,58,59] It has been reported that formation of the silica gel layer may have a pivotal role in the nucleation[60,61] and growth of calcium phosphates, and therefore on the bioactivity of the glass.[43,53,62] Other researchers did not find any direct evidence for this.[63] In simulated body fluid, precipitation of calcium phosphates onto sol-gel processed glasses seems to be promoted by[64] but independent of the phosphate content of the glass itself.[54] From these reports it seems that silicon dissolution is critical for glass bioactivity. Any compositional and microstructural modification of a bioactive glass and conditioning solution results in alterations of the reaction steps and silica gel formation.

One particular bioactive glass composition, Bioglass® (also known as 45S5), has found many non-load bearing applications: as replacement for the bony ossicular chain in the middle ear[65,66] to augment the orbital volume of the eye,[44,67] as a ridge maintenance implant[68] and bony defect filler in periodontics.[69-71] Bioglass® interactions with bone (*in vivo* and *in vitro*) have been extensively studied.[35,43,72-75] It is known that bioactive glasses are not strong enough to withstand loads, and attempts to coat metals or ceramics with Bioglass® resulted in unreliable glass-metal bonding.[76,77] Our research group recently developed a family of bioactive glasses in the SiO_2-CaO-MgO-Na_2O-K_2O-P_2O_5 system with compositions based on Bioglass®, (with the same P_2O_5 wt%, but variable SiO_2 and additional oxides) that were used to develop novel coatings using a functionally

graded approach. Nature is the first "engineer" of functionally graded materials, with structural and compositional transitions that serve the purpose of resisting breakage due to environmental forces (e.g bamboo, bone, the layered composition of the Earth itself).[78] Our research group (under the leadership of Dr. Antoni P. Tomsia at the Lawrence Berkeley National Laboratory) applied these principles to the development of bioactive glass coatings; several glass compositions were designed, and selectively coupled to meet the specific functions of matching the coefficient of thermal expansion of Ti6Al4V (for a reliable bond to the metal) and providing bioactivity (needed for a bond to bone).[77,79,80]

The scope of this work

In this research I conducted the experiments to provide a foundation to understand how to properly prepare and test cell interactions with functionally graded coatings (FGC) of novel bioactive glasses on Ti6Al4V prepared by the enameling technique.

The hypothesis is that the reaction products released from bioactive glasses exposed to buffered proteinaceous solutions and the resulting surface modifications significantly alter osteoblast behavior (e.g. adhesion and proliferation) and consequently determine the osteoconductive properties of the material.

The ultimate goal of this research is the proactive design of bioactive surfaces that elicit prompt and positive osteoblastic response, leading to faster healing times and true osteointegration.

In Chapter 2 the hypothesis is tested that two novel bioactive glass compositions in the as cast form, do not elicit adverse reactions and are cytocompatible. This was done prior to the fabrication and testing of functionally graded coatings (FCGs) following FDA recommendations.[81] Our novel glasses differ significantly from the well known

Bioglass®, and it was necessary to assess their cytocompatibility prior to coating fabrication to determine whether components of the glass needed to be removed or replaced due to cytotoxic effects. This seemingly trivial step later proved to be crucial: when the FGCs showed mild cytotoxicity (Chapter 5 "Incompletely Resolved Issues") without these data it would have been difficult to determine the source of the problem (glass composition, or contamination during the fabrication process).

In Chapter 3 the FGC fabrication process was validated by assessing its reproducibility. Furthermore the effect that the thermal treatment involved in the enameling technique had on glass microstructure, and bioactivity was assayed. Testing non reproducible samples has no utility in science.

Chapter 4 assessed the stability of the coatings under cell culture conditions. The dynamic exposure to protein containing solutions of both *in vivo* and *in vitro* cell culture conditions, can reportedly destabilize the glass silica network.[49,82-84] Bioglass® particles were hollowed by such conditions, resulting in calcium phosphate shells with complete dissolution of the internal silica network.[85] We hypothesized that a similar effect might have occurred on FGCs (even if the glass compositions were significantly different) with negative effects on coating stability (i.e. causing delamination). Furthermore we identified a preconditioning treatment that protects the subsurface silica network from fast degradation.

Chapter 5 reports negative results that are nevertheless very informative. In the process of testing osteoblastic proliferation on FGCs, initial sets of experiments yielded inconsistent results. Increasing the number of replicate experiments showed a transition to consistent results indicating a mild cytotoxic effect due to the FGCs. This together

with the results of Chapter 2 indicated that contamination occurred during the coating fabrication process. In this chapter it is illustrated that lower proliferation was due to a reduced cell viability induced by contaminants that leached into solution. The identification of the contaminant/s was attempted using inductively coupled plasma spray mass spectroscopy (ICP-MS) but was not conclusive. We could not determine whether the contaminant agent was located on the surface of FGCs only or in the bulk of the coating as well. Nevertheless the same preconditioning treatment that slowed down subsurface silica network degradation proved also to be effective in the "neutralization" of contaminant/s that were introduced in the FGC during the fabrication process.

Chapter 6 tested the hypothesis that preconditioned FGCs are cytocompatible and suitable substrates for osteoblast mineralization. Another objective was to determine whether FGCs can affect the expression of genes involved in osteogenesis by means of their dissolution products. This opens the possibility of modifying the composition of a material in order to induce the expression of a desired gene or set of genes.[86] We used real time reverse transcription polymerase chain reaction (real time RT-PCR) to test the effect on few selected genes. It has been reported that Bioglass® dissolution products alter human primary osteoblast gene expression. Unfortunately the use of microarray technology yielded a large amount of data that was difficult to interpret.[87]

Chapter 7 includes discussion, conclusions and future work.

General background

Osteogenesis

In vivo bone forms mainly through two processes that initiate during embryonic development: intramembraneous formation for flat bones (e.g. most of the bones of the

face, skull, and the pelvis); endochondral formation for long bones (e.g. vertebral column, limbs). The intramembraneous process requires the formation of an undifferentiated aggregation of mesenchymal cells into a membrane. This gets invaded by blood vessels and osteoprogenitor cells. Upon differentiation into osteoblasts these cells deposit organic bone matrix that will mineralize.[88] In endochondral ossification a cartilaginous model formed in embryonic development is replaced by bone in a step-wise fashion. Mineralization of some regions of the cartilage matrix will occur, followed by vascular invasion, differentiation of osteoprogenitor cells into osteoblasts, cartilage resorption and deposition of mature lamellar bone.[89-91] These two processes occur throughout life in bone healing of different types of fractures.[88]

In vitro it is possible to obtain, from bone fragments, a population of cells expressing significant levels of osteoblastic phenotypic markers (e.g. alkaline phosphatase, osteopontin and osteocalcin). Once in culture, these cells can undergo a program of proliferation, differentiation and mineralization.[92] These steps are similar to what happens *in vivo* and underline the biological relevance of osteoblast culture systems as models to study osteoblasts. During active proliferation genes associated with cell cycle and cell growth are up-regulated (e.g. histone, c-myc, c-fos, c-jun). Genes associated with the formation of the extracellular matrix (ECM) are also up-regualted (e.g. collagen type I, transforming growth factor β (TGF-β)). These are then down-regulated and maintained at a low basal level during the next stages of differentiation. During differentiation expression of osteoblast markers (e.g. alkaline phosphatase) is increased and ECM composition is modified. Just before the onset of mineralization alkaline phosphatase activity increases. It promotes hydrolysis of phosphates producing

orthophosphates essential for crystal formation.[93] When mineralization occurs, osteoblasts release matrix vesicles containing high concentrations of calcium and phosphates and calcium – phospholipid complexes, and other genes are up-regulated (e.g. osteopontin, osteocalcin).[94]

Bone matrix

Bone is a composite material made of organic (more than 20 wt% wet) and inorganic (about 65 wt% wet) components plus 10 wt % of water. The organic components, mainly collagen type I with small amounts of types V and XII, confer the ability to resist tension to the bone. The inorganic matrix, the mineral phase, allows bone to resist compression and withstand loading activities. Its other main role is as a reservoir of ions necessary for physiological functions (e.g. of the nervous system) and biochemical reactions. In fact about 99 % of the body's calcium, 85 % of phosphorus, and 40 to 60 % of the total body sodium and magnesium reside in the bone associated with mineral crystals. Bone crystals are mainly apatite, partially substituted with carbonated ions ($Ca_{10}[PO]_6CO_3$) with incorporation of other ions.[95] In bone, solid calcium phosphates form from soluble calcium and phosphates in the extracellular matrix. Upon precipitation, the crystallinity increases over time, but it is generally less than synthetic hydroxyapatite formed *in vitro* in SBF.[96,97] Implanting a bioactive material in bone will affect osteoblast metabolism locally and possibly systemically. A clear understanding of the degree of reactivity of such a material and its effect on bone is crucial for the selection of better implants.

Osteoblast interactions with biomaterials

It is well known that osteoblasts can discriminate between different surface chemistries and also between the same chemistries with different microcrystallinity and

topography.[98,99] Tissue culture experiments often give contradictory results and a sound comparison of the available data is difficult due to the variety of cell types used. For example, Bioglass® increased cell proliferation of fetal rat osteoblasts,[100] but had no effect on mice calvaria osteoblasts.[75] It is known that significant protein adsorption occurs on substrata within seconds.[101] Fibronectin was selectively adsorbed on calcium phosphate coated bioactive glasses and caused enhanced cell adhesion.[102] When different substrates adsorbed the same amounts of fibronectin, cell adhesion was enhanced only on calcium phosphate coated bioactive glasses, suggesting a substrate-dependent conformational change.[103] It is not clear whether an implant surface coated with calcium phosphates is preferable to a Si-rich 'gelated' one to enhance protein adsorption and how it affects osteoblast adhesion. *In vivo*, protein adsorption will occur simultaneously with the reactions leading to the formation of silica-gel, ultimately resulting in a Si-rich matrix containing a mixture of amorphous phosphates and proteins.[104] The gel matrix could preserve the embedded proteins (e.g. growth factors) from protease degradation, causing enhanced bone regeneration.[105] On the other hand the protein rich amorphous phosphate surface is permeable to fluids and leads to the degradation of the underlying silica network.[83,85] *In vitro* studies suggested that hydroxyapatite may exert a stimulatory effect on marrow stromal stem cell differentiation.[106] and osteoblast-like cell mineralization.[107] The mechanism is unknown: the calcium phosphate's topography might have an effect, as well as the adsorbed proteins and the products of dissolution. Some *in vivo* experiments indicated that primary calcification during bone healing is significantly affected by the surface properties of the implant and the effect was apparent also in the contralateral limb. Bone bonding and non-bone bonding implant materials elicited

specific enzymatic activity in matrix vesicle-enriched micrososmes (MVEM). Enzymatic activity in the MVEM isolated from the contralateral limb reproduced those of the treated limb with less intensity.[93,108] This indicates a systemic effect underlying the importance of products of dissolution on bone metabolism. Few papers addressed the response of osteoblasts to bioactive glass reaction products at the molecular level. Ionic products of dissolution of Bioglass® particles altered human osteoblast cell metabolism[75] and caused up-regulation of genes involved in cell proliferation and differentiation, identified by microarray analysis.[87,109] It has been reported that the level of mineralization of the extracellular matrix affects bone-implant bonding.[110] It is clinically desirable for osteoblasts to readily deposit mineralized matrix on the implant surface, supplying mechanical stability and minimizing motion-induced damage at the implant site.[111] *In vivo* studies of various bioactive glass-ceramics had one result: bone bonded with the materials through an intervening layer of calcium phosphates.[18] It is still unclear whether pre-conditioning of the implant to obtain precipitation of apatite-like calcium phosphates might be advantageous to osteoblast differentiation and mineralization. A biomaterial engineered to induce specific gene expression and enhance osteoblastic mineral deposition could be of significant clinical use.

Historical perspective

Dentistry dealt with replacing missing teeth significantly earlier than orthopedics faced the issue of replacing a joint. The ancient Egyptians described in the papyrus of Ebes (3500-1500 B.C.) several treatments for toothache, and wooden artificial teeth have been found in Egyptian sarcophagi. The Etruscans, or early Italians (~1000-200 B.C.) attempted to replace missing teeth with artificial ones, from calf or cow, re-shaped and

held in place by gold wires and screws. The ancient Chinese (~2700 B.C.) used acupuncture to relive toothache and believed there were "worms" excavating teeth. The Law of the Twelve Tables written in Rome in 450 B.C., considers legal the burial or cremation of corpses without removing the gold that was binding the teeth together, and specimens of bridgework emerged from the tombs. The Greeks worshipped Aesculapius, the God of Medicine, but it is to Hippocrates that the title of "father of Medicine" was granted. Hippocrates was born about 460 years B.C. and devoted his life to the study of medicine. He wrote about dental extraction, realized that teeth are formed before birth and invented crude dental instruments. As dentistry evolved certain superstitions persisted, in fact the ancient Chinese belief of the existence of dental worms survived throughout the Middle Ages until in 1728 Pierre Fauchard (from Brittany) published Le Chirurgien Dentiste (The Dentist Surgeon) marking the beginning of modern dentistry.[112,113] Dental root implants were introduced as early as 1807 by Jourdan and Maggiolo and not extensively used for over 100 years. Detailed report of this technique was given only in 1912 by Dr. E.J. Greenfield at the Washington meeting of the National Dental Association.[113]

In orthopedics diseased joints were usually removed without any attempt to replace them and restore function. Several reports of joint resections can be found between 1536 and 1831; at this latter date the publication of the book "The excision of diseased joints" by Dr. James Syme from the University of Edinburgh made the general practice of *resection arthroplasty* official.[114]

Removal of the affected joint was not followed by any attempt to restore function; total loss of motion or, ankylosis, was either expected or desired. In 1840 the innovative

concept of *interpositional arthroplasty* was introduced by Dr. Carnochan. The New York surgeon was reported to be the first to attempt to restore motion to a patient's ankylosed jaw, by placing a small piece of wood between the raw bony surfaces of the joint. This opened the field to several creative attempts to restore articular motion by the interposition of a variety of materials. Between 1878 and 1906, adipose tissue, muscle and connective tissue, thin platinum plate, pig's bladder, gold foil and periosteum were used by different surgeons in various countries.[115] Between 1920 and 1950 extensive research was conducted in *interpositional arthroplasy* with materials such as glass and Pyrex, rubber, plastics (Lucite and plexiglas), cellophane and nylon. In 1923, for the first time, glass cups were used in hip reconstructive surgery by Dr. Smith-Petersen from Boston. The glass cup, placed to cover the articulation, proved to be too brittle, and after attempts with Pyrex, in 1937 Dr. Smith-Petersen experimented more successfully with cobalt-chromium cups.

The field of *prosthetic arthroplasty* developed around 1890 when Themistocles Glueck introduced a new idea involving the fixation of an implant by means of a cement. An ivory prosthesis was fixed with a cement of colophony, pumice and gypsum.[116] Metals such as iron, platinum and stainless steel, were later used to provide a more lasting implant. In 1938 Charles Venable and Walter Stuck developed Vitallium, a cobalt-molybdenum-chromium alloy that resisted corrosion and was then used for hip replacement. In the early 1950s several metal hip prosthesis designs were developed and attempts were made to match them with a Smith-Petersen acetabular cup. In the 1950s and 1960s the design of prostheses improved, and the use of dental acrylic for fixation became more common in orthopedic surgery.[115,117] It took a combination of discoveries

to remove major roadblocks to the development of modern oral and orthopedic surgery: the use of surgical anesthesia (1842), the invention of the hypodermic syringe (1853) for more effective anesthetic delivery, the discovery of Roentgen rays (X-rays) (in 1895 but not used in dentistry until 1920) as a crucial diagnostic tool,[118] and the importance of antisepsis (brought about by Dr. Hunter's speech "The role of sepsis and antisepsis in medicine" in 1910 Note: surgeons used to operate with bare hands, unmasked face and wearing street clothes)[119] to mention just a few. The science of biomechanics together with an understanding of tissue reactions to materials and materials' reactions to bodily fluids is still evolving. The design, choice of material and fixation technique are active areas of research, prompted by the fact that in spite of exceptional accomplishments a high percentage of implants still fail.

Many of the dentists and surgeons of the past were excellent craftsmen. Each generation refined previous ideas and techniques and from their mistakes a true science evolved. Looking back at materials used in the past you may want to chuckle, but we did advance because of all these contributions and failures.

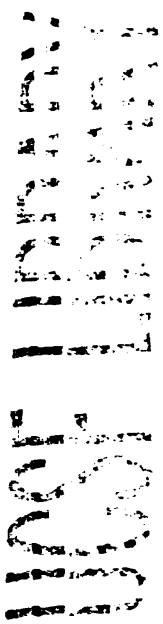

References

1. http://www.aahks.org.
2. Long M, Rack HJ. Titanium alloys in total joint replacement--a materials science perspective. Biomaterials 1998;19(18):1621-39.
3. Jaffin RA, Berman CL. The excessive loss of Branemark fixtures in type IV bone: a 5-year analysis. J Periodontol 1991;62(1):2-4.
4. LeGeros RZ, Craig RG. Strategies to affect bone remodeling: osteointegration. J Bone Miner Res 1993;8 Suppl 2:S583-96.
5. Hench LL, Ethridge EC. Orthopedic Implants. Biomaterials : an interfacial approach. New York: Academic Press; 1982. p 225-252.
6. Breen DJ, Stoker DJ. Titanium lines: a manifestation of metallosis and tissue response to titanium alloy megaprostheses at the knee. Clin Radiol 1993;47(4):274-7.
7. Case CP, Langkamer VG, James C, Palmer MR, Kemp AJ, Heap PF, Solomon L. Widespread dissemination of metal debris from implants. J Bone Joint Surg Br 1994;76(5):701-12.
8. Wang JC, Yu WD, Sandhu HS, Betts F, Bhuta S, Delamarter RB. Metal debris from titanium spinal implants. Spine 1999;24(9):899-903.
9. Sieber HP, Rieker CB, Kottig P. Analysis of 118 second-generation metal-on-metal retrieved hip implants. J Bone Joint Surg Br 1999;81(1):46-50.
10. Hirakawa K, Bauer TW, Stulberg BN, Wilde AH, Borden LS. Characterization of debris adjacent to failed knee implants of 3 different designs. Clin Orthop 1996(331):151-8.
11. Hirakawa K, Bauer TW, Stulberg BN, Wilde AH, Secic M. Characterization and comparison of wear debris from failed total hip implants of different types. J Bone Joint Surg Am 1996;78(8):1235-43.
12. Okazaki Y, Rao S, Ito Y, Tateishi T. Corrosion resistance, mechanical properties, corrosion fatigue strength and cytocompatibility of new Ti alloys without Al and V. Biomaterials 1998;19(13):1197-215.
13. Ghalambor N, Cho DR, Goldring SR, Nihal A, Trepman E. Microscopic metallic wear and tissue response in failed titanium hallux metatarsophalangeal implants: two cases. Foot Ankle Int 2002;23(2):158-62.
14. Gawkrodger DJ. Metal sensitivities and orthopaedic implants revisited: the potential for metal allergy with the new metal-on-metal joint prostheses. Br J Dermatol 2003;148(6):1089-93.
15. Regling G. Wolff's law and connective tissue regulation : modern interdisciplinary comments on Wolff's law of connective tissue regulation and rational understanding of common clinical problems. Berlin ; New York: W. de Gruyter; 1992. xii, 337 p.
16. Schulman A, Piliero SJ, Pentel L, Ott WR, Moskowitz HD. Composite materials for dental implants. Oral Surg Oral Med Oral Pathol 1975;40(2):183-93.
17. Warren AB, Caputo AA. Load transfer to alveolar bone as influenced by abutment designs for tooth-supported dentures. J Prosthet Dent 1975;33(2):137-48.

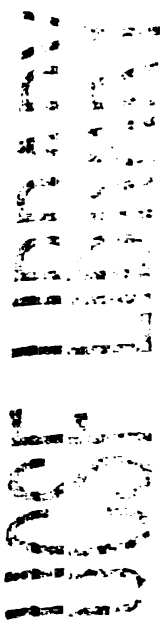

18. Hench LL. Bioceramics: from concept to clinic. J Am Ceram Soc 1991;74:1487-1510.
19. Kèuhn KD. PMMAs as bone cements. In: Kèuhn KD, editor. Bone cements : up-to-date comparison of physical and chemical properties of commercial materials. Berlin ; New York: Springer; 2000. p 21-34.
20. Muller C, Frigg R, Pfister U. Effect of flexible drive diameter and reamer design on the increase of pressure in the medullary cavity during reaming. Injury 1993;24 Suppl 3:S40-7.
21. Leunig M, Hertel R. Thermal necrosis after tibial reaming for intramedullary nail fixation. A report of three cases. J Bone Joint Surg Br 1996;78(4):584-7.
22. Baumgart F, Kohler G, Ochsner PE. The physics of heat generation during reaming of the medullary cavity. Injury 1998;29 Suppl 2:B11-25.
23. Ochsner PE, Baumgart F, Kohler G. Heat-induced segmental necrosis after reaming of one humeral and two tibial fractures with a narrow medullary canal. Injury 1998;29 Suppl 2:B1-10.
24. Holmes RE. Osteoconduction in hydroxyapatite-based materials. In: Brighton CT, Friedlaender GE, Lane JM, American Academy of Orthopaedic Surgeons., National Institute of Arthritis and Musculoskeletal and Skin Diseases (U.S.). editors. Bone formation and repair. Rosemont, IL: American Academy of Orthopaedic Surgeons; 1994. p 355-379.
25. Lemons JE. Materials for total joint replacement: Metals and Alloys. In: Petty W, editor. Total joint replacement. Philadelphia: Saunders; 1991. p 21-27.
26. Thomas KA, Kay JF, Cook SD, Jarcho M. The effect of surface macrotexture and hydroxylapatite coating on the mechanical strengths and histologic profiles of titanium implant materials. J Biomed Mater Res 1987;21(12):1395-414.
27. Geesink RG, de Groot K, Klein CP. Bonding of bone to apatite-coated implants. J Bone Joint Surg Br 1988;70(1):17-22.
28. Hayashi K, Matsuguchi N, Uenoyama K, Kanemaru T, Sugioka Y. Evaluation of metal implants coated with several types of ceramics as biomaterials. J Biomed Mater Res 1989;23(11):1247-59.
29. Oonishi H, Yamamoto M, Ishimaru H, Tsuji E, Kushitani S, Aono M, Ukon Y. The effect of hydroxyapatite coating on bone growth into porous titanium alloy implants. J Bone Joint Surg Br 1989;71(2):213-6.
30. Soballe K, Hansen ES, Brockstedt-Rasmussen H, Pedersen CM, Bunger C. Hydroxyapatite coating enhances fixation of porous coated implants. A comparison in dogs between press fit and noninterference fit. Acta Orthop Scand 1990;61(4):299-306.
31. Chang YL, Lew D, Park JB, Keller JC. Biomechanical and morphometric analysis of hydroxyapatite-coated implants with varying crystallinity. J Oral Maxillofac Surg 1999;57(9):1096-108; discussion 1108-9.
32. Koch B, Wolke JG, de Groot K. X-ray diffraction studies on plasma-sprayed calcium phosphate-coated implants. J Biomed Mater Res 1990;24(6):655-67.
33. Palka V, Brezovsky M, Zeman J, Cepera M. Phase changes after plasma spraying hydroxylapatite. Kovove Materialy 1993;31(6).

34. Ogiso M, Yamashita Y, Matsumoto T. Differences in microstructural characteristics of dense HA and HA coating. J Biomed Mater Res 1998;41(2):296-303.
35. LeGeros RZ, LeGeros J. P. Dense Hydroxyapatite. In: Hench LL and Wilson J, editor. An introduction to bioceramics. Singapore: World Scientific; 1993. p 139-180.
36. Bloebaum RD, Bachus KN, Rubman MH, Dorr LD. Postmortem comparative analysis of titanium and hydroxyapatite porous- coated femoral implants retrieved from the same patient. A case study. J Arthroplasty 1993;8(2):203-11.
37. Bloebaum RD, Dupont JA. Osteolysis from a press-fit hydroxyapatite-coated implant. A case study. J Arthroplasty 1993;8(2):195-202.
38. van Dijk K, Schaeken HG, Wolke JG, Jansen JA. Influence of annealing temperature on RF magnetron sputtered calcium phosphate coatings. Biomaterials 1996;17(4):405-10.
39. Choi JM, Kim HE, Lee IS. Ion-beam-assisted deposition (IBAD) of hydroxyapatite coating layer on Ti-based metal substrate. Biomaterials 2000;21(5):469-73.
40. Ramires PA, Romito A, Cosentino F, Milella E. The influence of titania/hydroxyapatite composite coatings on in vitro osteoblasts behaviour. Biomaterials 2001;22(12):1467-74.
41. Wheeler DL, Campbell AA, Graff GL, Miller GJ. Histological and biomechanical evaluation of calcium phosphate coatings applied through surface-induced mineralization to porous titanium implants. J Biomed Mater Res 1997;34(4):539-43.
42. Aksakal B, Yildirim OS, Okur A. Coating analysis of implant materials used in orthopaedic surgery. J Int Med Res 2003;31(5j):418-21.
43. Hench LL, Anderson O. Bioactive glasses. In: Hench HH WJ, editor. An introduction to bioceramics. Singapore: World Scientific; 1993. p 41-62.
44. Hench LL, Wilson J. Introduction. In: Hench LL, Wilson J, editors. An Introduction to bioceramics. Singapore ; River Edge, N.J.: World Scientific; 1993. p 1-24.
45. Fujita R, Yokoyama A, Nodasaka Y, Kohgo T, Kawasaki T. Ultrastructure of ceramic-bone interface using hydroxyapatite and beta-tricalcium phosphate ceramics and replacement mechanism of beta-tricalcium phosphate in bone. Tissue Cell 2003;35(6):427-40.
46. Porter AE, Patel N, Skepper JN, Best SM, Bonfield W. Effect of sintered silicate-substituted hydroxyapatite on remodelling processes at the bone-implant interface. Biomaterials 2004;25(16):3303-14.
47. Okada Y, Kobayashi M, Neo M, Kokubo T, Nakamura T. Ultrastructure of the interface between bioactive composite and bone: comparison of apatite and wollastonite containing glass-ceramic filler with hydroxyapatite and beta-tricalcium phosphate fillers. J Biomed Mater Res 2001;57(1):101-7.
48. Daculsi G, LeGeros RZ, Heughebaert M, Barbieux I. Formation of carbonate-apatite crystals after implantation of calcium phosphate ceramics. Calcif Tissue Int 1990;46(1):20-7.

49. Schepers EJ, Ducheyne P. Bioactive glass particles of narrow size range for the treatment of oral bone defects: a 1-24 month experiment with several materials and particle sizes and size ranges. J Oral Rehabil 1997;24(3):171-81.
50. Brink M, Turunen T, Happonen RP, Yli-Urpo A. Compositional dependence of bioactivity of glasses in the system Na2O- K2O-MgO-CaO-B2O3-P2O5-SiO2. J Biomed Mater Res 1997;37(1):114-21.
51. Filgueiras MR, LaTorre G, Hench LL. Solution effects on the surface reactions of three bioactive glass compositions. J Biomed Mater Res 1993;27(12):1485-93.
52. Filgueiras MR, La Torre G, Hench LL. Solution effects on the surface reactions of a bioactive glass. J Biomed Mater Res 1993;27(4):445-53.
53. Hamadouche M, Meunier A, Greenspan DC, Blanchat C, Zhong JP, La Torre GP, Sedel L. Bioactivity of sol-gel bioactive glass coated alumina implants. J Biomed Mater Res 2000;52(2):422-9.
54. Izquierdo-Barba I, Salinas AJ, Vallet-Regi M. In vitro calcium phosphate layer formation on sol-gel glasses of the CaO-SiO(2) system. J Biomed Mater Res 1999;47(2):243-50.
55. Jones JR, Sepulveda P, Hench LL. Dose-dependent behavior of bioactive glass dissolution. J Biomed Mater Res 2001;58(6):720-6.
56. Kokubo T, Kushitani H, Sakka S, Kitsugi T, Yamamuro T. Solutions able to reproduce in vivo surface-structure changes in bioactive glass-ceramic A-W. J Biomed Mater Res 1990;24(6):721-34.
57. Peitl Filho O, LaTorre GP, Hench LL. Effect of crystallization on apatite-layer formation of bioactive glass 45S5. J Biomed Mater Res 1996;30(4):509-14.
58. Li R, Clark AE, Hench LL. An investigation of bioactive glass powders by sol-gel processing. J Appl Biomater 1991;2(4):231-9.
59. Zhong J, Greenspan DC. Processing and properties of sol-gel bioactive glasses. J Biomed Mater Res 2000;53(6):694-701.
60. Takadama H, Kim HM, Kokubo T, and Nakamura T. Mechanism of biomineralization af apatite on a sodium silicate glass: TEM-EDX Study in vitro. Chem Mat 2001;13(3):1108-1113.
61. Karlsson KH, Hupa M, Backman R. Key Engineering Materials. Bioceramics 13. Phosphate precipitation at surface of bioactive glasses. Volume 192. Aedermannsdorf, Switzerland: Trans Tech Publications; 2000. p 219-22.
62. Li P, Ohtsuki C, Kokubo T, Nakanishi K, and Soga N. Apatite formation induced by silica gel in simulated body fluid. J Am Cer Soc 1992;75:2094-7.
63. Peltola T, Jokinen M, Veittola S, Rahiala H, Yli-Urpo A. Influence of sol and stage of spinnability on in vitro bioactivity and dissolution of sol-gel-derived SiO2 fibers. Biomaterials 2001;22(6):589-98.
64. Vallet-Regi M, Izquierdo-Barba I, Salinas AJ. Influence of P_2O_5 on crystallinity of apatite formed in vitro on surface of bioactive glasses. J Biomed Mater Res 1999;46(4):560-5.
65. Merwin GE, Atkins JS, Wilson J, Hench LL. Comparison of ossicular replacement materials in a mouse ear model. Otolaryngol Head Neck Surg 1982;90(4):461-9.
66. Reck R. Bioactive glass-ceramics in ear surgery: animal studies and clinical results. Laryngoscope 1984;94(2 Pt 2 Suppl 33):1-54.

67. Amato MM, Blaydon SM, Scribbick FW, Jr., Belden CJ, Shore JW, Neuhaus RW, Kelley PS, Holck DE. Use of bioglass for orbital volume augmentation in enophthalmos: a rabbit model (oryctolagus cuniculus). Ophthal Plast Reconstr Surg 2003;19(6):455-65.
68. Stanley HR, Hall MB, Clark AE, King CJ, 3rd, Hench LL, Berte JJ. Using 45S5 bioglass cones as endosseous ridge maintenance implants to prevent alveolar ridge resorption: a 5-year evaluation. Int J Oral Maxillofac Implants 1997;12(1):95-105.
69. Zamet JS, Darbar UR, Griffiths GS, Bulman JS, Bragger U, Burgin W, Newman HN. Particulate bioglass as a grafting material in the treatment of periodontal intrabony defects. J Clin Periodontol 1997;24(6):410-8.
70. Shapoff CA, Alexander DC, Clark AE. Clinical use of a bioactive glass particulate in the treatment of human osseous defects. Compend Contin Educ Dent 1997;18(4):352-4, 356, 358 passim.
71. Low SB, King CJ, Krieger J. An evaluation of bioactive ceramic in the treatment of periodontal osseous defects. Int J Periodontics Restorative Dent 1997;17(4):358-67.
72. Price N, Bendall SP, Frondoza C, Jinnah RH, Hungerford DS. Human osteoblast-like cells (MG63) proliferate on a bioactive glass surface. J Biomed Mater Res 1997;37(3):394-400.
73. Lobel KD, Hench LL. In vitro adsorption and activity of enzymes on reaction layers of bioactive glass substrates. J Biomed Mater Res 1998;39(4):575-9.
74. Wheeler DL, Eschbach EJ, Hoellrich RG, Montfort MJ, Chamberland DL. Assessment of resorbable bioactive material for grafting of critical-size cancellous defects. J Orthop Res 2000;18(1):140-8.
75. Silver IA, Deas J, Erecinska M. Interactions of bioactive glasses with osteoblasts in vitro: effects of 45S5 Bioglass, and 58S and 77S bioactive glasses on metabolism, intracellular ion concentrations and cell viability. Biomaterials 2001;22(2):175-85.
76. Hench LL, Andersson O. Bioactive glass coatings. In: Hench LL, Wilson J, editors. An Introduction to bioceramics. Singapore ; River Edge, N.J.: World Scientific; 1993. p 239-260.
77. Gomez-Vega JM, Saiz E, Tomsia AP. Glass-based coatings for titanium implant alloys. J Biomed Mater Res 1999;46(4):549-59.
78. Suresh S. Graded materials for resistance to contact deformation and damage. Science 2001;292(5526):2447-51.
79. Pazo A, Saiz E, Tomsia AP. Silicate glass coatings on Ti-based implants. Acta Materialia 1998;46:2551-2558.
80. Gomez-Vega JM, Saiz E, Tomsia AP, Marshall GW, Marshall SJ. Bioactive glass coatings with hydroxyapatite and Bioglass particles on Ti-based implants. 1. Processing. Biomaterials 2000;21(2):105-11.
81. International A. Section 13: Medical Devices and Services. American Society for Testing and Materials. Annual book of ASTM Standards. Philadelphia, PA: ASTM International.; 2001. p 243-249.
82. Sepulveda P, Jones JR, Hench LL. In vitro dissolution of melt-derived 45S5 and sol-gel derived 58S bioactive glasses. J Biomed Mater Res 2002;61(2):301-11.

83. Radin S, Ducheyne P, Rothman B, Conti A. The effect of in vitro modeling conditions on the surface reactions of bioactive glass. J Biomed Mater Res 1997;37(3):363-75.
84. Schepers E, de Clercq M, Ducheyne P, Kempeneers R. Bioactive glass particulate material as a filler for bone lesions. J Oral Rehabil 1991;18(5):439-52.
85. Radin S, Ducheyne P, Falaize S, Hammond A. In vitro transformation of bioactive glass granules into Ca-P shells. J Biomed Mater Res 2000;49(2):264-72.
86. Hench LL, Polak JM. Third-generation biomedical materials. Science 2002;295(5557):1014-7.
87. Xynos ID, Edgar AJ, Buttery LD, Hench LL, Polak JM. Gene-expression profiling of human osteoblasts following treatment with the ionic products of Bioglass 45S5 dissolution. J Biomed Mater Res 2001;55(2):151-7.
88. Buckwalter JA, Glimcher MJ, Cooper RR, Recker R. Bone biology. II: Formation, form, modeling, remodeling, and regulation of cell function. Instr Course Lect 1996;45:387-99.
89. Pechak DG, Kujawa MJ, Caplan AI. Morphological and histochemical events during first bone formation in embryonic chick limbs. Bone 1986;7(6):441-58.
90. Syftestad GT, Weitzhandler M, Caplan AI. Isolation and characterization of osteogenic cells derived from first bone of the embryonic tibia. Dev Biol 1985;110(2):275-83.
91. van de Wijngaert FP, Schipper CA, Tas MC, Burger EH. Role of mineralizing cartilage in osteoclast and osteoblast recruitment. Bone 1988;9(2):81-8.
92. Beresford JN, Graves SE, Smoothy CA. Formation of mineralized nodules by bone derived cells in vitro: a model of bone formation? Am J Med Genet 1993;45(2):163-78.
93. Schwartz Z, Swain LD, Marshall T, Sela J, Gross U, Amir D, Muller-Mai C, Boyan BD. Modulation of matrix vesicle enzyme activity and phosphatidylserine content by ceramic implant materials during endosteal bone healing. Calcif Tissue Int 1992;51(6):429-37.
94. Stein G, Lian JB. Molecular mechanisms mediating developmental and hormone-regulated expression of genes in osteoblasts: an integrated relationship of cell growth and differentiation. In: Noda M, editor. Cellular and Molecular Biology of Bone: Academic Press Inc; 1993. p 47-95.
95. Rey C, Collins B, Goehl T, Dickson IR, Glimcher MJ. The carbonate environment in bone mineral: a resolution-enhanced Fourier Transform Infrared Spectroscopy Study. Calcif Tissue Int 1989;45(3):157-64.
96. Matsushima N, Hikichi K. Age changes in the crystallinity of bone mineral and in the disorder of its crystal. Biochim Biophys Acta 1989;992(2):155-9.
97. Roberts JE, Bonar LC, Griffin RG, Glimcher MJ. Characterization of very young mineral phases of bone by solid state 31phosphorus magic angle sample spinning nuclear magnetic resonance and X-ray diffraction. Calcif Tissue Int 1992;50(1):42-8.
98. Sinha RK, Morris F, Shah SA, Tuan RS. Surface composition of orthopaedic implant metals regulates cell attachment, spreading, and cytoskeletal organization of primary human osteoblasts in vitro. Clin Orthop 1994(305):258-72.

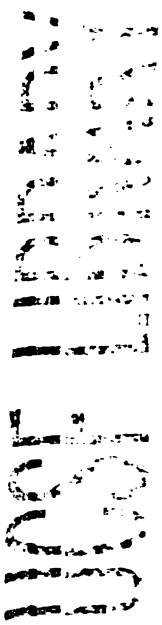

99. Boyan BD, Hummert TW, Dean DD, Schwartz Z. Role of material surfaces in regulating bone and cartilage cell response. Biomaterials 1996;17(2):137-46.
100. Vrouwenvelder WC, Groot CG, de Groot K. Behaviour of fetal rat osteoblasts cultured in vitro on bioactive glass and nonreactive glasses. Biomaterials 1992;13(6):382-92.
101. Baier RE, Dutton RC. Initial events in interactions of blood with a foreign surface. J Biomed Mater Res 1969;3(1):191-206.
102. El-Ghannam A, Ducheyne P, Shapiro IM. Effect of serum proteins on osteoblast adhesion to surface-modified bioactive glass and hydroxyapatite. J Orthop Res 1999;17(3):340-5.
103. Garcia AJ, Ducheyne P, Boettiger D. Effect of surface reaction stage on fibronectin-mediated adhesion of osteoblast-like cells to bioactive glass. J Biomed Mater Res 1998;40(1):48-56.
104. Ducheyne P, Qiu Q. Bioactive ceramics: the effect of surface reactivity on bone formation and bone cell function. Biomaterials 1999;20(23-24):2287-303.
105. Tabata Y, Yamada K, Miyamoto S, Nagata I, Kikuchi H, Aoyama I, Tamura M, Ikada Y. Bone regeneration by basic fibroblast growth factor complexed with biodegradable hydrogels. Biomaterials 1998;19(7-9):807-15.
106. Ohgushi H, Dohi Y, Yoshikawa T, Tamai S, Tabata S, Okunaga K, Shibuya T. Osteogenic differentiation of cultured marrow stromal stem cells on the surface of bioactive glass ceramics. J Biomed Mater Res 1996;32(3):341-8.
107. Chang YL, Stanford CM, Keller JC. Calcium and phosphate supplementation promotes bone cell mineralization: implications for hydroxyapatite (HA)-enhanced bone formation. J Biomed Mater Res 2000;52(2):270-8.
108. Schwartz Z, Amir D, Boyan BD, Cochavy D, Mai CM, Swain LD, Gross U, Sela J. Effect of glass ceramic and titanium implants on primary calcification during rat tibial bone healing. Calcif Tissue Int 1991;49(5):359-64.
109. Xynos ID, Edgar AJ, Buttery LD, Hench LL, Polak JM. Ionic products of bioactive glass dissolution increase proliferation of human osteoblasts and induce insulin-like growth factor II mRNA expression and protein synthesis. Biochem Biophys Res Commun 2000;276(2):461-5.
110. Gross U, Brandes J, Strunz V, Bab I, Sela J. The ultrastructure of the interface between a glass ceramic and bone. J Biomed Mater Res 1981;15(3):291-305.
111. Dee KC, Rueger DC, Andersen TT, Bizios R. Conditions which promote mineralization at the bone-implant interface: a model in vitro study. Biomaterials 1996;17(2):209-15.
112. Guerini V, National dental association. [from old catalog]. A history of dentistry from the most ancient times until the end of the eighteenth century. Philadelphia and New York,: Lea & Febiger; 1909. x, [17]-355 p. p.
113. Taylor JA. Ancient dentistry. History of dentistry; a practical treatise for the use of dental students and practitioners. Philadelphia and New York,: Lea & Febiger; 1922. p 19-33.
114. Osgood RB. The evolution of orthopaedic surgery. St. Louis,: The C.V. Mosby Company; 1925. 70 p. p.
115. McElfresh E. History of Arthroplasty. In: Petty W, editor. Total joint replacement. Philadelphia: Saunders; 1991. p 3-18.

116. Muster D. Themistocles Gluck, Berlin 1890: a pioneer of multidisciplinary applied research into biomaterials for endoprostheses. Bull Hist Dent 1990;38(1):3-6.
117. Le Vay D. The history of orthopaedics : an account of the study and practice of orthopaedics from the earliest times to the modern era. Carnforth, Lancs, UK ; Park Ridge, N.J., USA: Parthenon Pub. Group; 1990. xiii, 693 p. p.
118. Taylor JA. The history of anesthesia. History of dentistry; a practical treatise for the use of dental students and practitioners. Philadelphia and New York,: Lea & Febiger; 1922. p 113-118.
119. Taylor JA. Prosthetic dentistry, crown and bridge work, orthodontia, oral surgery. History of dentistry; a practical treatise for the use of dental students and practitioners. Philadelphia and New York,: Lea & Febiger; 1922. p 142-156.

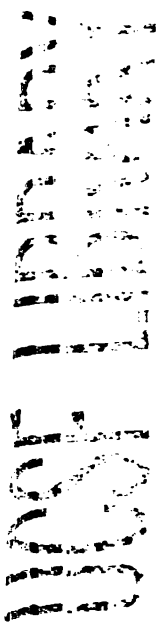

Chapter 2

The influence of novel bioactive glasses on *in vitro* osteoblast behavior

Reprinted from: Silvia Foppiano, Sally J. Marshall, Grayson W. Marshall, Eduardo Saiz and Antoni P. Tomsia. (2004) **The influence of novel bioactive glasses on *in vitro* osteoblast behavior.** *J Biomed Mater Res Part A* Sep 15;71A(2):242-249. With permission from Wiley.

Abstract

Implant success requires a direct bond between bone and implant surface. Bioinert implants, such as titanium alloys, are commonly plasma-spray-coated with a bone-bonding, bioactive material such as hydroxyapatite. Such coatings tend to be chemically and topographically inhomogeneous without reproducible properties. A family of bioactive glasses that can be enameled and reliably adheres to titanium alloy has been developed. In this study the cytocompatibility of two of these glass compositions was tested in the as-cast condition. The effects of these glasses on the early and late events of osseous tissue formation *in vitro* were determined with MC3T3-E1.4 mouse osteoblast-like cells. MC3T3-E1.4 cells were cultured on glasses containing 55 and 50 wt% SiO_2, with titanium alloy (Ti6Al4V) and tissue culture polystyrene as controls. Cellular adhesion and proliferation, and alkaline phosphatase activity were studied over 5-15 days in culture. Qualitative and quantitative assays of mineralization were conducted. The osteoblast-like cells showed increased proliferation when grown on a bioactive glass containing 50 wt% silica. However, the adhesion, differentiation and mineralization behavior were similar on both glass compositions used in this study. These bioactive glasses proved to be cytocompatible substrata for osteoblast-like cell culture, and yielded higher cellular proliferation than titanium alloy.

Introduction

The long term success of orthopedic and dental implants depends on osteointegration.[1] A number of factors affecting osteointegration include: implant material, design, surface chemistry and topography, quality of the bone, wound healing process, and operator error.[2] Bioinert materials with suitable mechanical properties, such as stainless steel,

titanium and cobalt chromium alloys (i.e. 316L, Ti6Al4V and Co-Cr-Mo), are commonly used for making load bearing implants.[3] Their retention relies mostly on mechanical interaction. Bioinert implants often become encapsulated in fibrous tissue, which results in the lack, or improper transfer of stress across the interface, thereby loosening the implant or fracturing the adjacent bone.[4]

To improve implant-bone bonding, metal alloys are commonly coated with hydroxyapatite (HA) by plasma spray[5,6] or other techniques.[7-10] Each technique presents pitfalls that result in partial crystallization and/or poorly controlled macro and micro porosity that affect the reproducibility, stability and long term performance of the coatings.[11] Metal alloys also can be coated with some bioactive glasses by the plasma spray technique,[12] subject to the same drawbacks. Glasses of bioactive compositions allow the formation of a biological apatite layer, similar to natural bone, on their surfaces *in vitro* when immersed in simulated body fluid (SBF). This is a cell and protein-free solution reproducing the ionic concentrations of blood plasma.[13,14] The formation of this layer is thought to be responsible for the bone-bonding characteristics of bioactive glasses.[15,16] Bioglass®, has found many non-load bearing applications and its interactions with bone *in vivo*, and with osteoblast cultures *in vitro*, have been extensively studied.[17-22] It is known that bioactive glasses are not strong enough to withstand loads, and attempts to use Bioglass® as an implant coating resulted in unreliable glass-metal bonding.[3,23]

A family of bioactive glasses has been developed that can be enameled onto Ti6Al4V yielding a reliable coating[23] while retaining bioactivity.[24] These glasses have the same phosphate content as Bioglass®, but differ in the amounts of other oxides. They also contain potassium and magnesium oxides, which are absent in Bioglass®, and allow a

better match to the coefficient of thermal expansion of Ti6Al4V. An enameled bioactive coating may provide the desired interfacial attachment to bone, extending implant life. More uniform surface texture, better adhesion and controlled chemical composition of bioactive glass coatings may make them more reproducible and reliable than plasma sprayed HA. To successfully fabricate functionally graded coatings on Ti6Al4V, the compositional limit for the top layer is about 53 wt% SiO_2. Since the chemical compositions of the glasses in this study differ significantly from Bioglass®, it is logical to test their cytocompatibility. As suggested by ASTM F748-98,[25] we first tested the glasses as cast without engaging in the coating fabrication process, to determine whether the glasses contain components that, once leached into solution, may adversely affect osteoblast-like cell activity. It was hypothesized that these glasses do not have a detrimental effect on osteoblast-like cellular behavior and are cytocompatible. The objective of this study was to screen for possible adverse reactions and/or differences in cellular response to the two glass compositions. We assayed cell adhesion, proliferation, differentiation and mineralization behavior of the mineralizing subclone of the mouse osteoblast-like cell line MC3T3-E1: MC3T3-E1.4 applied to two bioactive glasses and to the control substrates, Ti6Al4V and tissue culture polystyrene.

Materials and methods

Glass preparation

Glasses in the SiO_2-Na_2O-K_2O-CaO-MgO-P_2O_5 system were prepared by mixing the reagents in propanol using a high speed stirrer for 1 hour followed by drying at 80°C for 12 hours.[23] The P_2O_5 content was 6 wt% for both glasses, therefore designated 6P followed by their SiO_2 content in weight percent (Table 1).

The reagents were SiO_2 (99.5% Cerac Inc. Milwaukee, WI), $CaCO_3$ (99.9%, J.T. Baker Phillipsburg, NJ), MgO (98.6%, J.T. Baker, Phillipsburg, NJ), K_2CO_3 (99% Allied Chemical, Minneapolis, MN), $NaHCO_3$ (99.5% J.T. Baker, Phillipsburg, NJ), and Na_2HPO_4 (99.7% Allied Chemical, Minneapolis, MN). After drying, the mixture was fired in air in a Pt crucible for 5 hours at 1400°C. The melt was cast in a pre-heated (200°C) graphite mold yielding glass bars (~2 x 2 x 8 cm) that were annealed at 500 °C for 6 hours to relieve internal stresses. The annealed bars were subsequently cut perpendicularly to the long axis into square samples (~ 2 x 2 x 0.2 cm) with a low speed diamond saw (Isomet, Buehler, Ltd., Lake Bluff, IL). Each sample was metallographically polished with diamond suspension to 1 μm (Buehler, Ltd., Lake Bluff, IL). Samples were then reduced to squares of 1.5 x 1.5 x 0.2 cm by grinding down the sides. The resulting glass squares fit snugly into the wells of 12 well tissue culture polystyrene plates (B-D Falcon, Becton Dickinson, Franklin Lakes, NJ), which prevented the samples from moving and therefore avoided the breakage of the cell layer when the plates were handled for medium replenishment. Cutting and polishing was done in isopropyl alcohol due to the reactivity of the glasses in aqueous solutions. Titanium alloy (Ti6Al4V Goodfellow Ltd., Huntingdon, UK), similarly cut into squares and polished, served as control together with tissue culture polystyrene (TCPS) (the bottom of the wells). Prior to sterilization in dry heat at 250 °C, the samples were cleaned by sonication in acetone and isopropyl alcohol for 5 minutes each. Sterile samples were placed in 12 well tissue culture plates under sterile conditions.

Cell culture

MC3T3-E1.4 mouse osteoblast-like cells were obtained from Dr. Tamara N. Alliston (Dr. Rik Derynck's laboratory, University of California, San Francisco). This is a well characterized mineralizing subclone of the mouse osteoblast-like MC3T3-E1 cell line.[26-30] Cells were grown in an incubator at 37°C and 5% CO_2 atmosphere, in α-modified Eagle's medium (α-MEM) supplemented with 10% fetal bovine serum (FBS) and 1% antibiotics (penicillin and streptomycin) and passaged every 4-5 days. Cells were used between passage 10 and 20. In all experiments cells were plated at an initial density of 50,000 cells/cm^2; previous studies showed that this cell density results in optimal expression of osteoblast markers.[30]

Cell adhesion

Cells (50,000 cells/cm^2 density) were seeded in 30 μL aliquots on the center of each sample and control material. Cells were allowed to adhere for 10 minutes before the wells were gently flooded with the medium (1 mL/well). We consistently used 1 mL medium/well to reduce the variability of glass dissolution which is known to be a function of the solution volume.[31] Three hours after flooding, the supernatant containing non-adhering cells was removed, and replaced with fresh medium. The number of adhering cells was assayed using a commercial kit (CellTiter 96® Promega Corp. Madison, WI), based on the metabolic activity of living cells (3-(4,5-dimethylthiazol-2-yl)-2,5-diphenyl tetrazolium bromide) (MTT) assay). The MTT solution added to each well was incubated for 4 hours at 37 °C. After the formation of the crystal formazan product the square samples (glasses and Ti6Al4V) were transferred from the original tissue culture plate and placed into the wells of a new one. This way only the crystals formed on the samples were dissolved. To dissolve the formazan product solutions were

added according to the Promega protocol, keeping the ratio of solution volume to sample surface area constant at 2 $\mu L/mm^2$. This was done to compensate for the difference in surface available to the cells, since the samples did not cover the bottom of the wells completely. The overnight protocol was chosen to ensure complete solubilization of the dark blue formazan product. The optical density was measured at 570 nm in a spectrophotometer (Spectronic Genesys 5, Spectronics Instruments, Rochester, NY). A calibration curve was determined to convert absorption into number of cells; the relationship was linear. The data was normalized to the sample surface area ($cells/cm^2$). Experiments were performed in triplicate with N=3 for each material in each experiment.

Cell proliferation

Cell proliferation was assayed according to the following schedule: on day 1, cells were seeded as described above; on day 2, cells were synchronized by serum starvation for 48 hours, replacing the medium with a fresh one containing 1% FBS. On day 4, cells were allowed to re-enter the cell cycle by replacing the medium with a fresh one containing 10% FBS. After 24 hours, the proliferating cells were assessed using the MTT assay as described above. Experiments were performed in triplicate with N=3 for each material in each experiment.

Alkaline phosphatase

To determine the effect of the glasses on early events of osseous tissue formation *in vitro*, alkaline phosphatase activity, a marker of osteoblast differentiation, in the absence of ascorbic acid (AA) treatment, was analyzed. Cells were seeded as described above, the medium was replaced at 2-day intervals throughout the experiment. Alkaline phosphatase activity was measured in cell layers after 5, 8, 11 and 15 days in culture. At

each time point the glasses and Ti6Al4V were transferred to a new tissue culture plate to avoid lysis of cells not on the materials. Cell layers were rinsed twice with phosphate buffer solution (PBS) without calcium or magnesium, incubated with 100 μL sodium dodecyl sulfate solution (0.05% in PBS). Alkaline phosphatase activity was measured, from 10 μL of cell lysate, as released p-nitrophenol from a p-nitrophenyl phosphate substrate after 15 min of incubation at 37 °C (Sigma Diagnostics procedure No 104, Sigma Diagnostics Inc., St. Louis, MO). A Sigma Unit of phosphatase activity is the amount of enzyme that will release 1 μmol p-nitrophenol per hour. The optical density was measured at 410 nm in a spectrophotometer. The enzyme activity was expressed as units per mg of total proteins. Estimation of protein content was carried out using a Bio-Rad Protein assay (BioRad Laboratories, Hercules, CA); optical density was measured at 595 nm in the same spectrophotometer. To determine the effect of the materials on cellular response to AA, experiments at day 3 and 8 were repeated in presence of AA (50 μg/mL medium) and alkaline phosphatase was measured as described above. Experiments were done at least twice with N=3 per material per experiment.

Mineralization

Alizarin S staining

Cells were seeded as described above. Cells were treated with AA (50 μg/mL medium) for 10 days and then with AA and inorganic phosphate (NaH_2PO_4) (10 mM) for an additional 5 days. Medium was replaced at 2 day intervals throughout the experiment. Cells were washed 3 times with PBS without calcium or magnesium prior to fixation with 100% ethanol for 15 minutes. Cell layers were stained with alizarin S solution for 30 minutes, rinsed and photographed under an optical microscope (Olympus BX50 Olympus

America Inc., Melville, NY) with a ccd camera (DVC 1300C camera RGB color, DVC Company, Austin, TX). Experiments were performed in triplicate with N=3 for each material in each experiment. To ensure that no artifact staining occurred due to the presence of phosphate in the glass compositions the following control experiments were carried out: 1) samples were prepared as described above, and half the cell layer covering the glass was removed prior to staining. 2) glass as cast was stained with alizarin S.

Quantitative measurement of inorganic phosphate

To quantify the amount of mineralized matrix produced by the cells on the different materials, cells were seeded and treated with ascorbic acid and inorganic phosphate to induce mineralization as described above. After 15 days in culture, cells were washed 3 times with PBS without calcium or magnesium and the cell layer grown on glasses and Ti6Al4V was scraped off the sample with a rubber policeman and transferred to a new tissue culture plate. This was done to avoid measuring phosphate released from the glasses themselves or from the tissue grown on the tissue culture wells adjacent to the test substrates, since the glass and Ti6Al4V substrates did not cover the bottom of the wells entirely. The mineralized tissue was incubated for 24 hours in 15% trichloroacetic acid (TCA). The amount of TCA added was kept constant at 2 $\mu L/mm^2$ of sample surface. 50 μL of supernatant was then assayed. Inorganic phosphate concentration was determined by spectrophotometry (355 nm) using the method of Heinonen and Lahti.[32] The absorbance value in Klett units (KU) (1 KU corresponds to the absorbance of 0.005) was converted into concentration using a calibration curve made using the same method. Experiments were performed in triplicate with N=3 for each material in each experiment.

Scanning electron microscopy (SEM) analysis

Cell layers cultured and treated for mineralization were prepared for SEM analysis (Topcon ISI SX 40A scanning electron microscope, Milpitas, CA) as follows. Cell layers were dehydrated with a series of graded ethanol solutions, then treated with hexamethyldisilazane (HMDS) and sputter-coated with Au-Pd (200 nm).

Results:

Cell adhesion

Figure 1 shows the results from a representative experiment (N=3): the number of viable adhering cells was significantly lower on TCPS with respect to Ti6Al4V and the glasses (ANOVA, Student Newman Keuls (SNK) $p<0.05$).

Cell proliferation

As shown in Figure 2, proliferation was significantly different on each material (ANOVA, SNK $p<0.05$). Cells proliferated on the materials in the following order from lowest to highest: TCPS, Ti6Al4V, 5P55, and 6P50.

Alkaline phosphatase

At days 5, 8, 11 and 15 alkaline phosphatase activity was low or undetectable for all samples and controls with no significant differences. This result was not surprising since the alkaline phosphatase production of this cell line is known to be extremely low in the absence of ascorbic acid (AA) treatment.[28] Thus exposure of the cell line to the test and control materials had no effect on alkaline phosphatase expression in the absence of AA. To determine whether the cell culture was being handled correctly and retained its ability to respond to AA treatment in the presence of the materials we repeated some experiments, on the same substrates, but treated with 50 μg/ml AA. Alkaline phosphatase activity increased significantly after ascorbic acid treatment (with respect to

no AA treatment) on each material, but no significant difference between samples and controls was found (data not shown).

Mineralization

Alizarin S staining

Fresh samples were prepared and treated with alizarin S to assess the level of background staining. No staining was found on samples and controls (data not shown). Figure 3 shows alizarin S staining for control samples where part of the cell layer was removed prior to staining. The area of the sample not covered by the cell layer had a pale pink staining. Figure 4 shows alizarin S staining of the mineralizing cell layer on glasses and control materials. Distinct nodular colonies can be distinguished and a morphological difference in the mineral distribution is apparent. Tissue culture polystyrene (Figure 4 A) and Ti6Al4V (Figure 4 B) showed well localized areas of mineralization with intense staining. Areas clearly devoid of calcium and unstained, also are present. Glasses 6P50 (Figure 4 C) and 6P55 (Figure 4 D) appear to be mineralizing differently, as indicated by the more extensive and less intense staining patterns. Scanning electron microscopy analysis (Figure 5) revealed areas with the morphology of mineral nodules and abundant collagen-like fibers. Three-dimensional structures attributed to bone nodules are indicated by the black arrowheads in Figure 5 (A: tissue culture polystyrene, B: Ti6Al4V, C: 6P55, D: 6P50). On all materials a collagen-like extracellular matrix was present, but it appeared more evident on the glasses (Figure 5C, D and E, large black arrows).

Quantitative measurement of inorganic phosphate

Figure 6 shows the concentration of inorganic phosphate released from the mineralizing cell layer. Significantly higher concentration of inorganic phosphate was released from the cell layer grown onto TCPS (ANOVA, SNK $p<0.05$).

Discussion

The ultimate goal is to fabricate a functionally graded coating on titanium alloy implants, yielding a reproducible and reliable bioactive surface. The characterization of bioactive glasses for this purpose has important implications in the development of such new implants and possibly in skeletal reconstruction. This is the first time that the *in vitro* biocompatibility of these bioactive glasses has been evaluated with osteoblast-like cells. The MC3T3-E1 cell line is known to be phenotypically heterogeneous due to its mesenchymal origin and multiple passaging.[27] For this reason we chose its subclone, the MC3T3-E1.4, which is well characterized and has the ability to form a mineralized bone matrix *in vitro*.[26,28-30] Bioactive glasses should support osteoblast proliferation and differentiation. Lack of cellular adhesion on these materials indicates cytotoxicity since these cells require adhesion for survival. Three hours after seeding, mouse osteoblast-like cells adhered on all samples and controls. Bioactive glasses, by means of their reactivity in aqueous solutions, produce a silica gel layer on their surfaces[17] which could affect cell adhesion. Cells could be passively stuck on the glass surface but not be viable. To measure cell adhesion we chose the MTT assay, which accounts only for viable cells. The data indicate that MC3T3-E1.4 osteoblast-like cells adhered on tissue culture polystyrene in lower numbers compared to bioactive glasses containing 50 and 55 wt% silica and to titanium alloy. At day 5 proliferation was significantly different on each

material. The lowest proliferation on TCPS, could be due to the lower initial number of adhering cells. Differences in proliferation on the other materials are probably due to the intrinsic properties of the materials since there was no initial difference in the number of adhering cells. MC3T3-E1.4 cells are known to respond to AA treatment by increasing alkaline phosphatase activity. To identify possible changes in alkaline phosphatase activity due exclusively to the bioactive glasses, alkaline phosphatase activity was measured without AA treatment. The natural low alkaline phosphatase activity was not significantly altered by any of the materials. Control experiments were conducted to determine whether the glasses impaired cellular response to AA treatment. Alkaline phosphatase increased in response to AA treatment in the presence of the materials but no significant difference between materials was observed. Thus bioactive glasses in this study did not appear to perturb osteoblast-like cell alkaline phosphatase activity. Cultures maintained for 15 days in αMEM under mineralizing conditions differentiated, forming three-dimensional nodular colonies. Alizarin S staining and microscopic analysis indicated that these three dimensional nodules consisted of aggregated cells embedded in the mineralizing extracellular matrix. Bioactive glasses allowed a more diffuse mineralization pattern, while titanium alloy and tissue culture polystyrene presented localized mineralized areas. Microscopic analysis revealed the presence of abundant extracellular matrix (fibrous in nature), probably collagen that is necessary for mineralization.[33,34] The collagen organization in the osteoblastic extracellular matrix can be affected by different calcium-phosphate based bioactive substrates.[35] The surface reactivity of the bioactive glasses may play a role in the way collagen is distributed, yielding a uniform and less intense mineralization pattern. Alizarin S, which binds to

calcium,[36] could have yielded false positive results for two main reasons: 1) the glasses contain calcium and 2) in aqueous solutions, these glasses react to form a superficial layer of calcium-containing mineral. We eliminated these possibilities by testing for background staining of the glass alone, prior to immersion in any fluid, which yielded no staining. Secondly, mineralizing tissue grown on samples was partially removed prior to staining. After Alizarin S treatment the exposed glass did not stain significantly. Therefore the stain seen on the glasses was a result of mineralization and not a result of false staining of calcium components of the glasses. We then quantified the mineral formation since the Alizarin S staining could not be quantified due to different optical properties of the glasses compared to the alloy.

The quantity of mineralized tissue grown on the glasses and titanium alloy contained similar amounts of inorganic phosphate, while mineralization was significantly higher on TCPS. The results of this work suggest that these bioactive glasses have significant potential for use as coatings, and have no deleterious effects on an osteoblast-like cell function as studied here. Further quantitative analysis of markers of osteoblast differentiation may reveal subtle differences in the effect of bioactive glass coatings on cellular behavior. Future research will involve the fabrication of functionally graded enameled coatings with a bioactive surface containing about 55 wt% silica and their detailed analysis.

Conclusions

The cytocompatibility of bioactive glasses, as cast, containing 50 and 55 wt% SiO_2 was tested using the mouse MC3T3-E1.4 osteoblastic cell line as an *in vitro* bone-model. We found significantly higher cell adhesion onto bioactive glasses and Ti6Al4V with respect

to tissue culture polystyrene. Proliferation was significantly different on all materials: highest on the glass containing 50 wt% silica, followed by the glass containing 55 wt% silica, Ti6Al4V and lowest on TCPS. Alkaline phosphatase activity was not affected by the glasses or control materials. Mineralization occurred on all materials with morphological differences. The mineralizing tissue grown onto bioactive glasses and titanium alloy contained similar amounts of inorganic phosphate. The results suggest that the bioactive glasses studied here do not have any significant negative effect on osteoblast-like cell function and are cytocompatible.

Acknowledgements

The authors would like to thank Dr. Tamara N. Alliston for her support with cell culture techniques and Dr. Pamela DenBesten for allowing the use of her facilities and the National Institutes of Health/National Institute of Dental and Craniofacial Research for support through grant R01DE11289.

LeGeros RZ and Craig RG, Strategies to affect bone remodeling: osteointegration. J Bone Miner Res, 1993;8:S583-96.
Hench LL and Ethridge EC. Tissue reactions. In: Hench LL and Ethridge, EC editors. Biomaterials An Interfacial Approach. Academic press 1982;105-148.
Hench LL and Andresson O. Bioactive glass coatings. In: Hench LL, Wilson J, editors. An Introduction to Bioceramics Singapore: World Scientific 1993;239-259.
Long M and Rack HJ, Titanium alloys in total joint replacement--a materials science perspective. Biomaterials, 1998;19(18): 1621-39.
Geesink RG, de Groot K, Klein CP. Bonding of bone to apatite-coated implants. J Bone Joint Surg Br, 1988;70(1):17-22.
Hayashi K, Matsuguchi N, Uenoyama K, Kanemaru T, Sugioka Y. Evaluation of metal implants coated with several types of ceramics as biomaterials. J Biomed Mater Res, 1989;23(11):1247-59.
Choi JM, Kim HE, Lee IS. Ion-beam-assisted deposition (IBAD) of hydroxyapatite coating layer on Ti-based metal substrate. Biomaterials, 2000;21(5):469-73.
van Dijk K, Schaeken HG, Wolke JG, Jansen J. Influence of annealing temperature on RF magnetron sputtered calcium phosphate coatings. Biomaterials, 1996;17(4):405-10.
Wheeler DL, Campbell AA, Graff GL, Miller GJ. Histological and biomechanical evaluation of calcium phosphate coatings applied through surface-induced mineralization to porous titanium implants. J Biomed Mater Res, 1997;34(4):539-43.
Ramires PA, Romito A, Cosentino F, Milella E. The influence of titania/hydroxyapatite composite coatings on in vitro osteoblasts behaviour. Biomaterials 2001;22(12):1467-74.
Lacefield WR. Hydroxylapatite Coatings. In: Hench LL and Wilson J editors. An introduction to Bioceramics Singapore: World Scientific 1993;223-238. 12.
Oliva A, Salerno A, Locardi B, Riccio V, Della Ragione F, Vardino P, Zappia V. Behaviour of human osteoblasts cultured on bioactive glass coatings. Biomaterials;1998;19(11-12):1019-25.
Kokubo T, Kushitani H, Sakka S, Kitsugi T, Yamamuro T. Solutions able to reproduce in vivo surface-structure changes in bioactive glass-ceramic A-W. J Biomed Mater Res, 1990;24(6):721-34.
Ohgushi H, Dohi Y, Yoshikawa T, Tamai S, Tabata S, Okunaga K, Shibuya T. Osteogenic differentiation of cultured marrow stromal stem cells on the surface of bioactive glass ceramics. J Biomed Mater Res. 1996;32(3):341-8.
Hench LL, Splinter RJ, Allen WC, Greenlee TK. Bonding mechanisms at the interface of ceramic prosthetic materials. J Biomed Mater Res 1971;2:117-41.
Hench LL, Paschall HA. Direct chemical bond of bioactive glass-ceramic materials to bone and muscle. J Biomed Mater Res 1973;4:25-42.
Hench LL and Andersson O. Bioactive glasses. In: Hench LL and Wilson J editors. An Introduction to Bioceramics. Singapore: World Scientific 1993;41-62.

18. Price N, Bendall SP, Frondoza C, Jinnah RH, Hungerford DS. Human osteoblast-like cells (MG63) proliferate on a bioactive glass surface. J Biomed Mater Res, 1997;37(3):394-400.
19. Lobel KD and Hench LL, In vitro adsorption and activity of enzymes on reaction layers of bioactive glass substrates. J Biomed Mater Res, 1998;39(4): 575-9.
20. Radin S, Ducheyne P, Falaize S, Hammond A. In vitro transformation of bioactive glass granules into Ca-P shells. J Biomed Mater Res, 2000;49(2):264-72.
21. Radin S, Ducheyne P, Rothman B, Conti A. The effect of in vitro modeling conditions on the surface reactions of bioactive glass. J Biomed Mater Res, 1997;37(3):363-75.
22. Silver IA, Deas J, Erecinska M. Interactions of bioactive glasses with osteoblasts in vitro: effects of 45S5 Bioglass, and 58S and 77S bioactive glasses on metabolism, intracellular ion concentrations and cell viability. Biomaterials, 2001;22(2):175-85.
23. Gomez-Vega JM, Saiz E, Tomsia AP, Marshall GW, Marshall SJ. Bioactive glass coatings with hydroxyapatite and Bioglass particles on Ti-based implants. 1. Processing. Biomaterials 2000;21:105-11.
24. Gomez-Vega JM, Saiz E, Tomsia AP. Glass-based coatings for titanium implant alloys. J Biomed Mater Res 1999;46:549-59.
25. American Society for Testing and Materials. Annual Book of ASTM Standards. Philadelphia, PA. Section Thirteen: Medical Devices and Services, Vol 13.01 F748-98 2001;243-49.
26. Wang D, Butler JP, Ingber DE. Isolation and characterization of MC3T3-E1 preosteoblast subclones with distinct in vitro and in vivo differentiation/mineralization potential. J Bone Miner Res, 1999;14:893-903.
27. Huang W, Carlsen B, Rudkin GH, Shah N, Chung C, Ishida K, Yamaguchi DT, Miller TA. Effect of serial passage on gene expression in MC3T3-E1 preosteoblastic cells: a microarray study. Biochem Biophys Res Commun, 2001;281:1120-6.
28. Quarles LD, Yohay DA, Lever LW, Caton R, Wenstrup RJ. Distinct proliferative and differentiated stages of murine MC3T3-E1 cells in culture: an in vitro model of osteoblast development. J Bone Miner Res, 1992;7:683-92.
29. Franceschi RT and Iyer BS, Relationship between collagen synthesis and expression of the osteoblast phenotype in MC3T3-E1 cells. J Bone Miner Res, 1992;7:235-46.
30. Franceschi RT, Iyer BS, Cui Y. Effects of ascorbic acid on collagen matrix formation and osteoblast differentiation in murine MC3T3-E1 cells. J Bone Miner Res, 1994;9:843-54.
31. Jones JR, Sepulveda P, Hench LL. Dose-dependent behavior of bioactive glass dissolution. J Biomed Mater Res, 2001;58:720-6.
32. Heinonen JK, and Lahti RJ. A new and convenient colorimetric determination of inorganic orthophosphate and its application to the assay of inorganic pyrophosphatase. Anal Biochem 1981;113:313-317.
33. Owen TA, Aronow M, Shalhoub V, Barone LM, Wilming L, Tassinari MS, Kennedy MB, Pockwinse S, Lian JB, Stein GS. Progressive development of the

rat osteoblast phenotype in vitro: reciprocal relationships in expression of genes associated with osteoblast proliferation and differentiation during formation of the bone extracellular matrix. J Cell Physiol 1990;143:420-30.
34. Karsenty G. The genetic transformation of bone biology. Genes Dev, 1999;13:3037-51.
35. Davies JE and Matsuda T. Extracellular matrix production by osteoblasts on bioactive substrata in vitro. Scanning Microsc, 1988;2:1445-52.
36. [http://madlib.med.utah.edu/webpath/hthtml/manuals/alizarins.pdf].

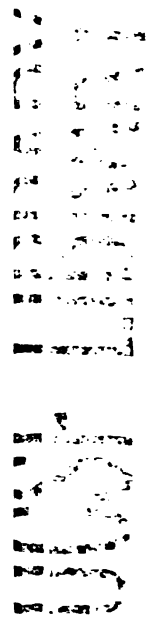

Tables

Table 1. Glass compositions in weight %

	SiO_2	Na_2O	K_2O	CaO	MgO	P_2O_5
6P50	49.8	15.5	4.2	15.6	8.9	6.0
6P55	54.5	12.0	4.0	15.0	8.5	6.0

Figures and Captions

Figure 1

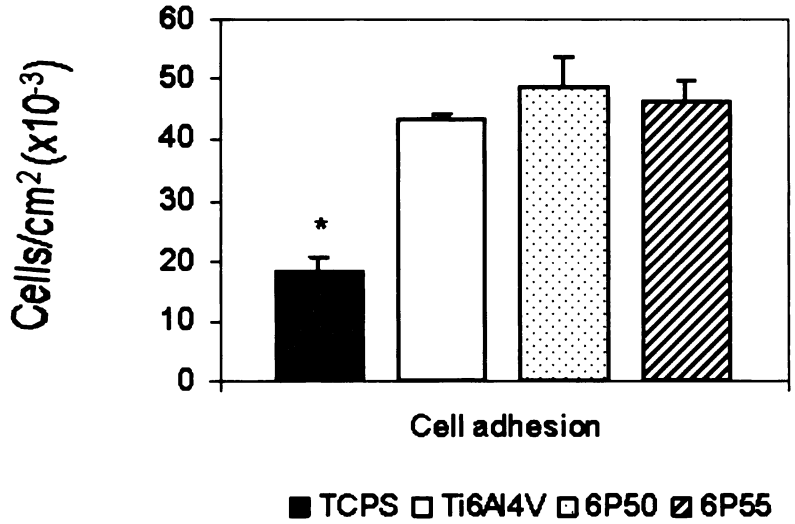

Figure 1. Cell adhesion: Cells adhered in lower numbers onto TCPS. (*)=significantly different respect to all other materials (ANOVA, SNK $p<0.05$).

Figure 2

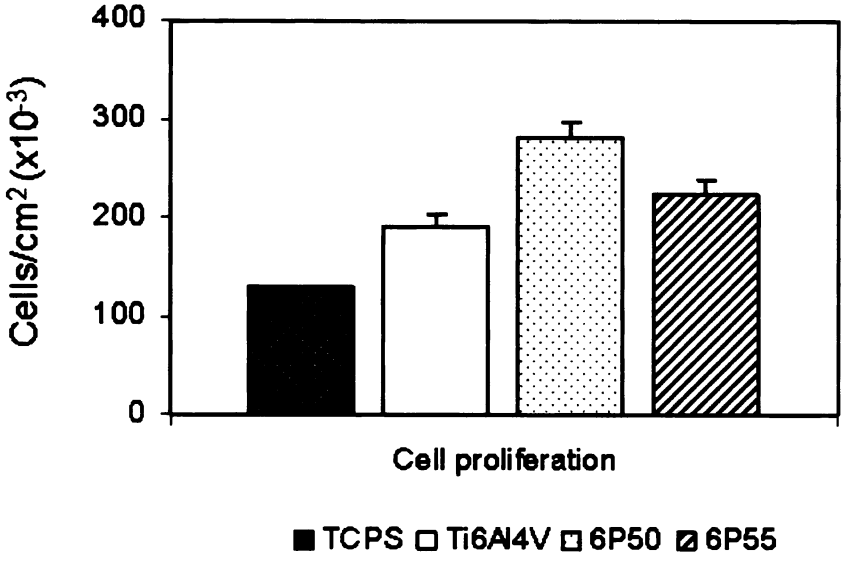

Figure 2. Cell proliferation: after 5 days in culture MC3T3-E1.4 mouse osteoblast-like cells proliferated significantly differently on all materials. Lowest proliferation occurred on TCPS followed by Ti6Al4V, glass 6P55 and glass 6P50 (ANOVA, SNK $p<0.05$).

Figure 3

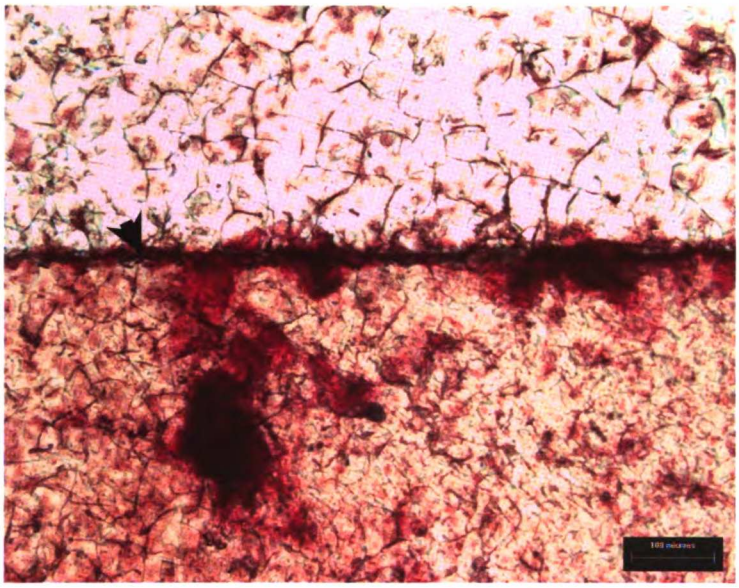

Figure 3. Mineralization, control experiment: tissue grown onto glass 6P50 was cut (black arrow) prior to staining with alizarin S. The tissue stained for alizarin S (area below the arrow, area devoid of tissue shows pale pink staining (area above the arrow). Similar results were obtained with glass 6P55.

Figure 4

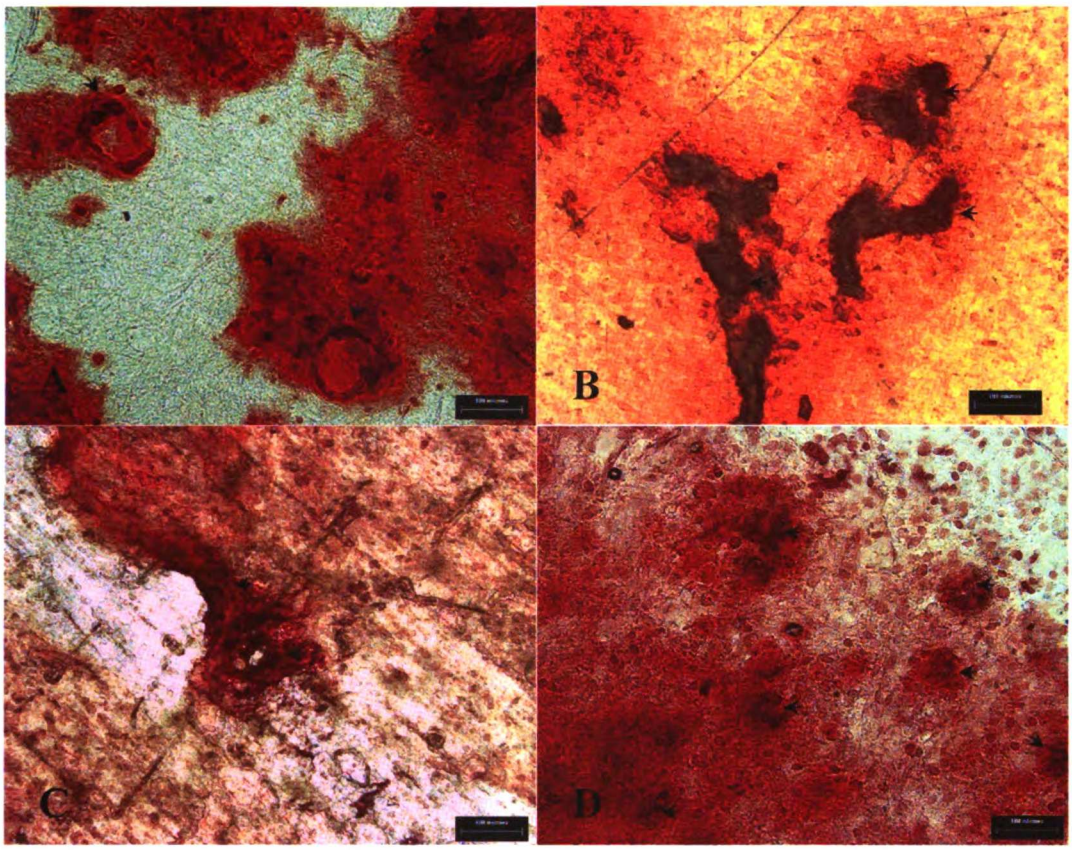

Figure 4. Mineralization by alizarin S staining: Mineralizing bone nodules showed a dark red staining (black arrowheads). The nodules appeared to be round in shape on tissue culture polystyrene (A) and on the glasses 6P55 (C) and 6P50 (D). On Ti6Al4V (B) mineralizing nodules had a more irregular shape. The staining was overall more intense and well defined on tissue culture polystyrene (A) and Ti6Al4V (B), where non mineralizing, unstained, areas are also clearly visible. Note that Ti6Al4V is not transparent and the reflected light confers a yellowish color to the unstained areas. On glasses 6P55 (C) and 6P50 (D) mineralization appeared to be more diffuse and less intense; non-mineralizing areas are not well defined.

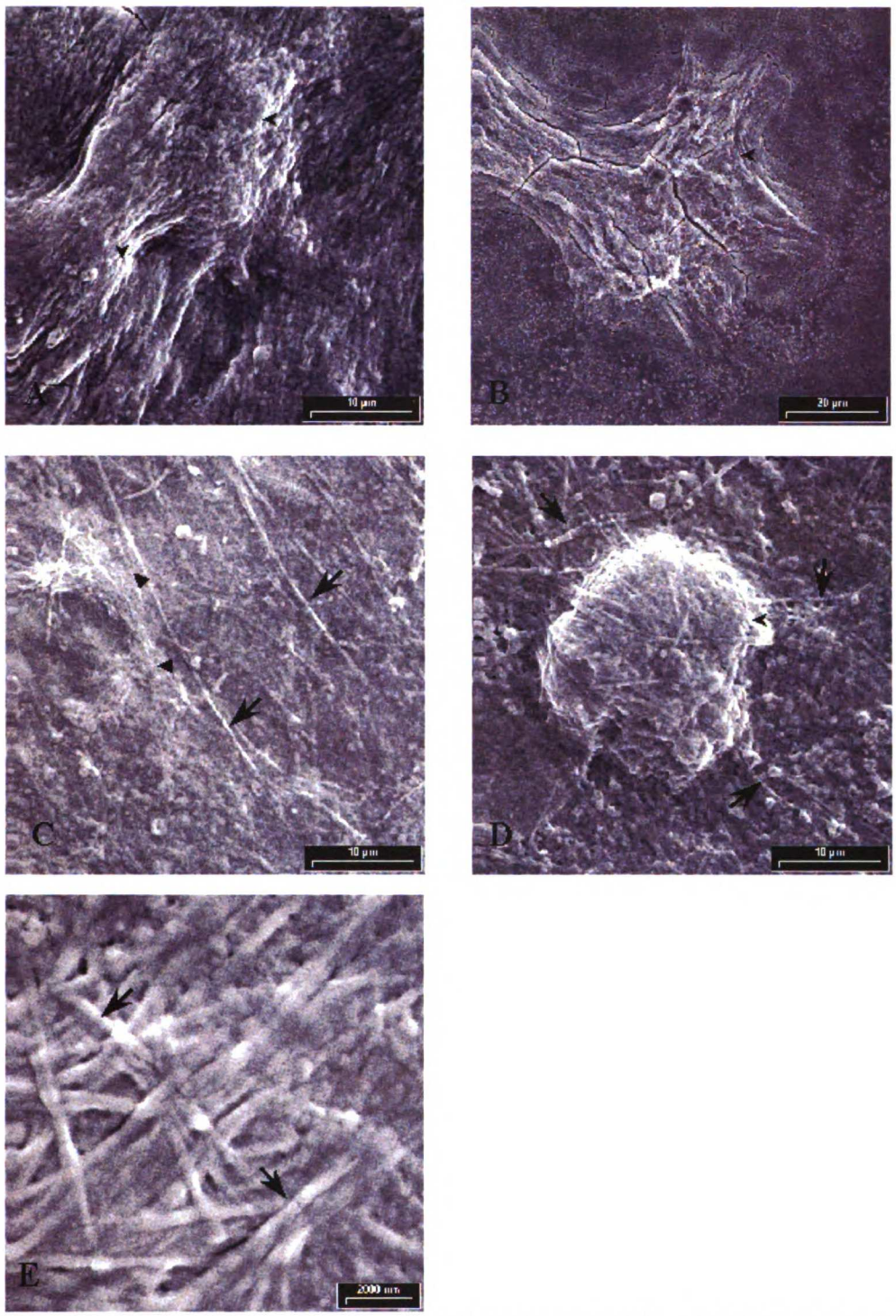

Figure 5. SEM analysis of mineralized areas: bone nodules of different size were observed on all materials (black arrowheads). The nodules appeared rounded on tissue culture polystyrene (A), and on glasses 6P55 and 6P50 (C and D respectively), while on Ti6Al4V (B) had a more irregular shape. The bone-like matrix contained collagen-like fibers which was detectable on all materials, but on the glasses was more evident even at low magnification (large black arrows). Representative collagen matrix on glass 6P50 is shown in (E).

Figure 6

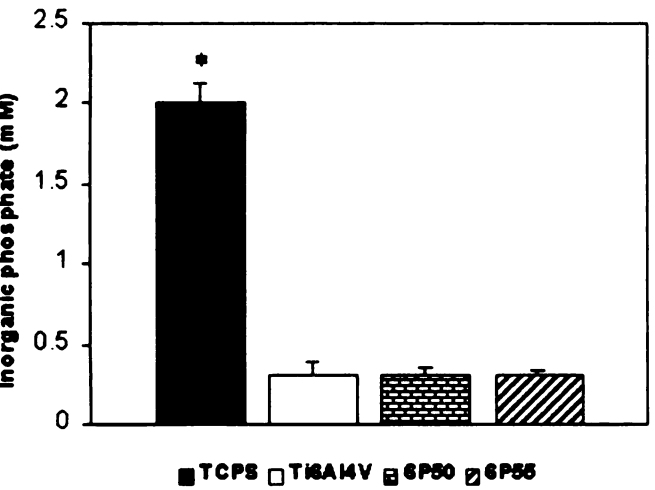

Figure 6. Quantitative mineralization: mineralizing tissue grown onto TCPS released a significantly higher concentration on inorganic phosphate respect to mineralizing tissue grown onto Ti6Al4V and bioactive glasses (*) (ANOVA, SNK $p<0.05$).

Chapter 3

Functionally graded bioactive coatings: the effect of fabrication process on glass bioactivity in simulated body fluid

The data reported in Chapter 3 and Chapter 4 will be combined into one single paper and submitted for publication

Abstract

The structure of functionally graded coatings (FGC) of bioactive glasses on titanium alloy (Ti6Al4V) prepared by the enameling technique, was compared to that of the as cast glass used for the reactive surface layer of the FGC. X-ray diffraction (XRD) and scanning electron microscopy (SEM) analyses showed that the fabrication process caused 5.9 ± 3.0 vol% crystallization of the coating while the glass as cast was amorphous. Two crystalline phases were identified by XRD: sodium calcium phosphate and calcium magnesium silicate. Immersion in simulated body fluid (SBF) caused the surface of the coating to react and form an amorphous layer rich in phosphate which, over 4 weeks, crystallized into apatite-like mineral identified by Fourier Transform Infrared Spectroscopy (FTIR), XRD and SEM. Similar reactions occurred on the surface of the glass as cast. Despite partial crystallization of the coatings' surface, there was no apparent difference in *in vitro* bioactivity in SBF due to the presence of crystalline phases.

Introduction

Current techniques for coating implants with hydroxyapatite, such as plasma spraying and others, have drawbacks that render the coatings inhomogeneous, not reliable and prone to delamination.[1-4] Functionally graded coatings (FGC) of bioactive glasses that reliably adhere to titanium alloy when enameled have been developed. These glasses differ significantly from Bioglass®. The properties and composition of the glass coating are graded to fulfill different functions. The glass composition in contact with Ti6Al4V offers a better coefficient of thermal expansion match and is more resistant to corrosion because of its higher silica content, while the glass on the surface provides a dynamic (i.e.

reactive) bioactive surface.[5,6] Bioactive glasses bond directly to bone *in vivo* through the formation of a carbonate-containing hydroxyapatite layer that forms on the material's surface.[7,8] To predict *in vivo* bioactivity, *in vitro* assays have been widely applied using simulated body fluid (SBF), a solution closely matching the ion concentrations and pH to those of human plasma.[9,10] In this study functionally graded coatings of titanium alloy were fabricated using a glass containing 61 wt% silica in contact with the alloy and a bioactive glass containing 55 wt% silica as surface coating. A recent *in vitro* study showed good cytocompatibility of the latter glass.[11] The objective of this work was to determine the effect of the coating fabrication process on the microstructure and on bioactivity, *in vitro*, in SBF of the top surface glass.

Materials and Methods

Glass and coating fabrication

Glasses in the SiO_2-Na_2O-K_2O-CaO-MgO-P_2O_5 system were prepared by mixing the reagents in propanol using a high speed stirrer for 1 hour and drying at 80°C for 12 hours. Both glasses contain 6 wt% P_2O_5 and are designated 6P followed by their SiO_2 content in weight percent (Table 1). The reagents were: SiO_2 (99.5% Cerac Inc., Milwakee, WI), $CaCO_3$ (99.9%, J.T. Baker, Phillipsburg, NJ), MgO (98.6%, J.T. Baker, Phillipsburg, NJ), K_2CO_3 (99.4 % Mallinkratt, Paris, KY), $NaHCO_3$ (99.5% J.T. Baker, Phillipsburg, NJ), and Na_2HPO_4 (99% Sigma, St. Louis, MO). The mixture was dried and fired in air in a Pt crucible for 5 hours at 1400 °C (glass 6P55) or 1450 °C (glass 6P61). The melt was cast in a pre-heated (200 °C) graphite mold yielding glass bars (~2 x 2 x 8 cm). Glass 6P55, when used as cast, was annealed at 500 °C for 6 hours to relieve internal stresses. The annealed bar was cut with a low speed diamond saw (Isomet, Buehler Ltd., Lake

Bluff, IL) perpendicularly to the long axis, resulting in square specimens (~ 2 x 2 x 0.2 cm). Each specimen was metallographically polished with diamond suspension to 1 μm (Buehler Ltd., Lake Bluff, IL). The size of the specimens' was reduced to 1.5 x 1.5 x 0.2 cm by grinding the sides. Cutting and polishing was done in isopropyl alcohol due to the reactivity of the glass in aqueous solutions. Titanium alloy (Ti6Al4V, Goodfellow Ltd., Huntingdon, UK) was similarly cut and finished to 1 μm with diamond suspension (Buehler, Ltd., Lake Bluff, IL). Ti6Al4V was cleaned by ultrasonication with ethanol and acetone for 10 minutes each. Functionally graded coatings were prepared as previously described.[5] Briefly, the glasses (6P61 and 6P55) were separately milled in a planetary agate mill. A suspension of 6P61 glass powder (particle size < 37 μm) in 100% ethanol was deposited on Ti6Al4V (1.5 x 1.5 x 0.1 cm) prepared as described above. Glass particles were allowed to settle and the process was carefully repeated using glass 6P55 (particle size < 37 μm) without disturbing the first powder layer. After drying in air at 80 °C for 48 hours the green coatings were fired in air in a dental furnace (Unitek Ultra Mat II, 3M, Maplewood, MN). The furnace was pre-heated at 640 °C; the firing temperature of 800 °C was reached with heating ramp of 40 °C/min while the furnace was evacuated to 0.1 atm. At 800 °C air was let into the firing chamber. Samples were fired for 10 sec in air at 1 atm and quenched.

SEM and XRD analyses

Glass 6P55 as cast and the FGC were etched with a solution of HNO_3:HF:H_2O (5:5:90 vol%) for 10 seconds, sputter-coated with Au-Pd (200 nm) and analyzed by scanning electron microscopy (SEM) (Topcon ISI SX 40A scanning electron microscope, Milpitas, CA) to visualize the microstructure. The amount of surface crystallization was assessed

by image analysis (Sigma AIA2 Analysis, Noran, Madison, WI). Twenty seven images were analyzed from 3 separate samples (9 images per sample). The percentage of surface area occupied by crystalline phases relative to the total surface area of the image was calculated. Samples were analyzed by glancing angle X-ray diffraction (XRD) (Siemens D5000, Siemens, Munich, Germany) to identify the crystalline phases. Peaks were identified by comparison to published material.[5,12]

Assessment of *in vitro* bioactivity in simulated body fluid (SBF)

In vitro bioactivity in SBF of the FGC and of glass 6P55 as cast was studied by Fourier Transform Infrared Spectroscopy (FTIR) (Laser Precision Analytical, Laser Precision Corp., Irvine, CA), XRD and SEM. Samples were prepared as described above, placed in 6 well tissue culture plates and immersed in SBF (Table 2) for 1, 2, 3, and 4 weeks at 37 °C, replenishing the solution every week. The surface area to volume ratio (SA/V of SBF solution) was fixed at 0.56 cm^{-1}. The SA/V relevant to *in vivo* conditions is difficult to estimate. The 0.56 cm^{-1} ratio was arbitrarily chosen to completely cover each sample and prevent significant SBF evaporation over the course of seven days. Samples were analyzed at weekly intervals by FTIR and after 4 weeks by XRD. Samples were sputter coated and analyzed by SEM as described above.

Results

SEM and XRD analyses

The etched FGC microstructure contained separated phases that were round in shape with diameters in the order of 5-6 μm. (Figure 1A). Image analysis indicated that the separated phases occupied 5.9 ± 3.0 vol%. Glass as cast (Figure 1B) had some surface

defects such as porosity but no visible phase separation. Figure 2 compares the glancing angle x-ray diffraction patterns of glass 6P55 as cast and of the FGC, where crystalline peaks are present only in the FGC pattern. The absence of peaks in the pattern of glass 6P55 as cast indicated that the glass was amorphous. Thus the coating fabrication process caused partial crystallization of the glass. The crystalline peaks in the XRD pattern of the FGC were consistent with sodium calcium phosphate (2.4 CaO $0.6Na_2O$ P_2O_5), and calcium magnesium silicate ($CaMg(SiO_3)_2$).

Assessment of *in vitro* bioactivity in simulated body fluid (SBF)

FTIR analysis showed that the FGC and glass as cast behaved similarly in SBF. The FTIR spectra of the FGC (Figure 3A (a)) and the glass as cast (Figure 3B (d)) contained reflection peaks of Si-O-Si bending mode (~450 cm^{-1}), the Si-O···alkali ion bond (~910 cm^{-1}) and the Si-O-Si network stretch (~1040 cm^{-1}).[13,14] After 1 week in SBF (Figures 3 (b) and (e)) the Si-O···alkali ion bond (~910 cm^{-1}) was much less prominent, indicating that the alkali ions were partially leached out of the glass.[15] The P=O stretching mode was present at ~1100 cm^{-1}. The absence of the peaks of P-O bending mode at ~520, ~ 555, and ~605 cm^{-1} indicated that this is an amorphous phosphate.[10] After 4 weeks in SBF (Figures 3 (c) and (f)) three bands of P-O bend (at ~520 cm^{-1} that appears as a shoulder of the peak at ~555 cm^{-1}, ~555 cm^{-1} and ~600 cm^{-1}) and of P-O stretch (~1050 and ~1100 cm^{-1}) indicated the presence of a crystalline phosphate consistent with apatite.[10,13,16] In Figures 3 (c) and (f) the very small peaks at ~840 cm^{-1} could be from the C-O stretching mode of a carbonated group as in carbonated apatite.[10] SEM analysis of the FGC and glass 6P55 as cast after 4 weeks in SBF showed the morphology typical of HA (Figures 4A and B respectively). Glancing angle XRD confirmed the presence of

HA on FGC (Figure 5).[12] The broad peaks indicate small crystallite size.[17] The XRD pattern of 6P55 as cast was similar (data not shown)

Discussion

The use of functionally graded bioactive coatings on titanium alloy may offer a more reproducible and reliable alternative to other coating techniques. In previous work the cytocompatibility of glass 6P55 was tested with an established *in vitro* bone model.[11] The results prompted the fabrication and study of functionally graded coatings using the same glass as the surface coating. In this work the effect of the fabrication process on the microstructure and *in vitro* bioactivity in simulated body fluid was evaluated. Functionally graded coatings with different compositions have been studied previously, and, in each case, partial crystallization of the coating was reported.[5] SEM microstructural analysis and X-ray diffraction of glass 6P55 as cast indicated that the glass was amorphous prior to the coating fabrication process. The enameling process caused the glass to partially crystallize, as expected. XRD analysis identified the crystalline phases as being mainly sodium calcium phosphate and calcium magnesium silicate. The amount of crystallinity in the coatings was previously reported as being about 5 vol%.[5] In this study we fabricated FGC with different compositions and we found that on average 6% of the coatings' surface was crystalline. This finding confirms that the fabrication process consistently causes limited crystallization. There was no major difference in reactivity in SBF over a one month period between the amorphous glass and the partially crystalline coating. After one week in SBF amorphous calcium phosphate formed on the surface of all samples and over the following 3 weeks it crystallized into an apatite-like mineral identified by XRD and SEM. The presence of

crystalline phases tends to slow the reactions in SBF.[18,19] We studied the reactivity of the glasses using an arbitrarily fixed surface area/volume ratio (0.56 cm^{-1}) and exchanged the fluid at weekly intervals. Both factors are known to affect the rate of reaction[20] and may not have allowed discrimination of differences in reactivity between the amorphous glass and the partially crystalline one in this study.

Conclusions

The coatings prepared for this study were reproducible and remained bioactive. These bioactive coatings could potentially be used as implant materials. The current results suggest that the FGC approach shows considerable promise and that further evaluations of the cytocompatibility of the coatings should be undertaken as the next logical step in their development.

Acknowledgements

The authors would like to thank Larry Watanabe and Grace Nonomura for their help with sample preparation, and the National Institutes of Health/National Institute of Dental and Craniofacial Research for support through grant R01DE11289.

References

1. Hayashi K, Matsuguchi N, Uenoyama K, Kanemaru T, Sugioka Y. Evaluation of metal implants coated with several types of ceramics as biomaterials. J Biomed Mater Res 1989;23(11):1247-59.
2. Lacefield WR. Hydroxylapatite coatings. In: Hench LL and Wilson J, editor. An introduction to bioceramics. Singapore: World Scientific; 1993. p 223-238.
3. van Dijk K, Schaeken HG, Wolke JG, Jansen JA. Influence of annealing temperature on RF magnetron sputtered calcium phosphate coatings. Biomaterials 1996;17(4):405-10.
4. Choi JM, Kim HE, Lee IS. Ion-beam-assisted deposition (IBAD) of hydroxyapatite coating layer on Ti-based metal substrate. Biomaterials 2000;21(5):469-73.
5. Gomez-Vega JM, Saiz E, Tomsia AP. Glass-based coatings for titanium implant alloys. J Biomed Mater Res 1999;46(4):549-59.
6. Gomez-Vega JM, Saiz E, Tomsia AP, Marshall GW, Marshall SJ. Bioactive glass coatings with hydroxyapatite and Bioglass particles on Ti-based implants. 1. Processing. Biomaterials 2000;21(2):105-11.
7. Kokubo T. Bioactive glass ceramics: properties and applications. Biomaterials 1991;12(2):155-63.
8. Hench LL. Bioceramics: from concept to clinic. J Am Ceram Soc 1991;74:1487-1510.
9. Kokubo T, Kushitani H, Sakka S, Kitsugi T, Yamamuro T. Solutions able to reproduce in vivo surface-structure changes in bioactive glass-ceramic A-W. J Biomed Mater Res 1990;24(6):721-34.
10. Filgueiras MR, LaTorre G, Hench LL. Solution effects on the surface reactions of three bioactive glass compositions. J Biomed Mater Res 1993;27(12):1485-93.
11. Foppiano S, Marshall SJ, Marshall GW, Saiz E, Tomsia AP. The influence of novel bioactive glasses on in vitro osteoblast behavior. J Biomed Mater Res 2004;71A(2):242-249.
12. Elliott JC. Appendix: Calculated X-ray diffraction patterns of the calcium orthophosphates. In: Elliott JC, editor. Structure and chemistry of the apatites and other calcium orthophosphates. Amsterdam: Elsevier Science; 1994.
13. Ohgushi H, Dohi Y, Yoshikawa T, Tamai S, Tabata S, Okunaga K, Shibuya T. Osteogenic differentiation of cultured marrow stromal stem cells on the surface of bioactive glass ceramics. J Biomed Mater Res 1996;32(3):341-8.
14. Jones JR, Sepulveda P, Hench LL. Dose-dependent behavior of bioactive glass dissolution. J Biomed Mater Res 2001;58(6):720-6.
15. Hench LL andAndersson O. Bioactive glasses. In: Hench LL and Wilson J, editor. An introduction to bioceramics. Singapore: World Scientific; 1993. p 41-62.
16. el-Ghannam A, Ducheyne P, Shapiro IM. Formation of surface reaction products on bioactive glass and their effects on the expression of the osteoblastic phenotype and the deposition of mineralized extracellular matrix. Biomaterials 1997;18(4):295-303.

17. LeGeros RZ, LeGeros JP. Dense Hydroxyapatite. In: Hench LL and Wlson J editor. An introduction to bioceramics. Singapore: World Scientific; 1993. p 139-180.
18. Zhang Q, Chen J, Feng J, Cao Y, Deng C, Zhang X. Dissolution and mineralization behaviors of HA coatings. Biomaterials 2003;24(26):4741-8.
19. Shi D, Jiang G, Bauer J. The effect of structural characteristics on the in vitro bioactivity of hydroxyapatite. J Biomed Mater Res 2002;63(1):71-8.
20. Radin S, Ducheyne P, Falaize S, Hammond A. In vitro transformation of bioactive glass granules into Ca-P shells. J Biomed Mater Res 2000;49(2):264-72.

Tables

Table 1. Glass compositions in weight %

	SiO_2	Na_2O	K_2O	CaO	MgO	P_2O_5
6P61	61.1	10.3	2.8	12.6	8.9	6.0
6P55	54.5	12.0	4.0	15.0	8.5	6.0

Table 2. Ion concentration (in di H_2O) of SBF (mM)

	Ion concentration (mM)						
	Na^+	K^+	Ca^{2+}	Mg^{2+}	Cl^-	HCO_3^-	HPO_4^{2-}
SBF	142	5	2.05	1.5	148	4.2	1

Figures and captions

Figure 1

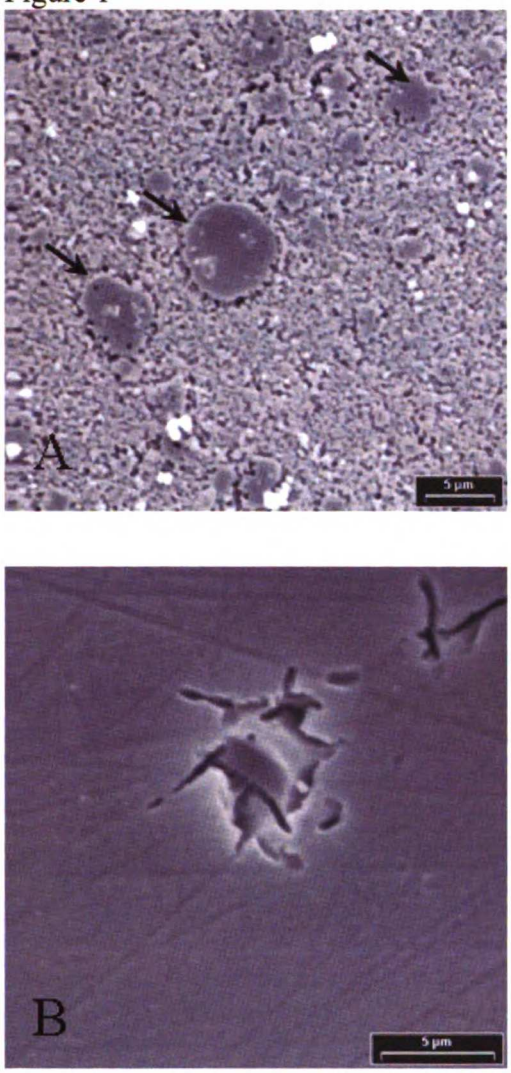

Figure 1: SEM image of the functionally graded coating after etching (A). Round separated phases are present (black arrows). Glass as cast shows intrinsic irregularities but no phase separation (B).

Figure 2

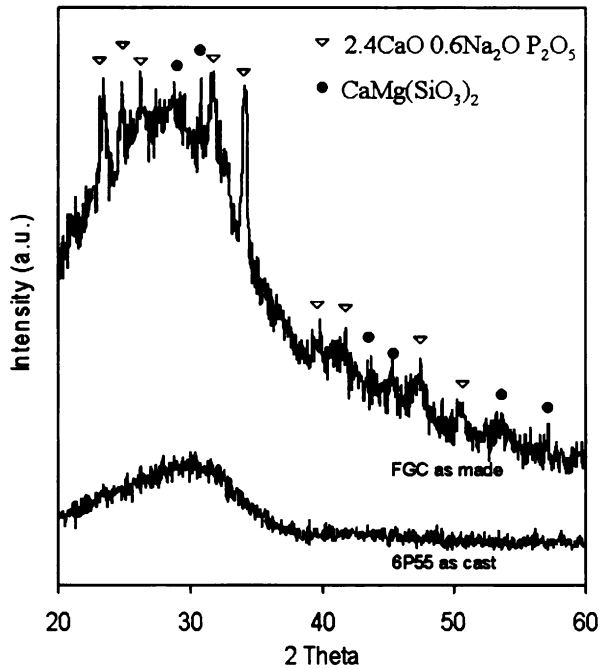

Figure 2: Glancing angle x-ray diffraction pattern of FGC as fabricated and glass 6P55 as cast. Partial crystallization occurred only on the surface of the coating, glass as cast is amorphous.

Figure 3

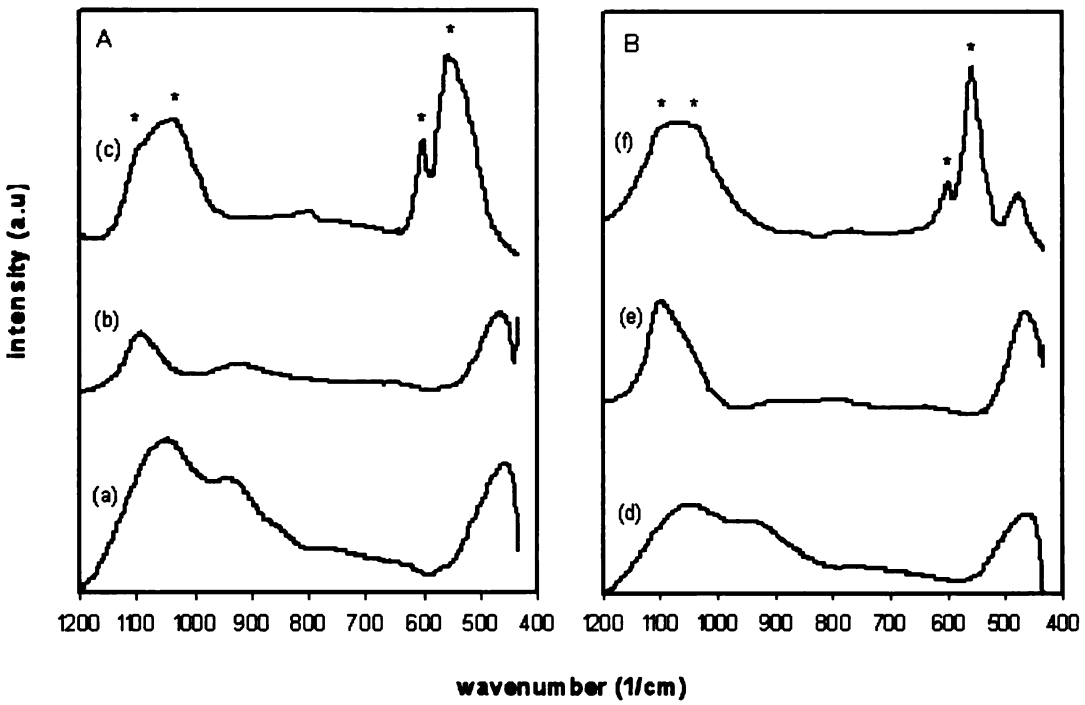

Figure 3: FTIR of FGC (A) and glass 6P55 as cast (B) as made (a and d), after 1 week in SBF (b and e), and after 4 weeks in SBF (c and f). Peaks associated with hydroxyapatite are indicated by *.

Figure 4

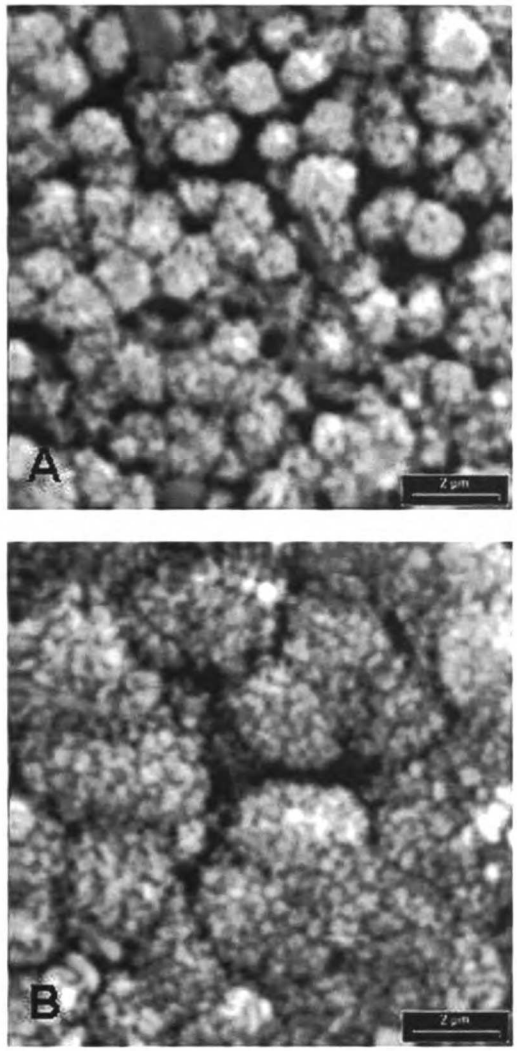

Figure 4: SEM images of the surface of FGC (A) and glass 6P55 as cast (B) after immersion for 4 weeks in SBF. Both surfaces present the typical morphology of hydroxyapatite.

Figure 5

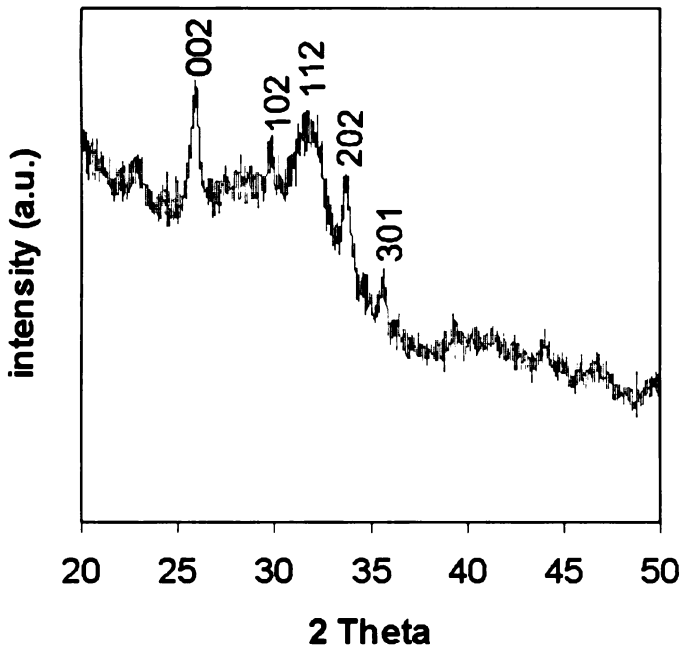

Figure 5: Glancing angle x-ray diffraction pattern of FGC after immersion for 4 weeks in SBF. The marked peaks correspond to hydroxyapatite. The peaks are broad, indicating small crystallite size.

Chapter 4

Functionally graded bioactive coatings: Reproducibility of fabrication process and stability of the coating under cell culture conditions

Abstract

We recently developed functionally graded bioactive glass coatings (FGC) that reliably adhere to titanium alloy (Ti6Al4V). Ti6Al4V coated in such way could potentially be used as a load bearing implant material. This paper had two goals: assessing the reproducibility of functionally graded coatings (FGC) fabricated by the enameling process and determining whether cell culture conditions undermine the integrity of the coating. Bioactive glasses react differently in protein containing simulated body fluid (SBF) than in SBF alone. Furthermore, studies using dynamic immersion in protein containing solutions have shown that bioactive glass particles are undermined and this may correspond to delamination of coatings. Thus studying these materials under cell culture conditions is important.

The reproducibility of the fabrication process was assessed by measuring the thickness and crystallinity of coatings from three different batches using glancing angle x-ray diffraction (XRD) and scanning electron microscopy (SEM). MC3T3-E1.4 mouse pre-osteoblast cells were cultured and induced to mineralize, on FGCs, either as made or pre-conditioned in simulated body fluid (SBF). Sample surfaces were analyzed by XRD, Fourier Transform Infrared Spectroscopy (FTIR), and SEM prior to cell culture. FGCs as made were glassy with partial crystallization (average 6 vol%). The coating fabrication process yielded reproducible samples. Pre-conditioning caused formation of a crystalline phosphate on the surface. After cell culture, samples were exposed to low vacuum to verify the integrity of the coating. FGCs as made were suitable substrata for cell culture, but the glass silica network below the reacted surface was compromised. Pre-conditioning in SBF prevented sub surface silica network dissolution and stabilized the

coatings. Incubation in SBF is recommended prior to *in vitro* and *in vivo* testing to provide a stable coating.

Introduction

Implants for load bearing orthopedic or dental applications, face the dual challenge of osteointegration while withstanding complex forces. Bioinert metal alloys (Ti6Al4V, Co-Cr and others) have been used as implant materials because they can support loads while provoking only minor reactions in the body.[1-5] The degree of the reactions can vary depending not only on intrinsic properties of bioinert materials but also on the site of implantation, degree of trauma and implant fit.[6,7] Bioactive materials, that elicit formation of normal tissue and form a direct bond with bone, have been extensively investigated to improve osteointegration.[7] Glasses of specific compositions such as Bioglass®, and calcium phosphate-containing materials such as hydroxyapatite (HA) can provide the desired bioactivity but cannot withstand loads.[8] A bioactive material coating on a bioinert metal alloy may allow osteointegration and load-bearing capabilities. Several different techniques have been developed and/or applied to yield such coatings, with plasma sprayed HA being the most common and currently used to fabricate commercially available implants.[9,10] Plasma sprayed HA does not retain its original characteristics and yields non reliable coatings prone to delamination.[11,12] Bioglass® can not be used to fabricate FGCs because of its coefficient of thermal expansion (CTE) mismatch with Ti6Al4V and high crystallization upon firing.[13,14] Functionally graded coatings (FGC) of bioactive glasses on titanium alloy that retain bioactivity after the fabrication process[14,15] have the potential for use as load bearing implants. The surface reactions occurring on bioactive glasses have been studied extensively.[16-19] An important

property of Bioglass® and other bioactive glasses is the reactivity when exposed to simulated body fluid. Initial reactions involve the exchange of alkali ion with hydronium ion (H_3O^+ or H^+). This causes a rise in pH in the immediate environment.[5] Frequently bioactive glasses are preconditioned in SBF or other solutions to initiate the surface reactions and avoid the rise in pH during the assessment of cytocompatibility and osteogenic potential.[20-25] There is a significant difference in the reaction kinetics leading to the formation of apatite, depending on the presence or absence of proteins in the "conditioning" solution. *In vivo* and *in vitro* the presence of proteins, combined with periodic solution exchange, appears to cause a delay in apatite formation prolonging the dissolution of Si species.[25-28] A proposed mechanism involves the absorption of proteins within the surface silica-gel reaction layer, and its consequent increased permeability. This would allow further release of Si and delay apatite formation.[25,28] When bioactive glass powder was used this resulted in excavation of the particles, yielding hollow Ca P-rich shells.[29] The sub-surface silica network degradation that occurred in the excavated particles suggests that bioactive glass coatings may undergo a similar degradation that could result in delamination. Evidence indicates that glass silica network dissolution occurs also in absence of proteins.[30] *In vitro* experiments showed that in the absence of proteins the subsurface silica dissolution is significantly slowed down by a calcium phosphate-rich reaction layer which forms on the surface.[25,28] The presence of proteins always allowed higher rates of silica dissolution regardless of the mode of immersion (static vs. dynamic).[29] In this study, the hypothesis that the integrity of the coatings may be compromised by cell culture conditions was tested using mouse pre-osteoblastic cells (MC3T3-E1.4) culture on FGC with or without pre-conditioning in SBF. The cell line

chosen for this study is a well established *in vitro* bone model.[31-36] Cell culture conditions consist of both the presence of proteins (fetal bovine serum) as well as the periodic exchange of solution. To evaluate the possible 'excavation' below the coating surface we applied suction (low vacuum) to identify the weakest interface. As a basic requirement prior to any further investigation we also assessed the reproducibility of the fabrication process. This was evaluated by determining possible batch to batch coating thickness and microstructure variability. The objective of this work was to provide a basic protocol for treatment of functionally graded coatings prior to *in vivo* evaluation.

Materials and Methods

Glass and coating fabrication

Glasses in the SiO_2-Na_2O-K_2O-CaO-MgO-P_2O_5 system were prepared by mixing the reagents in propanol using a high speed stirrer for 1 hour and drying at 80°C for 12 hours as previously described.[14] Table 1 gives the glass compositions by weight %. Reagents: SiO_2 (99.5% Cerac Inc., Milwakee, WI), $CaCO_3$ (99.9%, J.T. Baker, Phillipsburg, NJ), MgO (98.6%, J.T. Baker, Phillipsburg, NJ), K_2CO_3 (99.4 % Mallinkratt, Paris, KY), $NaHCO_3$ (99.5% J.T. Baker, Phillipsburg, NJ), and Na_2HPO_4 (99% Sigma, St. Louis, MO). The mixture was dried and fired in air in a Pt crucible for 5 hours at 1400 °C (glass 6P55) or 1450 °C (glass 6P61). The melt was cast in a pre-heated (200°C) graphite mold yielding glass bars (~2 x 2 x 8 cm). Functionally graded coatings were prepared as previously described.[14] Briefly, the glasses (6P61 and 6P55) were separately milled in a planetary agate mill. Titanium alloy (Ti6Al4V, Goodfellow Ltd., Huntingdon, UK) was cut into plates (1.5 x 1.5 x 0.1 cm) with a low speed diamond saw (Isomet, Buehler Ltd., Lake Bluff, IL) and metallographically polished to a 1 μm finish with diamond

suspension (Buehler Ltd., Lake Bluff, IL). Ti6Al4V was cleaned by ultrasonication with ethanol and acetone for 10 minutes each. Glass 6P61 offers a good coefficient of thermal expansion (CTE) match with Ti6Al4V (CTE_{6P61}=10.2 $CTE_{Ti6Al4V}$=9.1-9.8 (10^{-6} $°C^{-1}$)).[15] A suspension of its powders (particle size < 37 μm) in 100% ethanol was deposited on Ti6Al4V prepared as described above. Glass particles were allowed to settle and the process was carefully repeated using glass 6P55, avoiding disturbance of the first layer of glass 6P61 powder. After drying in air at 80 °C for 48 hours the green coatings were fired in air in a dental furnace (Unitek Ultra Mat II, 3M, Maplewood, MN). The furnace was pre-heated at 640 °C; the firing temperature of 800 °C was reached (heating ramp of 40 °C/min) while the furnace was evacuated to 0.1 atm. At 800 °C air was let into the firing chamber. Samples were fired for 10 sec in air at 1 atm and quenched.

Reproducibility of the fabrication process: microstructure and thickness of coatings

The crystallinity of the coating was assessed by glancing angle x-ray diffraction (XRD) (Siemens D5000, Siemens, Munich, Germany). The surfaces of the FGCs were etched with a solution of HNO_3:HF:H_2O (5:5:90 vol%) for 10 seconds, sputter-coated and analyzed by scanning electron microscopy (SEM) (TOPCON ISI SX 40A scanning electron microscope, Milpitas, CA U.S.A. and S-4300SE/N Schottky Hitachi emission scanning electron microscopy High-Technologies America, Inc. Pleasanton, CA), to visualize the underlying structure. To quantify the amount of crystallinity the crystallized surface area was measured from 3 different samples (9 pictures /sample) using image analysis software (Sigma AIA2 Analysis, Noran, Madison, WI). FGCs as made and not etched were analyzed by SEM for comparison to etched samples. To measure the coating thickness FGCs were embedded in epoxy resin, cross sectioned and metallographically

polished to 1 μm. Embedded samples were cleaned by sonication in acetone, and analyzed by SEM. The coating thickness was measured by image analysis (N=3) (Sigma AIA2 Analysis, Noran, Madison, WI). All experiments were performed on one sample from each of three separate batches made on different days to assess the reproducibility of the fabrication process.

Coating stability in the presence of MC3T3-E1.4 mouse pre-osteoblastic cells

FGCs were either pre-conditioned in SBF or used as made. Prior to cell culture the surfaces were analyzed by Fourier Transform Infrared Spectroscopy (FTIR) (Laser Precision Analytical, Laser Precision Corp., Irvine, CA), glancing angle XRD and SEM to assess differences in surface composition and crystallinity. SBF was prepared by adding the appropriate amounts of salts to deionized water to reach the concentrations reported in Table 2. Preconditioning was carried out for 2 weeks at 37 °C, exchanging the solution after the first week to provide an apatite-like surface. The surface area to volume of SBF solution ratio, was fixed at 0.56 cm^{-1}. FGCs were sterilized at 250 °C for 1 hour and placed in 12 well tissue culture plates under sterile conditions. MC3T3-E1.4 mouse pre-osteoblast cells were cultured in an incubator at 37°C and 5% CO_2 atmosphere, in α-modified Eagle's medium (α-MEM), supplemented with 10% fetal bovine serum (FBS) and 1% antibiotics (penicillin and streptomycin) and passaged every 4-5 days. In all experiments cells were plated at an initial density of 50,000 cells/cm^2 and the media was replaced at 2 day intervals. Experiments were carried out for 20 days, providing cells with ascorbic acid (AA) treatment (50 μg/mL medium) for 10 days, and then with AA and inorganic phosphate (NaH_2PO_4) (10 mM) for an additional 10 days to induce mineralization. Cells were rinsed with phosphate buffered saline (PBS), fixed

with 4% paraformaldehyde (20 min) and exposed to low vacuum (≤80 millitorr) in a vacuum chamber (Hummer VII, Anatech Ltd., Alexandria, VA). Samples were sputter coated for SEM analysis.

Results

Reproducibility of the fabrication process: Coating microstructure and thickness

SEM analysis of the coating surfaces (Figure 1A) shows the presence of microcracks. Otherwise the samples were smooth. Etching (Figure 1B), clearly revealed round separated phases. XRD analysis showed that the fabrication process caused partial crystallization as previously reported (manuscript in preparation).[14] The crystalline phases were consistent from batch to batch and were identified as being sodium calcium phosphate (2.4 CaO 0.6 Na_2O P_2O_5) and calcium magnesium silicate($CaMg(SiO_3)_2$) (Figure 2). The average crystallization from the three samples was 5.9±3.0 vol%. Figure 3 is an SEM image of the cross section of a coating. The average coating thickness measured from 3 different samples was 86.0±11.5 μm. The coating was devoid of internal porosity, and the superficial microcracks did not propagate to the surface of Ti6Al4V.

Coating surface analysis before and after pre-conditioning in SBF

Results from FTIR analysis of FGC before and after immersion in SBF are in Figure 4. FTIR analysis of FGC as made shows the reflection peaks of the Si-O-Si bending mode (~450 cm^{-1}), the Si-O···alkali ion bond (~910 cm^{-1}) and the Si-O-Si network stretch (~1040 cm^{-1})[37,38] typical of the unreacted glass (A in Figure 4). After the immersion sequence in SBF (B in Figure 4) Si-O-Si network stretch (~1040 cm^{-1}) is no longer visible and the Si-O···alkali ion bond (~910 cm^{-1}) is much less prominent, indicating that

the alkali ions were partially leached out of the glass surface. The P=O stretching mode is present at ~1100 cm^{-1}. The presence of the peaks of P-O bending mode at ~520 cm^{-1}, and ~ 555 cm^{-1} (which appears as a shoulder of the peak at 520 cm^{-1}) indicates the presence of a crystalline phosphate.[39-41] Other small unidentified peaks are present. XRD analysis of the FGCs before immersion in SBF indicates the presence of crystalline phases as described above (and Figure 5(1)). After pre-conditioning the peaks corresponding to the crystalline phases are lower in intensity (Figure 5(2)) but no HA peaks are yet clearly visible. SEM analysis indicates changes in surface morphology due to the reactions after pre-conditioning (Figure 6 and Figure 1A).

Coating stability in the presence of MC3T3-E1.4 mouse pre-osteoblastic cells

MC3T3-E1.4 osteoblast-like cells cultured on FGCs not pre-conditioned in SBF and induced to mineralize reached confluence and mineralized as assayed by alizarin S staining (data not shown). Under vacuum treatment the cell layer and a superficial layer of reacted glass peeled off the surface (Figure 7). In Figure 7A the SEM image shows the detached cell layer/reacted glass; the plane of focus (*) shows the confluent cells. In Figure 7B the light globular features are the crystalline phases that were formed during the coating fabrication process. The interface between crystalline phases and matrix reacted, and during vacuum treatment, the round crystals were subsequently loosened from the glassy matrix. The side view of the peeled layer (Figure 7C) clearly shows the thickness of the reacted glass (black double arrow), the original FGC-cells interface (white dotted line) and the thickness of the cultured tissue (white double arrow). Refer to Figure 7A for orientation. In Figure 7D in which the plane of focus (*) indicates the surface of the coating below the reacted glass, the separated phases are clearly visible. In

Figure 7E a gap between the crystalline phases and the surrounding matrix (black arrow) is visible; this is probably due to corrosion in the tissue culture fluids. The black arrowheads indicate the voids left by the crystalline phases that were loosened from the matrix during the sub-surface reaction as in Figure 7B. Figure 7F (2) is the EDS analysis of the area below the reacted glass shown in Figure 7E. It indicates the presence of abundant Si, low amounts of Ca and P relative to silicon, and amounts of K, Na and Mg, consistent with the glass components. Figure 7F (1) shows the SEM-EDS analysis of the glass involved in reactions just below the cell layer shown in Figure 7C. It shows that the reacted layer contained mainly P and Ca and little Si. This is consistent with the ongoing transformation of the surface into a calcium phosphate layer in the presence of proteins found under cell culture conditions. Figure 8 shows SEM images of MC3T3-E1.4 osteoblast-like cells cultured on the FGC pre-conditioned in SBF. Cells were confluent and bone nodule-like three dimensional features were present (Figure 8 black arrowheads). Some areas of the tissue layer cracked, on applying vacuum, but there was no separation of the layer.

Discussion

The functionally graded bioactive glass coatings evaluated in this study have been shown to reliably adhere on titanium alloy.[14,15] It is important to assess the reproducibility of the fabrication process and determine what surface treatment should be performed to promote the stability of the coatings prior to their further assessment. We found that the fabrication process was reproducible and yielded coating thickness values in agreement with a previous report.[15] The fabrication process resulted in a small amount of crystallization, which averaged 5.9±3.0 vol% . The crystalline phases were consistent

from batch to batch, and the coatings thickness was within a narrow range (75-97 μm). The amount of crystallization did not hinder *in vitro* bioactivity in SBF. The microcracks present on the coating surfaces were probably due to thermal stresses on the glass 6P55 surface which is expected to be under tension. The cracks never crossed through the glass coating to reach the titanium substrate and did not cause delamination. It is possible that the presence of crystalline phases slows or arrests crack propagation.[42] Bioactive glasses offer a dynamic surface that reacts in the presence of fluids. These materials are often pre-conditioned in SBF or protein containing solutions before cytocompatibility assays to avoid the initial pH increase occurring at the initial stages of glass reactions.[20-25] The parameters of the conditioning solution significantly affect the surface reactions leading to the formation of a Ca P-rich layer and ultimately HA. Both the presence of proteins and dynamic immersion better simulate *in vivo* conditions.[29] We chose cell culture conditions because they encompass both presence of proteins and solution exchange. Proteins slow down apatite formation and their presence in the Ca P-rich layer makes it permeable to fluids, resulting in prolonged leaching of Si (silicic acid).[25] This leaching results in excavation of bioactive glass powders. Conversely, the Ca P-rich layer formed in the absence of proteins (e.g. in SBF) had different permeability properties which subsequently protected the structure of the underlying glass network from complete dissolution.[25,29]

To determine whether preconditioning in SBF is a necessary step to provide a stable substrata for osteoblast-like cell culture, we compared the behavior of FGC as made, versus FGC preconditioned in SBF. We expected the surface of the not-conditioned FGC to react similarly to Bioglass® in the presence of proteins under dynamic conditions and

to show prolonged subsurface silica network degradation. For Bioglass® powder this can be identified as the glass particles are easily fractured and result in hollow shells. In this study a similar subsurface silica network degradation for the coatings became obvious when a low vacuum was applied. The Ca P rich surface layer separated from the underlying glass at the weak interface created by the degradation of the silica network. Again, similarly to Bioglass®, the preconditioned samples did not show this effect. After preconditioning all the interfaces present in the sample were strong enough to resist applied vacuum. This suggests that the initial crystalline phosphate layer formed in the absence of proteins was not as permeable and protected the inner layers of the coating from fast reaction. Thus, the reactions in the coatings were similar to those in other studies,[25] with minor differences due to the geometry of the samples. The FGCs examined in this study appeared to react more slowly than Bioglass® powders, possibly due to the following reasons: 1) lower ratio surface/volume for the FGC's flat surface compared to particles, 2) higher silica content of the FGC (about 10 wt% more than in Bioglass®) and 3) partial crystallization of the coating. Preconditioning in SBF caused surface modifications that provided a protective layer, slowing down the degradation of the sub-surface silica network. Silica network dissolution occurs at a slower rate in SBF than in protein containing solutions.[29] We can predict that if the reaction front was to reach glass 6P61, silica dissolution rate would be further slowed down because of the high silica content of this glass. Preconditioning in SBF may have additional beneficial effects such as: 1) removal of potential contaminants introduced by the fabrication process and 2) formation of an apatite-like biomimetic surface, improving biocompatibility. MC3T3-E1.4 mouse pre-osteoblastic cells reached confluence and

mineralized on both preconditioned and unconditioned FGCs but in the latter case cell culture conditions undermined the structure of the coating. More detailed cellular response to functionally graded coatings of the same composition used for this study is the focus of current investigation.

Conclusions

Functionally graded bioactive glass coatings on Ti6Al4V alloy fabricated by the enameling technique were reproducible. The FGCs were suitable substrata for cell culture without any prior surface modification. Nevertheless, the surface reactions occurring under cell culture conditions allowed prolonged sub-surface fluid exchange that could compromise the coating integrity. Preconditioning of the FGCs in SBF is recommended in order to make the surface Ca P-rich, with a somewhat protective effect on the underlying glass and ultimately preserving the integrity of the coating. This may be particularly important when the glass is partially crystalline, where the differential dissolution rate between glassy matrix and crystalline phases may widen that interface providing a preferential route for fluid exchange. Cytocompatibility assessment of pre-conditioned FGCs is currently under investigation.

Acknowledgements

The authors would like to thank Larry Watanabe for his help with SEM imaging, Mondhipa Ratnarathorn for helpful discussion and editing, and Dr. Pamela DenBesten for allowing the use of her facilities and the National Institutes of Health/National Institute of Dental and Craniofacial Research for support through grant R01DE11289.

References

1. Glantz PO, Bjorlin G, Sundstrom B. Tissue reactions to some dental implant materials. An in vivo study in white rats. Odontol Revy 1975;26(3):231-8.
2. Castleman LS, Motzkin SM, Alicandri FP, Bonawit VL. Biocompatibility of nitinol alloy as an implant material. J Biomed Mater Res 1976;10(5):695-731.
3. Levine DL, Staehle RW. Crevice corrosion in orthopedic implant metals. J Biomed Mater Res 1977;11(4):553-61.
4. Shettlemore MG, Bundy KJ. Toxicity measurement of orthopedic implant alloy degradation products using a bioluminescent bacterial assay. J Biomed Mater Res 1999;45(4):395-403.
5. Hench LL Anderson O. Bioactive glasses. In: Hench LL and Wilson J, editor. An introduction to bioceramics. Singapore: World Scientific; 1993. p 41-62.
6. Jaffin RA, Berman CL. The excessive loss of Branemark fixtures in type IV bone: a 5-year analysis. J Periodontol 1991;62(1):2-4.
7. LeGeros RZ, Craig RG. Strategies to affect bone remodeling: osteointegration. J Bone Miner Res 1993;8 Suppl 2:S583-96.
8. LeGeros RZ, LeGeros J. P. Dense Hydroxyapatite. In: Hench LL and Wilson J, editor. An introduction to bioceramics. Singapore: World Scientific; 1993. p 139-180.
9. Ducheyne P, Radin S, Heughebaert M, Heughebaert JC. Calcium phosphate ceramic coatings on porous titanium: effect of structure and composition on electrophoretic deposition, vacuum sintering and in vitro dissolution. Biomaterials 1990;11(4):244-54.
10. Lacefield WR. Hydroxylapatite coatings. In: Hench LL and Wilson J, editor. An introduction to bioceramics. Singapore: World Scientific; 1993. p 223-238.
11. Bloebaum RD, Bachus KN, Rubman MH, Dorr LD. Postmortem comparative analysis of titanium and hydroxyapatite porous- coated femoral implants retrieved from the same patient. A case study. J Arthroplasty 1993;8(2):203-11.
12. Chang YL, Lew D, Park JB, Keller JC. Biomechanical and morphometric analysis of hydroxyapatite-coated implants with varying crystallinity. J Oral Maxillofac Surg 1999;57(9):1096-108; discussion 1108-9.
13. Filgueiras MR, LaTorre G, Hench LL. Solution effects on the surface reactions of three bioactive glass compositions. J Biomed Mater Res 1993;27(12):1485-93.
14. Gomez-Vega JM, Saiz E, Tomsia AP. Glass-based coatings for titanium implant alloys. J Biomed Mater Res 1999;46(4):549-59.
15. Gomez-Vega JM, Saiz E, Tomsia AP, Marshall GW, Marshall SJ. Bioactive glass coatings with hydroxyapatite and Bioglass particles on Ti-based implants. 1. Processing. Biomaterials 2000;21(2):105-11.
16. Kokubo T, Ito S, Huang ZT, Hayashi T, Sakka S, Kitsugi T, Yamamuro T. Ca,P-rich layer formed on high-strength bioactive glass-ceramic A-W. J Biomed Mater Res 1990;24(3):331-43.
17. Radin SR, Ducheyne P. The effect of calcium phosphate ceramic composition and structure on in vitro behavior. II. Precipitation. J Biomed Mater Res 1993;27(1):35-45.

18. Ducheyne P, Radin S, King L. The effect of calcium phosphate ceramic composition and structure on in vitro behavior. I. Dissolution. J Biomed Mater Res 1993;27(1):25-34.
19. Radin SR, Ducheyne P. Effect of bioactive ceramic composition and structure on in vitro behavior. III. Porous versus dense ceramics. J Biomed Mater Res 1994;28(11):1303-9.
20. Ducheyne P, el-Ghannam A, Shapiro I. Effect of bioactive glass templates on osteoblast proliferation and in vitro synthesis of bone-like tissue. J Cell Biochem 1994;56(2):162-7.
21. el-Ghannam A, Ducheyne P, Shapiro IM. Bioactive material template for in vitro synthesis of bone. J Biomed Mater Res 1995;29(3):359-70.
22. Garcia AJ, Ducheyne P, Boettiger D. Effect of surface reaction stage on fibronectin-mediated adhesion of osteoblast-like cells to bioactive glass. J Biomed Mater Res 1998;40(1):48-56.
23. Xynos ID, Hukkanen MV, Batten JJ, Buttery LD, Hench LL, Polak JM. Bioglass 45S5 stimulates osteoblast turnover and enhances bone formation In vitro: implications and applications for bone tissue engineering. Calcif Tissue Int 2000;67(4):321-9.
24. Silver IA, Deas J, Erecinska M. Interactions of bioactive glasses with osteoblasts in vitro: effects of 45S5 Bioglass, and 58S and 77S bioactive glasses on metabolism, intracellular ion concentrations and cell viability. Biomaterials 2001;22(2):175-85.
25. Sepulveda P, Jones JR, Hench LL. In vitro dissolution of melt-derived 45S5 and sol-gel derived 58S bioactive glasses. J Biomed Mater Res 2002;61(2):301-11.
26. Schepers E, de Clercq M, Ducheyne P, Kempeneers R. Bioactive glass particulate material as a filler for bone lesions. J Oral Rehabil 1991;18(5):439-52.
27. Schepers EJ, Ducheyne P. Bioactive glass particles of narrow size range for the treatment of oral bone defects: a 1-24 month experiment with several materials and particle sizes and size ranges. J Oral Rehabil 1997;24(3):171-81.
28. Radin S, Ducheyne P, Rothman B, Conti A. The effect of in vitro modeling conditions on the surface reactions of bioactive glass. J Biomed Mater Res 1997;37(3):363-75.
29. Radin S, Ducheyne P, Falaize S, Hammond A. In vitro transformation of bioactive glass granules into Ca-P shells. J Biomed Mater Res 2000;49(2):264-72.
30. Saiz E, Goldman M, Gomez-Vega JM, Tomsia AP, Marshall GW, Marshall SJ. In vitro behavior of silicate glass coatings on Ti6A14V. Biomaterials 2002;23(17):3749-56.
31. Sudo H, Kodama HA, Amagai Y, Yamamoto S, Kasai S. In vitro differentiation and calcification in a new clonal osteogenic cell line derived from newborn mouse calvaria. J Cell Biol 1983;96(1):191-8.
32. Quarles LD, Yohay DA, Lever LW, Caton R, Wenstrup RJ. Distinct proliferative and differentiated stages of murine MC3T3-E1 cells in culture: an in vitro model of osteoblast development. J Bone Miner Res 1992;7(6):683-92.
33. Franceschi RT, Iyer BS. Relationship between collagen synthesis and expression of the osteoblast phenotype in MC3T3-E1 cells. J Bone Miner Res 1992;7(2):235-46.

34. Franceschi RT, Iyer BS, Cui Y. Effects of ascorbic acid on collagen matrix formation and osteoblast differentiation in murine MC3T3-E1 cells. J Bone Miner Res 1994;9(6):843-54.
35. Leis HJ, Hulla W, Gruber R, Huber E, Zach D, Gleispach H, Windischhofer W. Phenotypic heterogeneity of osteoblast-like MC3T3-E1 cells: changes of bradykinin-induced prostaglandin E2 production during osteoblast maturation. J Bone Miner Res 1997;12(4):541-51.
36. Wang D, Christensen K, Chawla K, Xiao G, Krebsbach PH, Franceschi RT. Isolation and characterization of MC3T3-E1 preosteoblast subclones with distinct in vitro and in vivo differentiation/mineralization potential. J Bone Miner Res 1999;14(6):893-903.
37. Ohgushi H, Dohi Y, Yoshikawa T, Tamai S, Tabata S, Okunaga K, Shibuya T. Osteogenic differentiation of cultured marrow stromal stem cells on the surface of bioactive glass ceramics. J Biomed Mater Res 1996;32(3):341-8.
38. Jones JR, Sepulveda P, Hench LL. Dose-dependent behavior of bioactive glass dissolution. J Biomed Mater Res 2001;58(6):720-6.
39. el-Ghannam A, Ducheyne P, Shapiro IM. Formation of surface reaction products on bioactive glass and their effects on the expression of the osteoblastic phenotype and the deposition of mineralized extracellular matrix. Biomaterials 1997;18(4):295-303.
40. Ohgushi H, Dohi Y, Yoshikawa T, Tamai S, Tabata S, Okunaga K, Shibuya T. Osteogenic differentiation of cultured marrow stromal stem cells on the surface of bioactive glass ceramics. J Biomed Mater Res 1996;32(3):341-8.
41. Filgueiras MR, LaTorre G, Hench LL. Solution effects on the surface reactions of three bioactive glass compositions. J Biomed Mater Res 1993;27(12):1485-93.
42. Ashby MF, Jones DRH. Micromechanisms of fast fracture. In: Ashby MF, Jones DRH, editors. Engineering materials : an introduction to their properties and applications. Oxford ; New York: Pergamon Press; 1980. p 129-135.

Tables

Table 1. Glass compositions in weight %

	SiO_2	Na_2O	K_2O	CaO	MgO	P_2O_5
6P61	61.1	10.3	2.8	12.6	8.9	6.0
6P55	54.5	12.0	4.0	15.0	8.5	6.0

Table 2. Ion concentration of SBF (mM) in deionized water

	Ion concentration (mM)						
	Na^+	K^+	Ca^{2+}	Mg^{2+}	Cl^-	HCO_3^-	HPO_4^{2-}
SBF	142	5	2.05	1.5	148	4.2	1

Figures and captions

Figure 1

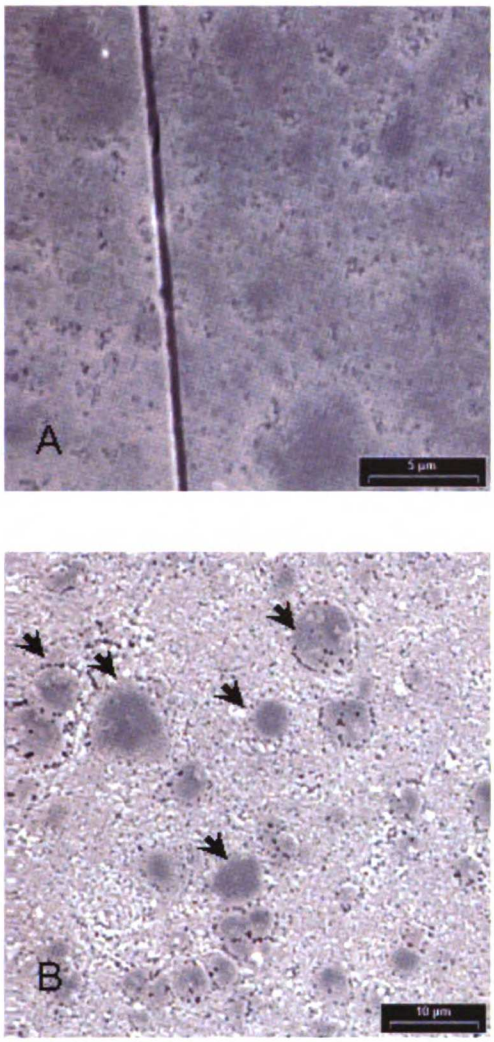

Figure 1. SEM image of FGC's surface with a microcrack (A). SEM image of FGC after etching (B). Crystalline phases round in shape (black arrows) are clearly visible.

Figure 2

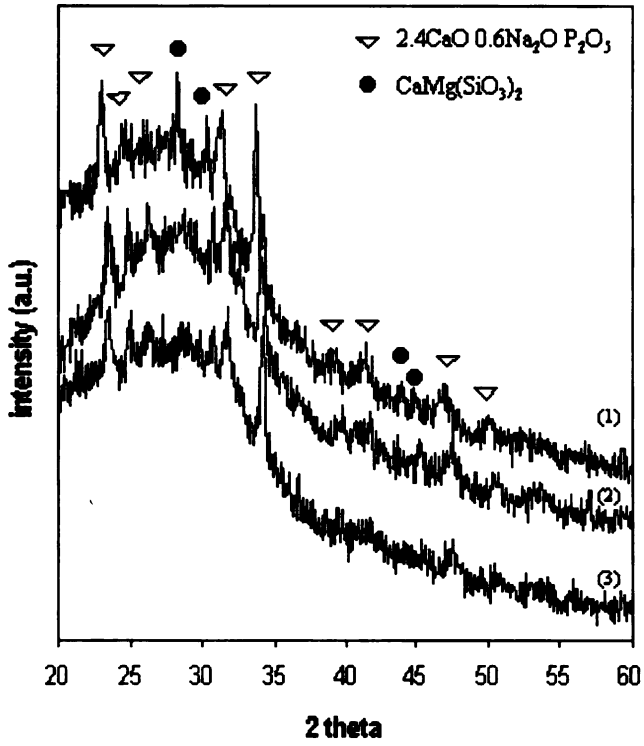

Figure 2. Thin film XRD patterns of FGCs from three different batches ((1), (2), (3)). Crystalline phases were consistently present and identified as being sodium calcium phosphate and diopside.

Figure 3

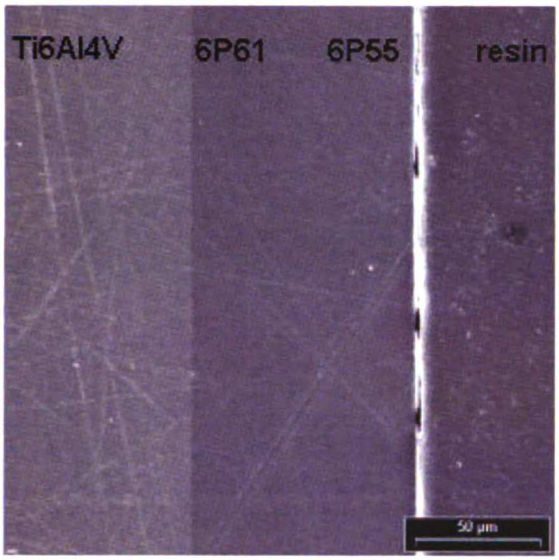

Figure 3. SEM image of FGC cross section.

Figure 4

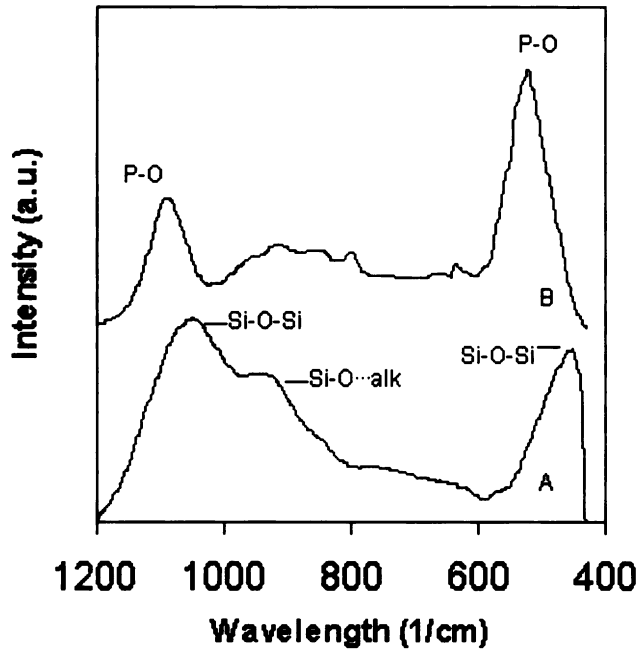

Figure 4. FTIR spectra of FGC as made (A); the labeled peaks indicate a glassy surface. FTIR spectra of FGC after conditioning in SBF (B); the labeled peaks indicate the presence of a crystalline phosphate on the surface.

Figure 5

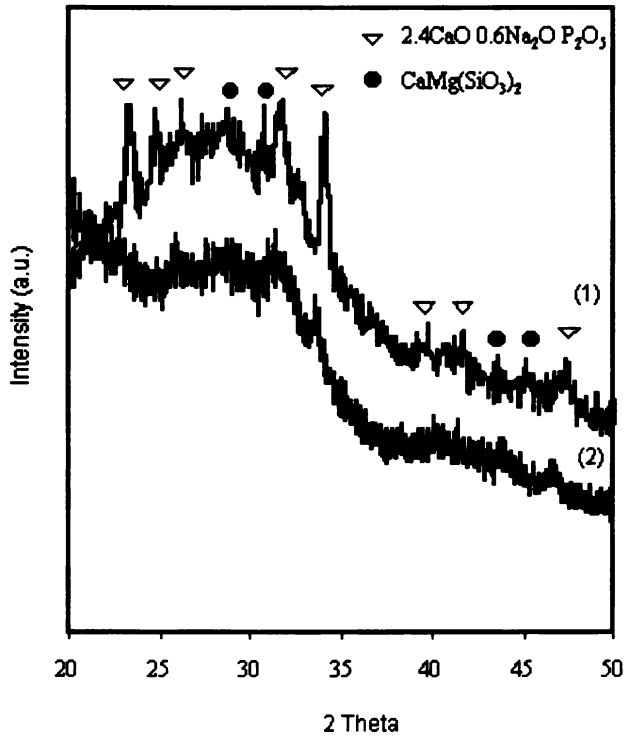

Figure 5. Thin film XRD patterns of FGC as made (1) and FGC after conditioning in SBF (2). FGC as made (1) showed the peaks of crystalline sodium calcium phosphate and magnesium calcium silicate. FGC pre-conditioned (2) had poorly defined peaks.

Figure 6

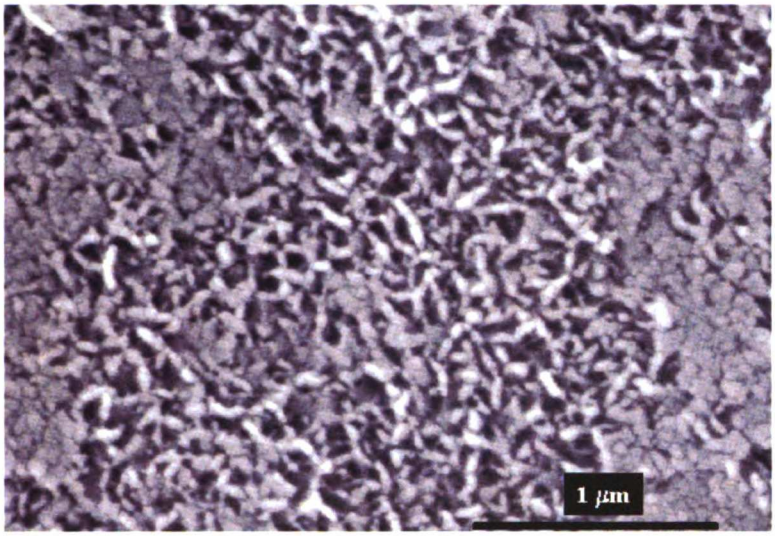

Figure 6. SEM image of FGC after conditioning in SBF. The morphology of the precipitate is similar to hydroxyapatite. The crystalline size is smaller than 1 μm.

Figure 7. SEM of MC3T3-E1.4 cells cultured on FGC as made, after exposure to vacuum (≤ 80 millitorr) (A to E). MC3T3-E1.4 osteoblast-like cells reached confluence but were detached from the sample by suction (A, * = plane of focus).
The surface reactions involved crystalline phases present in the original glass coating (B, scale bar: 2 μm). B is the magnification of an area corresponding to the solid line box from A.). The crystalline phases are visible as round three dimensional features (B black arrowheads).
Side view of the cell layer and reacted surface (C, scale bar: 2 μm). C is the magnification of an area corresponding to the white dotted line box from A) and shows the original cells-FGC interface (white dotted line). The thickness of the reacted layer is indicated by the black double headed arrow, the tissue grown over 20 days is indicated by the white double headed arrow.
Glass below the reacted surface (D, scale bar 50 μm, * = plane of focus) appears partially corroded.
E (scale bar: 5 μm) is the magnification of an area corresponding to the white dotted line box from D. The empty concavities (black arrowheads) resulted from the loosening of the crystalline phases from the glassy matrix. A noticeable space around the crystalline phases (black arrows), due to the differential dissolution rate between the matrix and the crystals, provides a preferential route for fluid movement.
F(1): EDS analysis of an area corresponding to the reacted FGC surface in Figure 7C showed presence of Ca and P with trace amounts of Si. F(2): EDS analysis of an area corresponding to the unreacted FGC in Figure 7E indicated the presence of all the elements in the original glass composition.

Figure 7

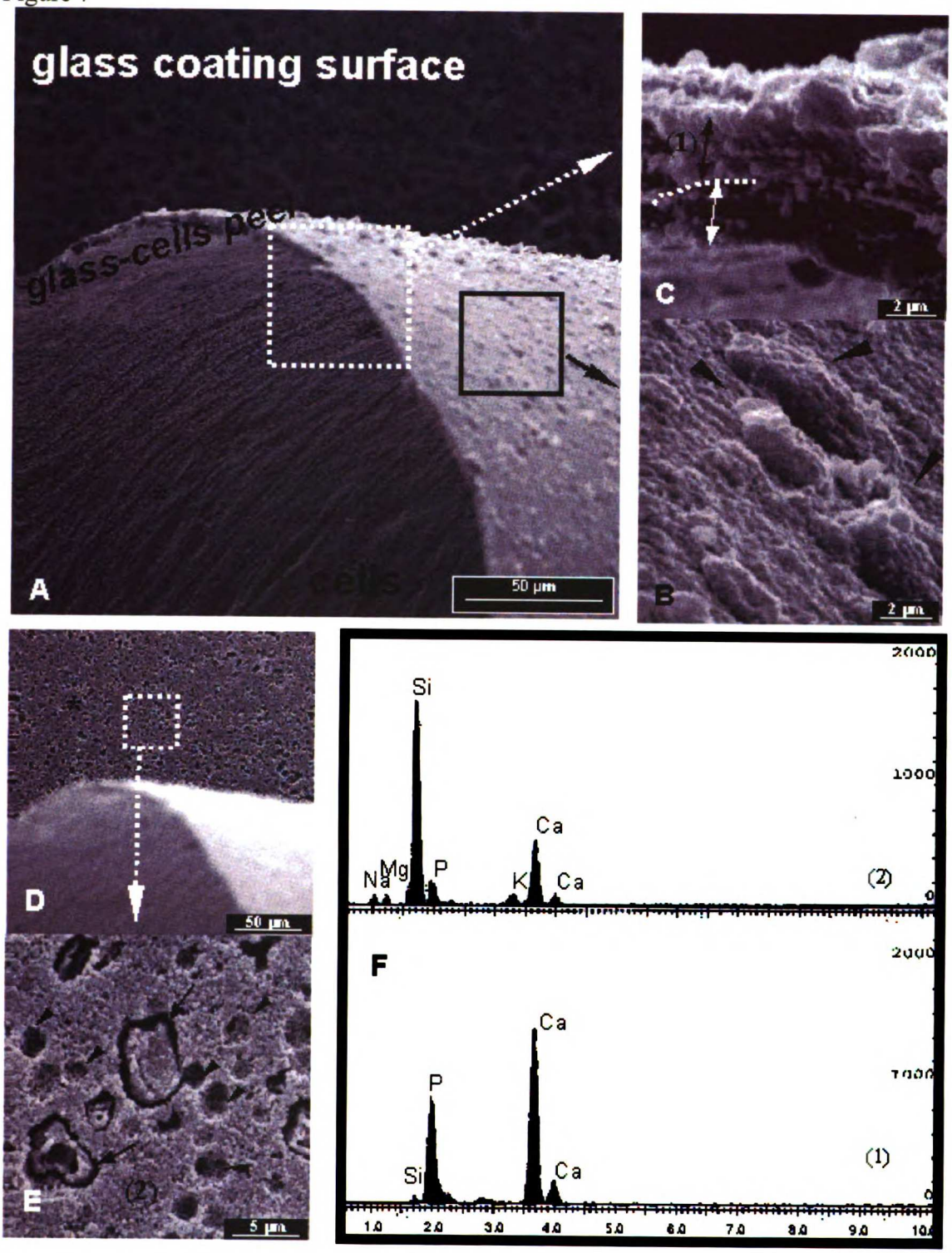
glass coating surface
glass-cells peel
A
50 μm
(1)
C
2 μm
B
2 μm
D
50 μm
E
(2)
5 μm
Si
Ca
Na
Mg
P
K
Ca
(2)
F
Ca
P
Si
Ca
(1)
1.0
2.0
3.0
4.0
5.0
6.0
7.0
8.0
9.0

Figure 8

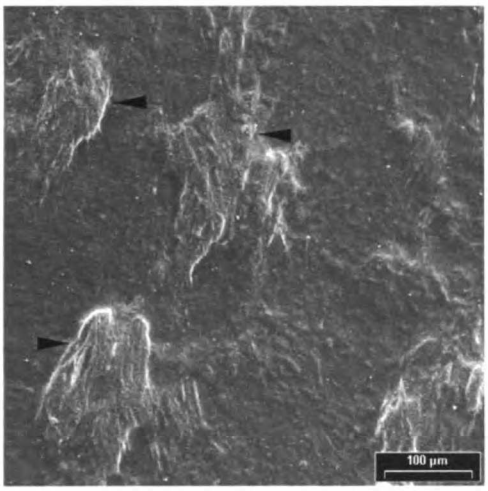

Figure 8. SEM image of MC3T3-E1.4 cells cultured on FGC pre-conditioned in SBF. Three dimensional structures associated with bone nodules are visible. The FGC's sub-surface was not disrupted by the applied suction. Scale bar: 100 µm.

Chapter 5

Incompletely Resolved Issues

Preface

This chapter will not be submitted for publication. It reports somewhat negative results which are informative from the standpoint of a researcher bridging the fields of materials science and biology. The findings indicate the importance of fabricating the functionally graded coatings (FGC) keeping in mind their possible ultimate application as implant materials. Careful handling of each component of the coatings (i.e. glass powders, and titanium alloy) as well as maintaining clean furnaces used for their fabrication is important to avoid contamination during the fabrication process. In the previous chapter MC3T3-E1.4 mouse pre-osteoblasts were cultured on FGCs that were not preconditioned, reaching confluence and subsequently mineralizing. The following cell proliferation assays on the FGCs yielded contradictory results. In the attempt to clarify these inconsistencies several repeat experiments were performed. Numerous coatings' batches and replicate experiments later, the results were consistent and indicated poor cell proliferation. There seemed to be an unknown and unavoidable contaminant that leached out of the coatings and was mildly cytotoxic. This chapter elucidates how we came to that conclusion, what was attempted to identify the possible contaminant and what was done to overcome this problem.

Abstract

In this study we determined that MC3T3-E1.4 osteoblast-like cell proliferation was significantly reduced on functionally graded coatings of bioactive glasses onto titanium alloy (FGC) in comparison to uncoated titanium alloy (Ti6Al4V) and tissue culture polystyrene (TCPS). This effect was also observed when the cells were never in direct contact with the materials and were cultured using the materials' extracts. FGCs prolonged the cells lag phase as demonstrated by proliferation curves. The viability of cells cultured onto FGCs was reduced to 70 % by the 5th day in culture, indicating that the prolonged lag phase was probably due to a lower number of viable cells. Pre-incubation of the FGCs in simulated body fluid (SBF) released ions in solution, among which were unexpectedly: vanadium, iron and nickel, as determined by inductively coupled plasma mass spectroscopy (ICP-MS). The toxicity of these ions had been previously reported,[1] but in concentrations higher than found in this study. MC3T3-E1.4 mouse pre-osteoblasts proliferated significantly more on preconditioned FGCs than on control materials, indicating that the preconditioning treatment in SBF had the effect of removing and/or preventing the leaching of the toxic agent.

Introduction

We are now able to fabricate functionally graded bioactive coatings (FGC) on titanium alloy (Ti6Al4V) that may be used as load bearing implants.[2,3] Previously we demonstrated that the fabrication process is reproducible and that cell culture conditions may compromise the stability of the coatings (Chapters 3 and 4). Preconditioning in SBF modified the FGC, resulting in a more stable coating (Chapter 4). This study investigated the effect of the FGCs not preconditioned, or preconditioned for 2 weeks in simulated

body fluid (SBF), on cell proliferation using the subclone 4 of the MC3T3-E1 mouse pre-osteoblastic cell line: MC3T3-E1.4. Proliferation of cells seeded directly on the materials was measured after 5 days in culture. Tissue culture polystyrene (TCPS) and Ti6Al4V served as controls. To uncouple possible topographical effects from chemical ones, proliferation of cells treated with FGC (not preconditioned) extract in full medium was measured. Proliferation curves were determined to establish the effect of the materials on proliferation over time. To determine whether cell proliferation was diminished because of a lower number of viable cells or a slower cellular metabolism, a viability assay was also conducted. Inductively coupled plasma-mass spectroscopy (ICP-MS) was used to identify ions released from the FGC.

Materials and Methods

Bioactive glasses were prepared by mixing the oxide powders (Table 1) in isopropyl alcohol. The solvent was evaporated and the glasses were fired in air at 1450 °C (glass 6P61) and 1400 °C (glass 6P55). The details of glass preparation can be found in previously published work.[2,4] Functionally graded coatings were prepared as previously described.[2] Briefly, the glasses (6P61 and 6P55) were separately milled in a planetary agate mill. Titanium alloy (Ti6Al4V Goodfellow Ltd., Huntingdon, UK) was cut (1.5 x 1.5 x 0.1 cm) with a low speed diamond saw (Isomet, Buehler, Ltd., Lake Bluff, IL) and polished to 1 μm with diamond suspension (Buehler, Ltd., Lake Bluff, IL). Ti6Al4V was cleaned by ultrasonication with ethanol and acetone for 10 minutes each. A suspension of glass 6P61 powders (particle size < 37 μm) in 100% ethanol was deposited on Ti6Al4V prepared as described above. Glass particles were allowed to settle and the process was carefully repeated using glass 6P55, without disturbing the first layer of glass

6P61 powder. After drying in air at 80 °C for 48 hours the green coatings were fired in air in a dental furnace (Unitek Ultra Mat II, 3M, Maplewood, MN). The furnace was pre-heated at 640 °C, the firing temperature of 800 °C was reached (heating ramp: 40 °C/min) while the furnace was evacuated to 0.1 atm. At 800 °C air was let into the firing chamber. Samples were fired for 10 sec in air at 1 atm and quenched. Ti6Al4V prepared as described above but uncoated was used as a control together with TCPS.

Cell culture

MC3T3-E1.4 mouse osteoblast-like cells were grown in an incubator at 37 °C and 5% CO_2 atmosphere, in α-modified Eagle's medium (α-MEM) supplemented with 10% fetal bovine serum (FBS) and 1% antibiotics (penicillin and streptomycin) (full medium) and passaged every 4-5 days. This is a well characterized mineralizing subclone of the mouse osteoblast-like MC3T3-E1 cell line.[5-8] In all experiments cells were plated at an initial density of 50,000 cells/cm^2. Experiments were performed three times with three samples for each material (N=3).

The effect of preconditioning in SBF on cell proliferation

Cell proliferation was assessed on FGCs without preconditioning and on FGCs preconditioned for 2 weeks in SBF at 37 °C, exchanging the solution weekly. Cells (50,000 cells/cm^2 density) were seeded in 30 μL aliquots on the center of each sample and control material. Cells were allowed to adhere for 10 minutes before the wells were gently flooded with the medium (1 mL/well). We consistently used 1 mL medium/well to reduce the variability of glass dissolution, which is known to be a function of the solution volume.[9] Cell proliferation was assayed according to the following schedule: on day 1, cells were seeded as described above; on day 2, cells were synchronized by serum

starvation for 48 hours, replacing the medium with a fresh one containing 1% FBS. On day 4, cells were allowed to re-enter the cell cycle by replacing the medium with a fresh one containing 10% FBS. After 24 hours, the number of proliferating cells was assayed using a commercial kit (CellTiter 96® Promega Corp. Madison, WI), based on the metabolic activity of living cells (3-(4,5-dimethylthiazol-2-yl)-2,5-diphenyl tetrazolium bromide) (MTT) assay). The MTT solution added to each well was incubated for 4 hours at 37 °C. After the formation of the crystal formazan product the square samples (glasses and Ti6Al4V) were transferred from the original tissue culture plate and placed into the wells of a new one. This way only the crystals formed on the samples were dissolved. To dissolve the formazan product solutions were added according to the Promega protocol; the overnight protocol was chosen to ensure complete solubilization of the dark blue formazan product. The optical density was measured at 570 nm in a spectrophotometer (Spectronic Genesys 5, Spectronics Instruments, Rochester, NY). A calibration curve was determined to convert absorption into number of cells; the relationship was linear. The number of cells was subsequently divided by the available surface to obtain cell density as number of cells/cm^2.

Proliferation rate

Proliferation curves were obtained by seeding and growing the cells on sample and control materials as previously described. Proliferation was measured by the MTT assay at days 5, 7 and 9. Cultures were synchronized 48 hours prior to the experiment endpoint by serum starvation. 24 hours prior to the experiment endpoint cells were allowed to re-enter the cell cycle by supplying the medium with 10% FBS. MTT assay was carried out as described above.

Proliferation in response to materials' extract

We used materials' extracts to uncouple the effect of surface topography from chemistry. An "incubation plate" was prepared with sterile FGC and Ti6Al4V placed in a 12 well tissue culture plate and, together with TCPS (the bottom of the wells), incubated with 1 mL of full medium for 24 hours at 37 °C. On day 1 cells were seeded on a new plate and treated with the extract. The incubation plate was replenished with medium containing 1% FBS. On day 2 cells were treated with the materials' extract containing 1% FBS. The incubation plate was replenished with full medium. On day 4 cells were treated with the materials extract and on day 5 proliferation was measured by the MTT assay as described above.

Cell viability

Cells were seeded on samples and controls and cultured with full medium for 6 days. At day 6 cells were trypsinized and pelleted. The pellet was resuspended to yield a 10^5 cells/mL dilution. One drop (0.01 mL) of cell suspension was mixed with one drop of 0.4% Trypan Blue stain (Gibco^{TM} Invitrogen Corp., Carlsbad, CA) and left for 5 min at room temperature. The number of non-viable, stained cells and the total number of cells were counted in an hemocytometer and the percentage of viable, unstained cells was calculated.

ICP-MS

To identify ions leached from the FGCs when immersed in solution a FGC extract in simulated body fluid (SBF) was prepared. Simulated body fluid was obtained by mixing the components in deionized water to reach the concentrations reported in Table 2. FGC extract was prepared by immersing 1 sample in 4 mL SBF for 2 weeks at 37°C, in a 45

mL volume sterile tube. A blank sample containing 4 mL of SBF was similarly prepared and stored. The ionic content of the extract was compared to the blank sample by inductively coupled plasma-mass spectroscopy (ICP-MS) (ChemTrace, (Freemont, CA).

Results

Cell proliferation on unconditioned materials

Cell density was significantly lower on FGCs after 5 days in culture (Figure 1) (ANOVA, SNK $p<0.05$). No significant difference was found between Ti6Al4V and TCPS.

Cell proliferation rate

The number of metabolically active cells on Ti6Al4V and TCPS increased throughout the experiment (Figure 2 pink and blue lines, respectively). The number of cells cultured on FGCs did not increase as much as cells seeded on TCPS and Ti6Al4V and appeared to be in the lag phase even after 9 days in culture (Figure 2 green line).

Viability

Figure 3 shows that after 5 days in culture, the average percentage of viable cells on FGCs was 66%. On TCPS and Ti6Al4V the percentage of viable cells was significantly higher (100%) (ANOVA, SNK $p<0.05$).

Proliferation in response to materials' extract

Cells cultured for 5 days with FGC extract proliferated significantly less than cells cultured with control extracts (Figure 4) (ANOVA, SNK $p<0.05$). This indicated that a component of the FGCs was released in solution that had the effect of slowing proliferation.

Proliferation on FGCs pre-conditioned in SBF for 2 weeks

Cells proliferated significantly more on FGC's pre-conditioned in SBF for 2 weeks (Figure 5) (ANOVA, SNK $p<0.05$) than on control materials, indicating that pre-conditioning removed the component or components responsible for the decreased cell viability.

ICP-MS

The trace metals released in SBF over the course of 2 weeks are reported in Table 3. The analysis indicates that the FGCs released significant amounts of calcium, iron, magnesium, nickel, potassium, sodium, and vanadium.

Discussion and conclusion

Initial experiments on non-preconditioned FGCs showed that cells were proliferating, reaching confluence and subsequently mineralizing, but proliferation experiments yielded inconsistent results. We increased the number of repeat experiments; after some FGCs batches proliferation at day 5 was reproducible and indicated that on FGCs cells were not proliferating as much as on control materials. This transition in the results suggests that some form of contamination occurred (most likely furnace contamination) that did not improve over time. Proliferation curves demonstrated that osteoblast proliferation on FGCs did not increase over time as much as on control materials, and after 9 days in culture cells were still in the lag phase. To determine whether cells were viable but metabolically slow, viability assay by trypan blue exclusion was performed. The results showed that about 30% of the cells seeded on FGC were not viable. Treating the cells with materials' extract indicated that the FGC's extract contained some agent that caused reduced proliferation and possibly cell death. Preconditioning FGCs in SBF for two weeks had the effect of reversing this trend and significantly promoting osteoblast

proliferation. It is not clear whether the toxic agent was located exclusively on the FGC surface or also in the bulk of the coating. Preconditioning in SBF might have had the following effects: 1) the toxic component/s was/were completely leached out; which could be the case if it/they was/were located on the surface only 2) the surface of the FGC had reacted to form an apatite-like layer that created a barrier for the toxic component/s or 3) the presence of the surface apatite-like layer slows down the leaching process, reducing the concentration of the toxic agent to a non-toxic level. Among the ions released from FGCs, vanadium, iron and nickel (in decreasing order of toxicity) had been previously reported as being toxic above a specific concentration.[1,10] We found that the concentration of vanadium in the extract was 0.01 mM (to convert mM into ppb: mM x molecular weight x 1000 = ng/mL or ppb). Hallab et al.[1] reported that vanadium in such concentration was not toxic to MG63 cells, but doubling that concentration to 0.02 mM caused a drop in MG63 human osteosarcoma viability of about 30%. MG63 is an osteosarcoma-derived cell line, more "robust" in nature compared to the spontaneously immortalized MC3T3-E1.4 cell line, which may explain the higher concentration at which the toxic effect could be noticed. In this study iron and nickel were present in the extract in concentrations of 0.0003 and 0.0004 mM respectively; these concentrations are not toxic.[1] It seems surprising that vanadium in the extract may be the cause of cell death, since cells were about 100% viable when cultured onto Ti6Al4V (uncoated) which also contains vanadium. The differences between the FGC and Ti6Al4V are the presence of the glass and the additional heat treatment that the enameling process requires. We exposed Ti6Al4V uncoated to the same thermal treatment of FGC but in the absence of any glass and then tested MC3T3-E1.4 proliferation on such substratum. The results

showed no difference in proliferation between Ti6Al4V and thermally treated Ti6Al4V (data not shown). We reasoned that some contaminant might have been included in the glass and we attempted to prepare FGCs on Pt sheet instead of Ti6Al4V. The resulting coatings showed poor adhesion but could be used as substrates for MC3T3-E1.4 culture. We tested for cellular proliferation as described above and found that cells proliferated significantly more on FGC-Pt samples than on FGC-Ti6Al4V (data not shown). The source and identity of the toxic component remains uncertain. To positively identify the toxic agent, preparation and analysis of extracts at various time points (to determine the rate of release), followed by cytotoxicity assays testing each agent singularly or in combination, would be recommended. This was outside the scope of this thesis, but the occurrence of contamination underscores the importance of carrying out each step of coating fabrication process with care and cleanliness as if it were a biological assay. The data reported in this and the previous chapter show that pre-conditioning in SBF is strongly recommended to provide a stable coating and to remove possible contaminants introduced during the glass fabrication and/or enameling process.

References

1. Hallab NJ, Vermes C, Messina C, Roebuck KA, Glant TT, Jacobs JJ. Concentration- and composition-dependent effects of metal ions on human MG-63 osteoblasts. J Biomed Mater Res 2002;60(3):420-33.
2. Gomez-Vega JM, Saiz E, Tomsia AP. Glass-based coatings for titanium implant alloys. J Biomed Mater Res 1999;46(4):549-59.
3. Gomez-Vega JM, Saiz E, Tomsia AP, Marshall GW, Marshall SJ. Bioactive glass coatings with hydroxyapatite and Bioglass particles on Ti-based implants. 1. Processing. Biomaterials 2000;21(2):105-11.
4. Foppiano S, Marshall SJ, Marshall GW, Saiz E, Tomsia AP. The influence of novel bioactive glasses on in vitro osteoblast behavior. J Biomed Mater Res 2004;71A(2):242-249.
5. Wang D, Christensen K, Chawla K, Xiao G, Krebsbach PH, Franceschi RT. Isolation and characterization of MC3T3-E1 preosteoblast subclones with distinct in vitro and in vivo differentiation/mineralization potential. J Bone Miner Res 1999;14(6):893-903.
6. Quarles LD, Yohay DA, Lever LW, Caton R, Wenstrup RJ. Distinct proliferative and differentiated stages of murine MC3T3-E1 cells in culture: an in vitro model of osteoblast development. J Bone Miner Res 1992;7(6):683-92.
7. Franceschi RT, Iyer BS. Relationship between collagen synthesis and expression of the osteoblast phenotype in MC3T3-E1 cells. J Bone Miner Res 1992;7(2):235-46.
8. Franceschi RT, Iyer BS, Cui Y. Effects of ascorbic acid on collagen matrix formation and osteoblast differentiation in murine MC3T3-E1 cells. J Bone Miner Res 1994;9(6):843-54.
9. Jones JR, Sepulveda P, Hench LL. Dose-dependent behavior of bioactive glass dissolution. J Biomed Mater Res 2001;58(6):720-6.
10. Morais S, Dias N, Sousa JP, Fernandes MH, Carvalho GS. In vitro osteoblastic differentiation of human bone marrow cells in the presence of metal ions. J Biomed Mater Res 1999;44(2):176-90.

Tables

Table 1. Glass compositions in weight %

	SiO_2	Na_2O	K_2O	CaO	MgO	P_2O_5
6P61	61.1	10.3	2.8	12.6	8.9	6.0
6P55	54.5	12.0	4.0	15.0	8.5	6.0

Table 2. Ion concentration of SBF (mM) in deionized water

	Ion concentration (mM)						
	Na^+	K^+	Ca^{2+}	Mg^{2+}	Cl^-	HCO_3^-	HPO_4^{2-}
SBF	142	5	2.05	1.5	148	4.2	1

Table 3. ICP-MS analysis concentrations in parts per billion (ppb)

		Detection Limit (ppb)	Blank	Sample (FGC)
Aluminum	(Al)	5	160	<5
Antimony	(Sb)	5	<5	<5
Arsenic	(As)	10	<10	<10
Barium	(Ba)	1	2.3	1.0
Beryllium	(Be)	5	<5	<5
Bismuth	(Bi)	5	<5	<5
Boron	(B)	10	140	164
Cadmium	(Cd)	1	<1	<1
Calcium	(Ca)	10	51,000	77,000
Chromium	(Cr)	5	<5	<5
Cobalt	(Co)	1	<1	<1
Copper	(Cu)	5	<5	<5
Gallium	(Ga)	1	<1	<1
Germanium	(Ge)	5	<5	<5
Gold	(Au)	10	<10	<10
Iron	(Fe)	10	<10	17
Lead	(Pb)	5	<5	<5
Lithium	(Li)	5	<5	<5
Magnesium	(Mg)	5	38,000	63,000
Manganese	(Mn)	5	<5	<5
Molybdenum	(Mo)	5	<5	<5

Nickel	(Ni)	5	6.9	23
Niobium	(Nb)	5	<5	<5
Potassium	(K)	10	200,000	220,000
Silver	(Ag)	5	<5	<5
Sodium	(Na)	10	2,200,000	2,300,000
Strontium	(Sr)	1	34	39
Tantalum	(Ta)	5	<5	<5
Thallium	(Tl)	1	<1	<1
Tin	(Sn)	5	<5	<5
Titanium	(Ti)	5	<5	<5
Vanadium	(V)	5	14	510
Zinc	(Zn)	5	<5	<5
Zirconium	(Zr)	1	2.0	<1

Figures and captions

Figure 1

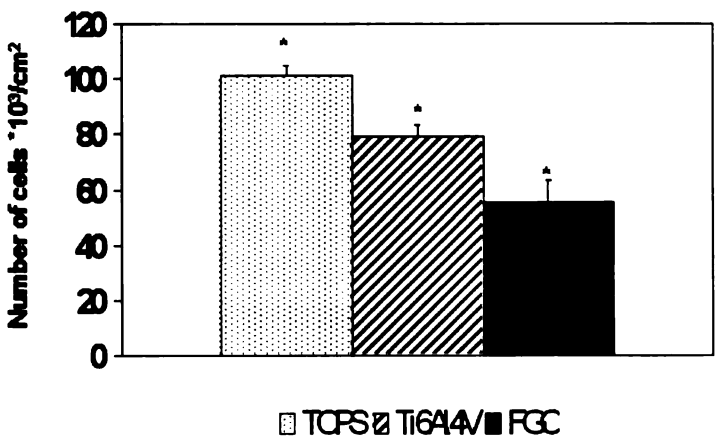

Figure 1. Cell proliferation: MC3T3-E1.4 mouse pre-osteoblast like cells proliferated significantly differently on all materials in the following order from higher to lower: TCPS> Ti6Al4V>FGC (*=significantly different ANOVA, SNK $p<0.05$)

Figure 2

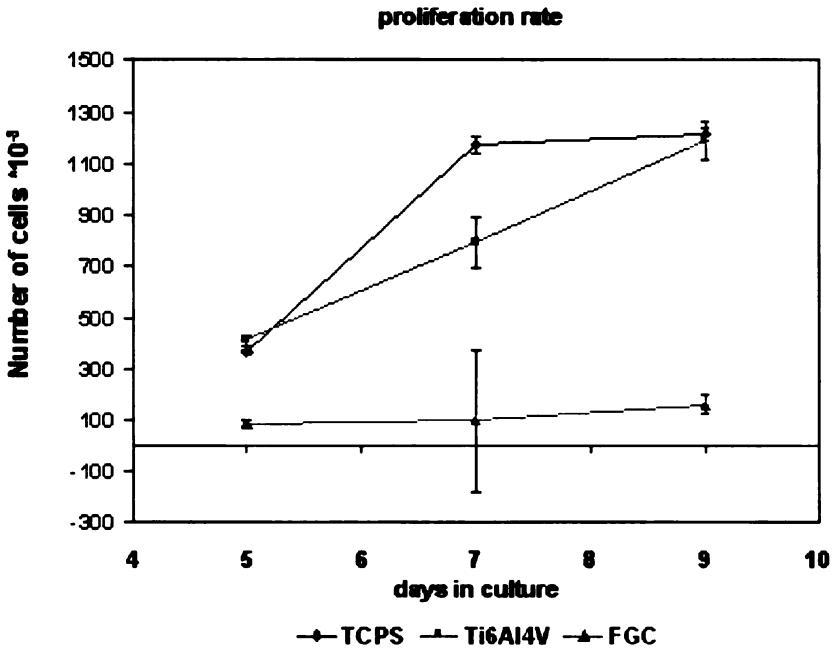

Figure 2. Proliferation rate: over 9 days in culture the number of cells on TCPS and Ti6Al4V increased (pink and blue line respectively). Cells cultured on FGC remained in the lag phase throughout the duration of the experiments (green line).

Figure 3

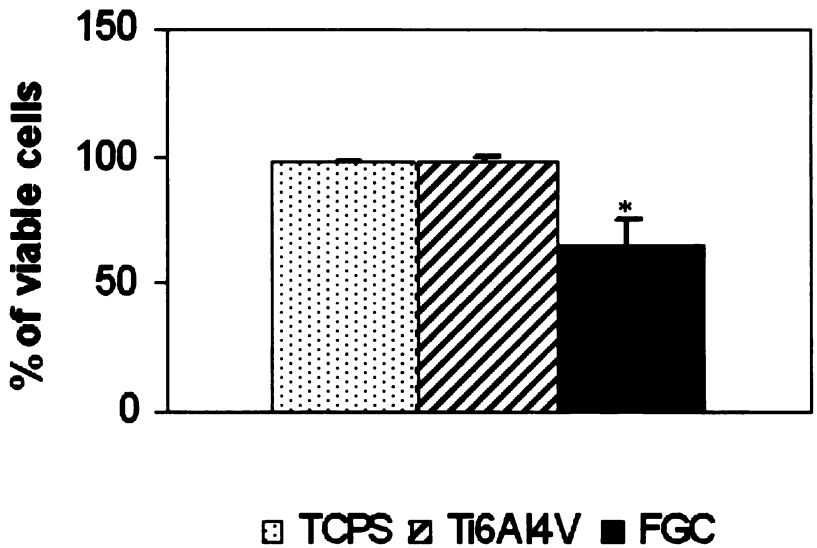

Figure 3. Cell viability: trypan blue exclusion indicated that after 5 days in culture about 100% of the cells were viable on TCPS and Ti6Al4V whereas on FGC only 70% of the cells survived (*=significantly different ANOVA, SNK $p<0.05$).

Figure 4

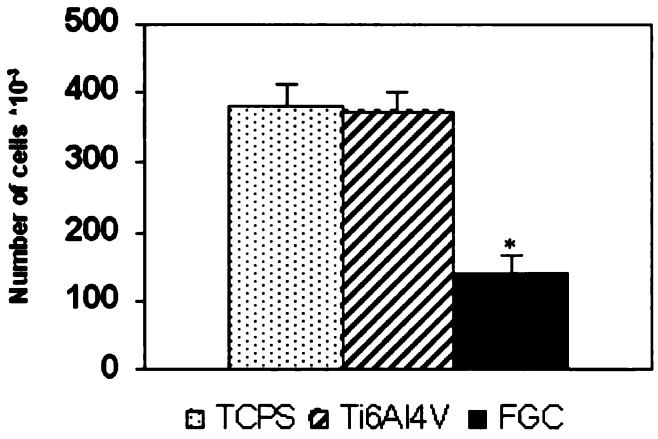

Figure 4. Cell proliferation in response to materials' extract: after 5 days in culture MC3T3-E1.4 cells proliferated similarly when treated with either TCPS or Ti6Al4V extract. Proliferation of cells treated with FGC extract was significantly lower (*=significantly different ANOVA, SNK $p<0.05$).

Figure 5

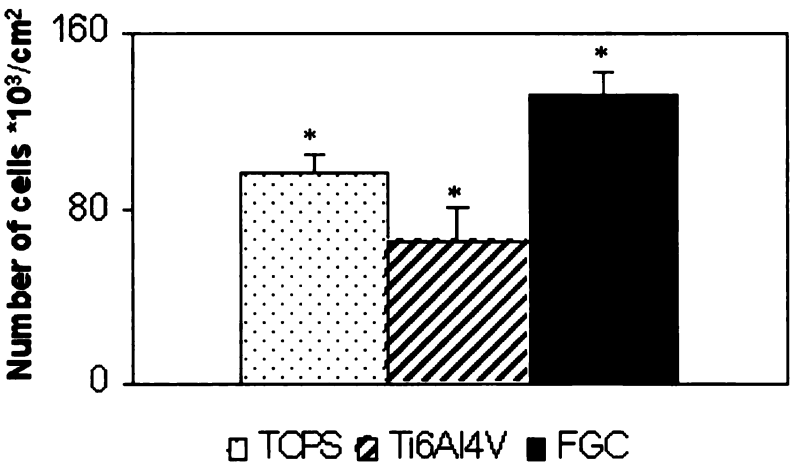

Figure 5. Cell proliferation on preconditioned materials: after 5 days in culture MC3T3-E1.4 mouse osteoblast-like cells proliferated significantly differently on all materials. Lowest proliferation occurred on Ti6Al4V followed by TCPS, and FGC (ANOVA, SNK $p<0.05$).

Chapter 6

Bioactive glass coatings affect osteoblast-like cells behavior

Abstract

Functionally graded coatings (FGC) of bioactive glass on titanium alloy (Ti6Al4V) were fabricated by the enameling technique. These innovative coatings may be an alternative to plasma sprayed hydroxylapatite coated implants. Previously (Chapter 4) we determined that a preconditioning treatment in simulated body fluid (SBF) was necessary to stabilize the coatings. This work had the primary goal of assessing the preconditioned FGCs' cytocompatibility, *in vitro* with MC3T3-E1.4 mouse pre-osteoblastic cells. We evaluated cell adhesion, proliferation, and mineralization on FGCs in comparison to uncoated Ti6Al4V and tissue culture polystyrene (TCPS). No difference in cell adhesion was identified, whereas proliferation was significantly different on all materials, highest on FGCs followed by TCPS and Ti6Al4V. Qualitative and quantitative mineralization assays indicated that mineralization occurred on all materials. The amount of inorganic phosphate released by the mineralizing layers was significantly different, highest on TCPS, followed by FGC and uncoated Ti6Al4V. The secondary objective of this work was to assess the ability of the FGCs to affect gene expression, indirectly, by means of their dissolution products, which was assessed by real time RT-PCR. FGCs dissolution products induced a two fold increase in the expression of Runx-2, and a 20% decrease in the expression of collagen type 1 with respect to TCPS extract. These genes are regulators of osteoblast differentiation and mineralization, respectively. The findings of this study indicate that preconditioned FGCs are cytocompatible and suggest that future work may allow composition changes to induce preferred gene expression.

Introduction

An enameling technique, combined with a functionally graded approach, was used to produce bioactive glass coatings on titanium alloy (Ti6Al4V) that resist delamination.[1,2] The glass in contact with Ti6Al4V contained 61 wt% Si, and small amounts of Mg and K oxides to provide an adequate match in coefficient of thermal expansion (CTE) with the alloy. The second layer of the coating was a glass containing 55 wt% Si, that is bioactive (Chapter 3).[1] Similar to findings with bioactive glass particles we found that the glass silica network of the coatings could be undermined unless the coatings were pretreated in SBF.[3-5] The preconditioning treatment partially transformed the coatings' surfaces into a crystalline apatite-like form (Chapter 4).

The mechanisms by which bioactive glasses, and their coatings, affect osteoblast behavior and metabolism are unclear. There is evidence indicating that bioactive glasses can control gene transcription through glass dissolution products.[6-8] The objective of this work was twofold: 1) to assess the *in vitro* biocompatibility of functionally graded bioactive glass coatings (FGC) after preconditioning treatment and 2) to test the hypothesis that FGCs so treated can affect the expression of genes involved in the early stages of osteogenesis by means of their dissolution products. To pursue our objectives cell adhesion, proliferation, and mineralization were assessed using the mineralizing subclone of the mouse pre-osteoblastic cell line MC3T3-E1: MC3T3-E1.4.[8] FGCs were pre-conditioned in SBF to provide a stable surface. Titanium alloy (Ti6Al4V) and tissue culture polystyrene (TCPS), pre-conditioned in the same way, served as controls. The second part of this study was investigated by preparing materials extracts and determining their effect on the expression of genes involved in the early stages of

osteoblast differentiation (Runx-2, α2 chain of collagen type I (Col 1), and alkaline phosphatase)[9] by quantitative real time reverse transcription polymerase chain reaction (real time RT-PCR).

Materials and Methods

Sample preparation

To fabricate FGCs, two bioactive glasses were prepared by mixing the reagents in propanol using a high speed stirrer as previously described.[1] The P_2O_5 content was 6 wt% for both glasses, designated 6P followed by their SiO_2 content in weight percent (Table 1). The reagents were SiO_2 (99.5% Cerac Inc., Milwaukee, WI), $CaCO_3$ (99.9%, J.T. Baker, Phillipsburg, NJ), MgO (98.6%, J.T. Baker, Phillipsburg, NJ), K_2CO_3 (99.4%, Mallinkrodt, Paris, KY), $NaHCO_3$ (99.5%, J.T. Baker, Phillipsburg, NJ), and Na_2HPO_4 (99%, Sigma, St.Louis, MO). The mixture was dried and then fired in air in a Pt crucible for 5 hours at 1400°C (glass 6P55) and 1450°C (glass 6P61). Functionally graded glass enameled coatings were prepared as previously described.[1] Glasses 6P61 and 6P55 were separately milled in a planetary agate mill. 6P61 glass powder (particle size < 37 μm) was suspended in 100% ethanol and deposited on polished (1 μm diamond suspension (Buehler, Ltd., Lake Bluff, IL)) Ti6Al4V squares (1.5 x 1.5 x 0.1 cm) (Ti6Al4V Goodfellow Ltd., Huntingdon, UK). Glass particles were allowed to settle and the process was carefully repeated using glass 6P55, without disturbing the first powder layer. The green coatings were dried in air at 80°C for 48 hours and then fired in air in a dental furnace (Unitek Ultra Mat II, 3M, Maplewood, MN). The furnace was pre-heated at 640°C, and the firing temperature of 800°C was reached at a rate of 40°C/min while evacuating the furnace to 0.1 atm. At 800°C air was let into the firing chamber, samples

were fired for 10 sec in air at 1 atm and quenched. Ti6Al4V of the same size and polished through 1 μm served as control together with tissue culture polystyrene (the bottom of the wells). Samples were cleaned by sonication in acetone and isopropyl alcohol for 5 minutes each, and sterilized in dry heat at 250°C. Sterile samples were placed in 12 well tissue culture plates under sterile conditions.

Samples and controls were preconditioned in 4 mL of filter sterilized (filter: 0.22 μm, GE Osmonics, Inc., Minnetoka, MN) SBF (Table 2). Preconditioning lasted for two weeks at 37°C, changing the solution at one week. Specimens were rinsed with phosphate buffered saline (PBS) prior to cell seeding. Experiments were performed in triplicate with N=3 for each material in each experiment.

Cell culture

MC3T3-E1.4 mouse osteoblast-like cells were grown in an incubator at 37°C and 5% CO_2 atmosphere, in α-modified Eagle's medium (α-MEM) supplemented with 10% fetal calf serum (FCS) and 1% antibiotics (penicillin and streptomycin) (full medium) and passaged every 4-5 days. In all experiments cells were plated at an initial density of 50,000 cells/cm^2.[1]

Cell adhesion

Cells were seeded in 30 μL aliquots on the center of sample and control materials. After 10 minutes the wells were gently flooded with the medium (1 mL/well). 1 mL medium/well was consistently used throughout the experiments. Three hours after flooding, the supernatant containing non-adhering cells was removed, and replaced with fresh medium. The number of adhering cells was assayed using a commercial kit (CellTiter 96® Promega Corp., Madison, WI), based on the metabolic activity of living

cells (3-(4,5-dimethylthiazol-2-yl)-2,5-diphenyl tetrazolium bromide) (MTT) assay). The MTT solution added to each well was incubated for 4 hours at 37°C. After the formation of the crystal formazan product the square samples (FGC and Ti6Al4V) were transferred to new tissue culture plates. This way only the crystals formed on the samples were dissolved. To dissolve the formazan product, solutions were added according to the manufacturer's protocol, keeping volume of solution to sample surface area ratio constant at 2 $\mu L/mm^2$. This was done to compensate for the difference in surface available to the cells. The overnight protocol was chosen to ensure complete solubilization of the dark blue formazan product. Optical density was measured at 570 nm in a spectrophotometer (Spectronic Genesys 5, Spectronics Instruments, Rochester, NY). A calibration curve allowed conversion of absorption to number of cells. The number of cells was then normalized to the sample surface area ($cells/cm^2$).

Cell proliferation

Cell proliferation was assayed after 5 days in culture. On day 1, cells were seeded as described above (see *cell adhesion)*. On day 2, cells were synchronized by serum starvation (1% FBS) for 48 hours. On day 4, cells were allowed to re-enter the cell cycle (10% FBS). After 24 hours the proliferating cells were assessed using the MTT assay as described above.

Mineralization

Cells were seeded as described above. Cells were treated with ascorbic acid (AA) (50 μg/mL medium) for 10 days and then with AA and inorganic phosphate (NaH_2PO_4) (10 mM) for an additional 5 days. Medium was replaced at 2 day intervals throughout the experiment. Cells were washed 3 times with PBS without Ca^{2+} or Mg^{2+} and then fixed

for 15 min in 100% ethanol. Cell layers were stained with alizarin S solution for 30 minutes, rinsed and photographed under an optical microscope (Olympus BX50 Olympus America Inc., Melville, NY) with a ccd camera (DVC 1300C camera RGB color, DVC Company, Austin, TX) connected to it.

Quantitative measurement of inorganic phosphate

Cells were seeded and treated with AA and NaH_2PO_4 as described above to induce mineralization. NaH_2PO_4 treatment was carried out for a total of 10 days. This was done to try to increase the amount of mineral in the tissue. After 20 days in culture, cells were washed 3 times with PBS without Ca^{2+} or Mg^{2+} and the cell layer grown on FGCs and Ti6Al4V was gently removed from the materials with a rubber policeman and transferred to a new tissue culture plate. This was done to avoid measuring phosphate possibly released from FGCs or from the tissue grown on the tissue culture wells adjacent to the test substrates. The mineralized tissue was incubated for 48 hours in 15% trichloroacetic acid (TCA). The volume of TCA added was kept constant at 2 $\mu L/mm^2$ of sample surface. 50 μL of supernatant were then assayed. Inorganic phosphate concentration was determined by spectrophotometry (355 nm) using the method of Heinonen and Lahti.[10] The absorbance value in Klett units (KU) (1 KU = 0.005 absorbance) was converted into concentration using a calibration curve made using the same method.

Quantitative real time RT-PCR

Cell culture

All samples and controls were preconditioned in SBF for 2 weeks as described above. *Incubation plates*: Materials extracts were prepared by immersing samples and materials in full media for 48 hours with a volume of solution to surface area ratio of 4.5 $\mu L/mm^2$.

Cells were seeded in six well tissue culture plates as described above, and treated with materials extract and AA (50 μg/mL medium) every 48 hours for 7 days. The incubation plates were replenished with the proper amount of full medium after each cell feeding.

RNA extraction and reverse transcription

At day 7 total RNA was extracted using the RNeasy extraction kit (Qiagen, Valencia, CA). The concentration and purity of the total RNA was determined by measuring the light absorbance at 260 nm and by calculating the A_{260}/A_{280} ratio, respectively. Two step RT-PCR was carried out in which reverse transcription was performed in a different tube than real time PCR. Reverse transcription was conducted using the Ericomp Powerblock II System (Long Island Scientific, East Setauket, NY). The same amount of total RNA from each sample within an experiment was used in a total volume of 20 μL containing 1 μL of oligo dT primer, 4 μL first strand buffer, 2 μL of 0.1 M DTT, 1 μL of 10 mM dNTP and 100 U of SuperScript™ II RNase H⁻ reverse transcriptase (Invitrogen, Carlsbad, CA). RT reaction was incubated at 42 °C for 60 min and terminated by heat inactivating the reverse transcriptase at 70 °C for 15 min.

Primers and probes

Primers and probes were Assays on Demand (Applied Biosystems, Foster City, CA) selected using the NCBIRefSeq sequences for glycerol-3 phosphatase dehydrogenase (Gapd) (accession number NM_008084), α2 chain of collagen type 1 (Col 1) (accession number NM_007743), alkaline phosphatase (Akp2) (accession number NM_007431), and core binding factor 1 (Runx-2) (accession number NM_009820). The Applied Biosystems patented fluorogenic probes incorporated reporter dye on the 5' end and

quencher dye on the 3' end, and spanned an exon/intron boundary to avoid genomic DNA amplification.

Real time PCR

Quantitative real time PCR was conducted with TaqMan® instrument (TaqMan-PCR ABI Prism 7900HT sequence detection system, Perkin Elmer Applied Biosystems, Foster City, CA) that detects accumulation of PCR product, and allows quantification in the exponential phase of PCR reactions. Serial dilutions of cDNA from cells cultured with the TCPS extract (control) were analyzed for the internal control and target genes (Gapdh, Col I, Runx-2 and Alk Phos). A standard curve was determined by plotting threshold cycle (C_T) versus the log of initial amount of cDNA and ensured comparable efficiency within the dynamic range. Alk Phos efficiency was not linear in the dynamic range so its real time RT-PCR data was discarded. Equal amounts of reaction mixture were amplified by PCR in a 1 x TaqMan® Universal Master mix containing AmpErase® UNG polymerase (Applied Biosystems, Foster City, CA). cDNA was amplified as follows: enzyme activation at 50°C for 2 min, 40 cycles of amplification associated with denaturation at 95 °C for 15 sec and extension at 60 °C for 1 min. A control without template and one without polymerase were used to exclude unspecific signals. Each sample was run in triplicate to test the consistency of the ABI Prism reading. Three replicate experiments were conducted to check for reproducibility.

Results

Cell adhesion and proliferation

Figure 1 shows the results from a representative experiment (N=3): the number of adhering cells per cm^2 was not significantly different among materials (ANOVA, Student

Newman Keuls (SNK) $p>0.05$). As shown in Figure 2, proliferation was significantly different on each material. Cells proliferated on the materials in the following order from lowest to highest: Ti6Al4V, TCPS, FGC (ANOVA, SNK $p<0.05$).

Qualitative mineralization: Alizarin S staining

Figure 3 shows alizarin S staining of the mineralizing cell layer on FGC and control materials. Distinct nodular colonies staining red can be distinguished.

Quantitative measurement of inorganic phosphate

Figure 4 shows the concentration of inorganic phosphate released from the mineralizing cell layer from each material in one representative experiment (N=3). Significantly different concentrations of inorganic phosphate were released from the cell layers cultured on each substratum in the following order from the lowest to the highest: Ti6Al4V, FGC, TCPS (ANOVA, SNK $p<0.05$).

Real time RT-PCR

Repeat runs of the same samples yielded consistent readings. Figure 5 shows the mean expression level, from three experiments, as percentage of the TCPS control. Real time RT-PCR showed that the Runx-2 expression level was 216 % of TCPS control in cultures treated with FGC extract, which was statistically significant (ANOVA, SNK $p<0.05$). Ti6Al4V did not elicit a significant change in Runx-2 expression with respect to TCPS (ANOVA, SNK $p>0.05$). Cultures treated with either Ti6Al4V or FGC extract expressed Col 1 at a significantly lower level, about 80 % of the TCPS control (ANOVA, SNK $p<0.05$).

Discussion

Functionally graded coatings of bioactive glasses on titanium alloy may be a potential alternative to plasma sprayed hydroxyapatite implant coatings, which have been shown to be unreliable.[11-14] We previously determined that a preconditioning treatment in SBF stabilizes FGCs prior to exposure to a protein containing environment. After preconditioning in SBF, SEM, FTIR and XRD analyses indicated the presence of a crystalline apatite-like mineral on the FGCs surface (Chapter 3). In this study, no significant change could be identified by SEM and FTIR on the surface of the control materials (data not shown). After preconditioning in SBF the FGCs were cytocompatible as shown by cell adhesion similar to controls, increased cell proliferation, and allowed cell differentiation and mineralization. An interesting finding was the significantly greater inorganic phosphate apparently included in the mineralizing cell layer cultured on the FGCs, as compared to the TiAl4V control. This suggests that the FGCs may offer more rapid mineralization. However we can not exclude the possibility that some of the apatite mineral coating on the FGCs was removed along with cells prior to these measurements. Mineralization onto TCPS was significantly higher than onto Ti6Al4V and FGC. The quantitative mineralization data together with qualitative alizarin S staining indicates that Ti6Al4V and FGC may delay but do not inhibit MC3T3-E1.4 mineralization, compared to TCPS. These differences could be due to the combined effect of surface chemistry and topography of the substrates. Microarray gene analysis indicated that Bioglass® extract affects gene expression in human primary osteoblastic cultures,[6,7] which suggests the possibility of designing materials capable of inducing the expression of specific genes.[8] Thus, in the second part of this study we conducted preliminary experiments to determine if FGCs also are able to induce gene expression.

We chose genes involved in the early stages of osteoblast differentiation, Runx-2, and Col 1, as target genes. Runx-2 is an osteoblast-specific transcription factor required for the differentiation of mesenchymal progenitor cells towards the osteoblastic lineage; in fact -/- Runx-2 mice do not have functional osteoblasts and show an exclusively cartilaginous skeleton.[15] Additionally Runx-2 is necessary to maintain a functional osteoblastic phenotype.[9] Collagen type 1 is the major collagenous extracellular matrix protein present in bone, and plays a central role in bone mineralization.[16] Using real-time RT-PCR we found that FGCs extract induced a two fold increase in the expression of Runx-2 compared to uncoated Ti6Al4V and TCPS, while Col 1 expression by the extracts of either FGCs or Ti6Al4V, was about 80% of the expression induced by TCPS extract. Thus FGCs dissolution products can induce selective gene expression important to osteoblast differentiation in a simplified *in vitro* model. The twofold induction of Runx-2 expression by FGCs extract could have important clinical implications. *In vivo* implants are in contact with a variety of cells present in bone including mesenchymal stem cells.[17] These innovative coatings may promote the differentiation of mesenchymal stem cells towards the osteoblastic lineage by stimulating Runx-2 expression, thereby favorably affecting osteointegration. The coating composition may be modified to simultaneously promote mineralization by the induction of genes involved in the process such as Col 1. This intriguing result will be the subject of future research.

Conclusions

FGCs preconditioned in SBF were cytocompatible and promoted osteoblast proliferation compared to uncoated titanium alloy and tissue culture polystyrene. Mineralization levels for FGC were higher than Ti6Al4V but less than TCPS. FGCs and Ti6Al4V are

able to affect osteoblast gene expression indirectly through their dissolution products into tissue culture media. Specifically FGCs extract induced a two fold expression of Runx-2, a key marker of osteoblast differentiation, compared to Ti6Al4V and TCPS. Future investigation will address the identification of the specific chemical cues behind the induction of gene expression, and the tailoring of materials composition to control such effect.

References

1. Gomez-Vega JM, Saiz E, Tomsia AP. Glass-based coatings for titanium implant alloys. J Biomed Mater Res 1999;46(4):549-59.
2. Gomez-Vega JM, Saiz E, Tomsia AP, Marshall GW, Marshall SJ. Bioactive glass coatings with hydroxyapatite and Bioglass particles on Ti-based implants. 1. Processing. Biomaterials 2000;21(2):105-11.
3. Radin S, Ducheyne P, Rothman B, Conti A. The effect of in vitro modeling conditions on the surface reactions of bioactive glass. J Biomed Mater Res 1997;37(3):363-75.
4. Radin S, Ducheyne P, Falaize S, Hammond A. In vitro transformation of bioactive glass granules into Ca-P shells. J Biomed Mater Res 2000;49(2):264-72.
5. Sepulveda P, Jones JR, Hench LL. In vitro dissolution of melt-derived 45S5 and sol-gel derived 58S bioactive glasses. J Biomed Mater Res 2002;61(2):301-11.
6. Xynos ID, Edgar AJ, Buttery LD, Hench LL, Polak JM. Ionic products of bioactive glass dissolution increase proliferation of human osteoblasts and induce insulin-like growth factor II mRNA expression and protein synthesis. Biochem Biophys Res Commun 2000;276(2):461-5.
7. Xynos ID, Edgar AJ, Buttery LD, Hench LL, Polak JM. Gene-expression profiling of human osteoblasts following treatment with the ionic products of Bioglass 45S5 dissolution. J Biomed Mater Res 2001;55(2):151-7.
8. Hench LL, Polak JM. Third-generation biomedical materials. Science 2002;295(5557):1014-7.
9. Karsenty G. The genetic transformation of bone biology. Genes Dev 1999;13(23):3037-51.
10. Heinonen JK, Lahti RJ. A new and convenient colorimetric determination of inorganic orthophosphate and its application to the assay of inorganic pyrophosphatase. Anal Biochem 1981;113:313-317.
11. Bloebaum RD, Bachus KN, Rubman MH, Dorr LD. Postmortem comparative analysis of titanium and hydroxyapatite porous- coated femoral implants retrieved from the same patient. A case study. J Arthroplasty 1993;8(2):203-11.
12. Bloebaum RD, Dupont JA. Osteolysis from a press-fit hydroxyapatite-coated implant. A case study. J Arthroplasty 1993;8(2):195-202.
13. Chang YL, Lew D, Park JB, Keller JC. Biomechanical and morphometric analysis of hydroxyapatite-coated implants with varying crystallinity. J Oral Maxillofac Surg 1999;57(9):1096-108; discussion 1108-9.
14. Lacefield WR. Hydroxylapatite coatings. In: Hench LL and Wilson J, editor. An introduction to bioceramics. Singapore: World Scientific; 1993. p 223-238.
15. Komori T, Yagi H, Nomura S, Yamaguchi A, Sasaki K, Deguchi K, Shimizu Y, Bronson RT, Gao YH, Inada M and others. Targeted disruption of Cbfa1 results in a complete lack of bone formation owing to maturational arrest of osteoblasts. Cell 1997;89(5):755-64.
16. Owen TA, Aronow M, Shalhoub V, Barone LM, Wilming L, Tassinari MS, Kennedy MB, Pockwinse S, Lian JB, Stein GS. Progressive development of the rat osteoblast phenotype in vitro: reciprocal relationships in expression of genes

associated with osteoblast proliferation and differentiation during formation of the bone extracellular matrix. J Cell Physiol 1990;143(3):420-30.
17. Bianco P, Robey PG. Stem cells in tissue engineering. Nature 2001;414(6859):118-21.

Tables

Table 1. Glass compositions in weight %

	SiO_2	Na_2O	K_2O	CaO	MgO	P_2O_5
6P61	61.1	10.3	2.8	12.6	8.9	6.0
6P55	54.5	12.0	4.0	15.0	8.5	6.0

Table 2. Ion concentration of SBF (mM) in deionized water

	Ion concentration (mM)						
	Na^+	K^+	Ca^{2+}	Mg^{2+}	Cl^-	HCO_3^-	HPO_4^{2-}
SBF	142	5	2.05	1.5	148	4.2	1

Figures and Captions

Figure 1

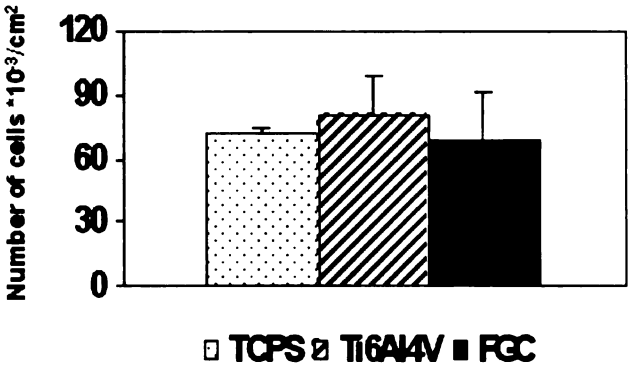

Figure 1. Cell adhesion: the number of adhering cells was not significantly different on all materials (ANOVA, SNK $p>0.05$).

Figure 2

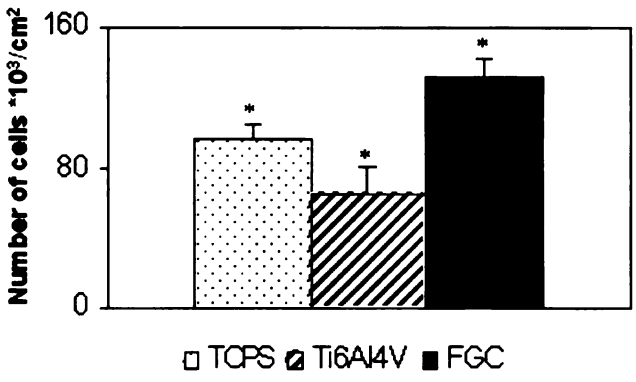

Figure 2. Cell proliferation: after 5 days in culture MC3T3-E1.4 mouse osteoblast-like cells proliferated significantly differently on all materials. Lowest proliferation occurred on Ti6Al4V followed by TCPS, and FGC (ANOVA, SNK $p<0.05$).

Figure 3

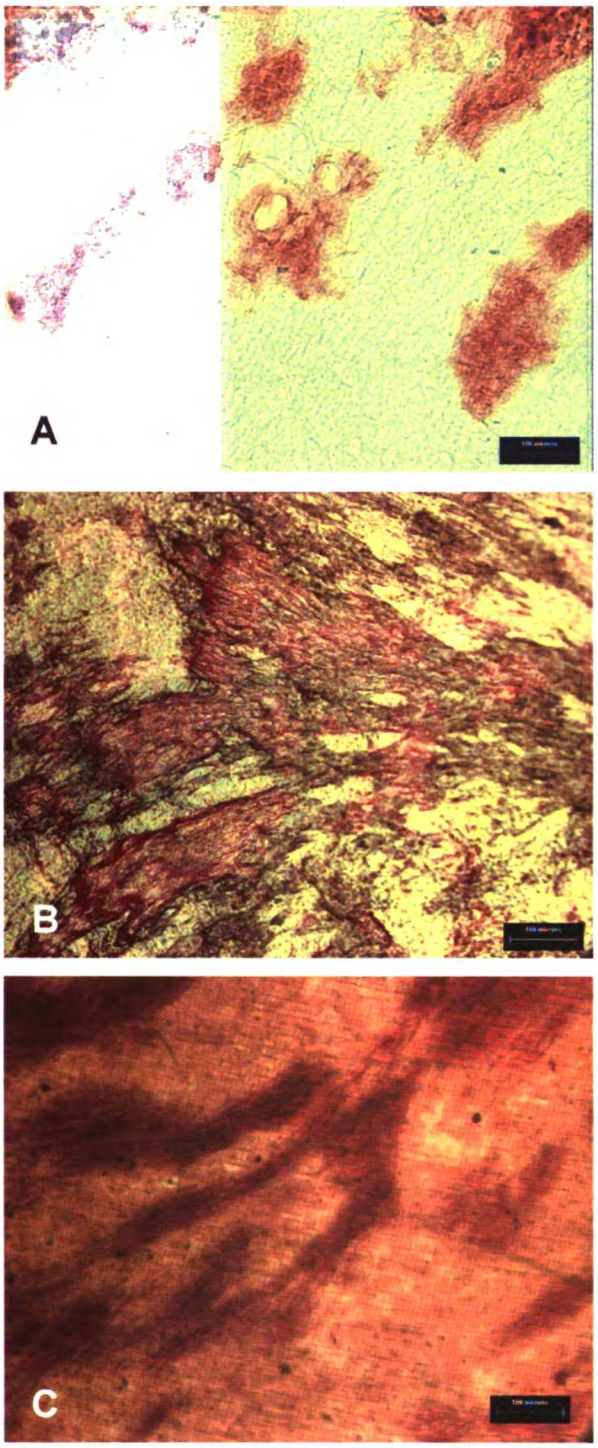

Figure 3. Mineralization by alizarin S staining: MC3T3-E1.4 mouse osteoblast-like cells mineralized on each substratum (A: TCPS, B: FGC, C: Ti6Al4V). Mineralizing areas showed a dark red staining. Scale bar: 100 μm.

Figure 4

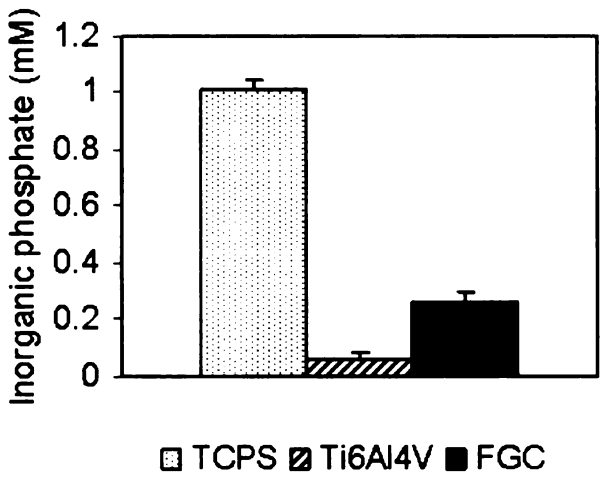

Figure 4. Quantitative mineralization: mineralizing tissue grown onto each material released a significantly different concentration of inorganic phosphate in the following order from the highest to the lowest: TCPS>FGC>Ti6Al4V (ANOVA, SNK $p<0.05$).

Figure 5

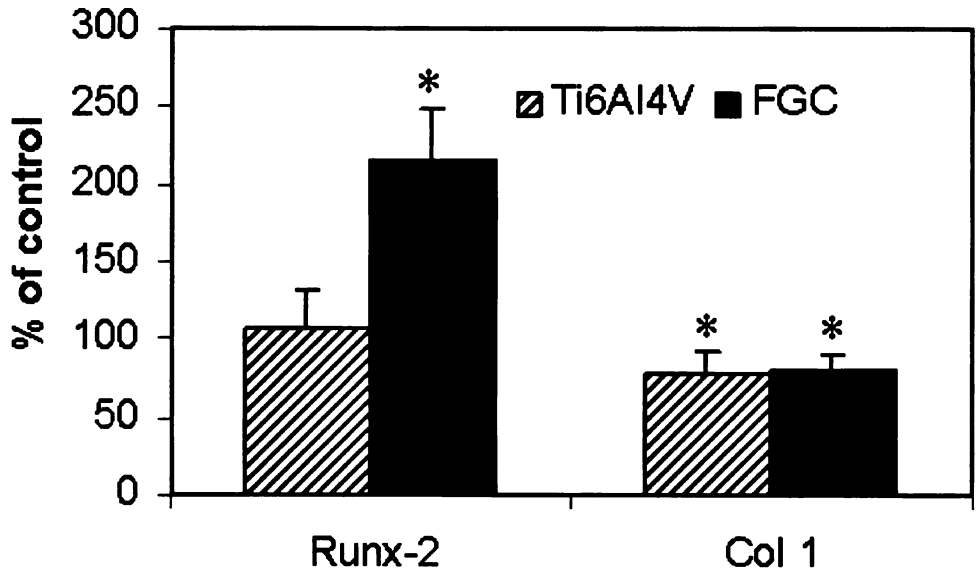

Figure 5. Real Time RT-PCR: FGCs extract induced a twofold increase in the expression of Runx-2 with respect to TCPS extract (control). FGC and Ti6Al4V extracts induced a 20% decrease in the expression of Col 1 respect to TCPS extract (control)(*=significantly different from control ANOVA, SNK $p<0.05$).

Chapter 7

Summary, Discussion, Conclusions and Future Work

Summary and discussion

Close to half a million Americans undergo either total knee or total hip joint replacement surgery yearly.[1] About 20% of these patients will need a second, revision, surgery which is usually not as successful, may cause additional damage to the surrounding tissues, and constitutes a significant increase in health care cost.[2]

Current implant materials for load bearing applications are typically metal alloys, strong enough to support the loads involved in daily activities, and bioinert to limit reactivity in the body that may cause inflammatory and other adverse reactions. Joint implants comprise articular surfaces made of alumina, ultra high molecular weight polyethylene (UHMWPE) or other materials to optimize tribology design, minimizing wear particles and adverse tissue reactions. This is an active area of research along with methods to obtain implant fixation into the surrounding bone.[2,3] Implants made of bioinert metal alloys rely on mechanical interlocking to achieve fixation which often can be improved by using bone cements. Common bone cements are polymers, such as polymethylmethacrylate (PMMA), and require the presence of monomers and an initiator to start radical polymerization. A radiopaque medium and occasionally an antibiotic also are present in the mix. Shrinkage of the polymer and heat of polymerization causing bone necrosis are common problems related to the use of bone cements. The ratios between the different components can be altered to minimize shrinkage. Polymerization heat has led to pre-cooling or pre-heating of the prosthesis to avoid bone necrosis. When the prosthesis is pre-cooled heat transfer occurs from cement to prosthesis and shrinkage of the polymer occurs at the same interface, increasing the risk of early loosening of the implant. Pre-heating of the prosthesis leads to higher transfer of heat to the bone increasing heat necrotic defects, again leading to loosening.[4]

To improve implant osteointegration, metal implants have been coated with hydroxyapatite (HA) by plasma spray. Such implants do not require the use of bone cement. Plasma sprayed HA coated implants are FDA approved and currently on the market, but coating delamination can occur because of the unreliable coating properties (HA re-crystallizes into different phases during plasma spray).[5]

Our research group developed a family of glasses, some bioactive and some with a coefficient of thermal expansion (CTE) compatible with Ti6Al4V, that can be enameled onto the alloy. Unfortunately these latter glasses are not bioactive because of their high silica content (above 60 wt%).[6] To overcome this, a functionally graded approach was pursued. We stratified the enameled coating with different glass compositions that fulfill different functions. We were able to couple a first glass layer, with a good CTE match to the alloy, with a second layer of bioactive glass, obtaining a functionally graded bioactive coating (FGC).[7,8]

In this thesis, for the first time some of these novel glasses in the as cast form, and their FGCs were tested for cytocompatibility with an *in vitro* bone model. We tested the glass as cast to determine whether any compositional change was needed to avoid negative cellular response (Chapter 2). In order to conduct cytocompatibility assays we first sterilized the glasses by gamma irradiation using an emission of 600 Curies of radiation per minute for a total of 12 hours. This procedure is commonly followed in our lab to sterilize biological samples, typically freshly extracted human teeth. After sterilization the glasses had acquired

a dark brown color because the gamma radiation created color centers. Color centers are formed when a high energy radiation bombards a material and an anion (or an electron) is ejected which causes loss of neutrality. A free electron can occupy the vacancy created by the loss of the anion (or electron) and fall into a trapping energy level. Within the energy trap there are discreet levels which can absorb light. Depending on the energy level onto which the electron falls different light is absorbed, conferring different color. Gemstones derive their color from color centers.[9,10] Thus, gamma irradiation changed the physical properties of our glasses and was not considered a suitable sterilization method. Sterilization and cleaning procedures have been shown to affect implant wear properties,[11] corrosion resistance,[12] and cellular response.[13,14] These reports indicate the importance of sterilization method, which should be assessed prior to *in vitro* and *in vivo* studies. Exposure of the samples to dry heat at 250 °C for 1 hour was the sterilization method of choice. The absence of vapor (which is present in autoclave) prevents initiation of surface reactions, and this temperature is sufficiently high to burn off any residue of cleaning solvent (ethanol and acetone) without reaching the transformation temperature of the glass (which is above 500 °C for each glass studied).

Glasses containing 50 and 55 wt% silica showed no cytotoxic response and were suitable substrates for osteoblast-like adhesion, proliferation and mineralization. MC3T3-E1.4 mouse pre-osteoblast cells adhered in significantly higher numbers onto bioactive glasses and Ti6Al4V with respect to tissue culture polystyrene (TCPS). Proliferation was significantly different on all materials: highest on the glass containing 50 wt% silica, followed by the glass containing 55 wt% silica, Ti6Al4V and lowest on TCPS. Alkaline phosphatase activity was not affected by the different substrates. Morphological differences were observed in the

mineralization pattern on the different materials: more diffuse on bioactive glasses and more localized on Ti6Al4V and TCPS. Distinct three dimensional structures of aggregated cells embedded in extracellular matrix, the latter with the morphology of collagen fibers, were present on all substrates. These structures stained with alizarin red and were identified as bone nodules. It is possible that the different mineralization pattern was due to diverse collagen organization on the bioactive substrates.[15] Quantification of inorganic phosphate released by the mineralized tissue indicated similar amounts of mineralization occurring on the glasses and Ti6Al4V and significantly higher on TCPS. No cytotoxic effect was encountered and no glass compositional change was required.

The ultimate application of our novel glasses is in the form of functionally graded coatings applied by the enameling technique. It is important to determine the effect of the fabrication process on glass microstructure and reactivity. The compositional limit for the top coating is about 53 wt% silica; FGCs of lower silica content cracked during cooling.[7] Glass 6P55, (containing 55 wt% silica) was coupled with glass 6P61 (containing 61 wt% silica) to fabricate a functionally graded coating on Ti6Al4V. Glass 6P61 has a coefficient of thermal expansion (CTE) compatible with Ti6Al4V (CTE_{6P61}=10.2 $CTE_{Ti6Al4V}$=9.1-9.8 (10^{-6} $°C^{-1}$)) and was enameled in direct contact with the metal. Glass 6P55 (CTE 11.0 (10^{-6} $°C^{-1}$)) is bioactive and was used as the top coating.[7] A diffuse interface is formed between the two glasses during the enameling procedure. Powder particles of 6P61 are in intimate contact with powder particles of glass 6P55 and the enameling temperature allows the particles to sinter. Smoother gradients can be obtained by interposition of a glass layer with silica content between 61 and 55 wt %.[7] The thermal treatment involved in the enameling procedure caused partial crystallization of the coating. X-ray diffraction (XRD) indicated

that two crystalline phases were formed: sodium calcium phosphate and sodium calcium silicate. Glass 6P55 as cast was entirely amorphous. Since there were structural and morphological differences between glass as cast and the coating, we tested for bioactivity in simulated body fluid (SBF). Serial immersion in SBF induced precipitation of HA on both 6P55 as cast and as a coating. It was expected that the coatings, being partially crystalline, would have slower reaction kinetics than glass as cast. The surface reactions were followed weekly by Fourier Transform Infrared Spectroscopy (FTIR) and no significant differences were found (Chapter 3). It is possible that differences could have been detected by performing FTIR analysis daily, but the amount of crystalline phases was very small (averaged 5.9 ± 3.0 vol%), and its effect may be minimal.

From the clinical point of view it is highly desirable that the implant characteristics be reproducible. This allows more predictable outcome in cellular response. We tested three different batches of coatings and the fabrication process yielded reproducible results: the amount and type of crystalline phases, as well as coating thickness, were consistent between batches (Chapter 4).

Several reports showed that the glass silica network continuously dissolves in solution, either SBF[16] or protein containing solutions.[17] Particular importance was paid to making *in vitro* testing conditions correspond closely to *in vivo* conditions.[18,19] In fact the glass transformations (i.e. complete silica dissolution and consequent excavation of particles) occurring *in vivo* could be reproduced *in vitro,* only in the presence of proteins and when solutions were replenished.[19] The presence of proteins always increased the rate of silica dissolution,[19] allowed the formation of a Ca P-rich surface but precluded its crystallization.[18] In the absence of proteins the reactions leading to silica dissolution were significantly

slowed.[19] In Chapter 4 we determined the effect of protein containing solutions on the stability of FGCs by using cell culture conditions, which comprise both the presence of proteins and exchange of solutions. We cultured MC3T3-E1.4 osteoblast-like cells on functionally graded coatings either as made or preconditioned in SBF. The preconditioning treatment produced a crystalline apatite-like surface on the coating identified by FTIR and scanning electron microscopy (SEM) (Chapter 4). After 20 days in culture under mineralizing conditions, the stability of the coating was assessed by applying vacuum (<80 millitorr). Vacuum had the effect of separating a superficial layer from the unconditioned (as made) coating. This layer comprised cells grown on the surface and a 4 μm thick layer of reacted glass containing Ca P and little Si immediately underneath them. Thus, under cell culture conditions the silica network kept on dissolving below the surface of the coating, creating a shifting pseudo-interface, which after 20 days was located about 4 μm below the original cell-coating interface. It is possible that continuing the experiment for longer times may shift this pseudo-interface further inwards. The pseudo-interface was the weakest link within the coating and pulled apart under the vacuum force, but *in vivo* other physical forces may have similar effects. Conversely, the same vacuum applied to samples preconditioned in SBF prior to cell culture had no apparent effect on the coating. Silica dissolution probably also was occurring in this case but the reactions may have been severely slowed because of the presence of the apatite-like layer on the surface induced by the preconditioning treatment, similar to previously reported results.[19] Delamination of the coating may occur if the pseudo-interface reaches the underlying alloy. It is difficult to calculate how much fluid exchange occurs *in vivo* at the implant surface, consequently it is difficult to predict how long silica dissolution must occur before the implant is compromised. Once the pseudo-interface

reaches glass 6P61 the reactions are likely to be slowed because of the high silica content of this glass. *In vivo*, by the time bone mineralization occurs, fluid motion at the implant surface may be reduced to the minimum required for bone remodeling. Thus, preconditioning in SBF is advantageous because it provides a more stable coating (Chapter 4), and removes possible contaminants (Chapter 5).

In the process of determining the cytocompatibility of the coatings we encountered some inconsistencies. Some mineralization experiments indicated that the cells reached confluence and mineralized, while in others, cells were not even confluent. Similar inconsistencies were observed in proliferation experiments. Increasing the number of repeat experiments required the fabrication of more samples, and with the new batches a clear shift in the results was observed. The results became consistently negative, with poor proliferation of MC3T3-E1.4 osteoblasts on FGCs. It was determined that reduced proliferation was not due to slower cellular metabolism but to the leaching of some chemical species from the FGCs which had the effect of decreasing cell viability from about 100% to about 70%. The noxious agent may completely leach out by immersion in SBF, or alternatively may be prevented from leaching out by the formation of apatite-like mineral on the glass surface. Indeed preconditioning of the coatings in SBF (similar to what was done in Chapter 4) had the effect of eliminating the problem. Coating extracts in SBF were prepared and analyzed by Inductively Coupled Plasma Mass Spectroscopy (ICP-MS) to identify the noxious agent. We screened for 34 different elements and compared the results to the analysis of a blank solution of SBF. We identified candidate elements which had been reported as being toxic that could have possibly caused reduced cell viability: V, Fe and Ni, in decreasing order of toxicity.[20,21] Iron and nickel were

found in very low concentrations (0.0003 and 0.0004 mM respectively), concentrations reported as not toxic.[21] The concentration of vanadium was about half of what had been reported as toxic to MG63 human osteoblast-like cells. The "robust" nature of this osteosarcoma-derived cell line compared to the spontaneously immortalized MC3T3-E1.4 mouse pre-osteoblast cell line used in our work may partly explain the difference in concentration at which a toxic effect was noticeable. The source of vanadium may have been the Ti6Al4V substratum for the coatings, but it seems strange that no cytotoxic behavior was found when Ti6Al4V uncoated was used. Exposing Ti6Al4V to the thermal treatment required for enameling, but in the absence of glass, had no noticeable effect on cell proliferation either. To exclude the possibility that some contaminant might have been included in the glass, an attempt to coat Pt sheet by the same technique was made. The coatings we obtained had poor adhesion but could still be used to test for cellular proliferation, and showed no cytotoxic effect. We are still uncertain about the source and identity of the toxic agent. Further experiments involving the preparation and analysis of extracts in various solutions, and at different time points, followed by testing of each agent at different concentrations, singularly or in combination, may help clarify this point. This was outside the scope of this thesis, but the occurrence of contamination underscores the importance of carrying out each step of the coating fabrication process with extreme cleanliness and care. The implant status may vary because of fabrication and handling, and can affect *in vitro* and *in vivo* performance. Thus characterization to ensure standardized and controlled properties is important (Chapters 2 and 3).[22,23] The data reported in Chapters 4 and 5 indicate that preconditioning in SBF is necessary to

provide a stable coating and to remove possible contaminants introduced during the glass fabrication and/or enameling process.

Chapter 6 tested the cytocompatibility of coatings preconditioned in SBF compared to similarly treated TCPS and uncoated Ti6Al4V. MC3T3-E1.4 osteoblasts adhered similarly to all materials but proliferated significantly more on preconditioned coatings. Cells mineralized on all substrata and higher inorganic phosphate was apparently incorporated in the mineralizing cell layer cultured on the coatings, as compared to the Ti6Al4V control. This suggests that the coatings may favorably affect mineralization with respect to uncoated Ti6Al4V. Mineralization onto TCPS was significantly higher than onto Ti6Al4V and FGCs. Quantitative mineralization data and qualitative alizarin red staining indicated that Ti6Al4V and FGC may slow but do not prevent MC3T3-E1.4 mineralization compared to TCPS. These differences may be due to the combined effect of surface chemistry and topography of the substrates which could possibly affect the extracellular matrix organization.[15]

There is evidence that Bioglass® extract affects gene expression in human primary osteoblastic cultures.[24,25] This exciting finding suggests the possibility of designing materials capable of inducing the expression of specific genes.[26] In the second part of Chapter 6 we conducted preliminary experiments to determine if preconditioned coatings also are able to alter gene expression by means of their dissolution products. Genes involved in the early stages of osteoblast differentiation, Runx-2 and Col 1, were chosen as target genes, and their expression was quantified by real time RT-PCR. Runx-2 is an osteoblast-specific transcription factor required for the differentiation of mesenchymal progenitor cells towards the osteoblastic lineage[27] and is necessary to maintain a

functional osteoblastic phenotype.[28] Collagen type 1, the principal collagenous extracellular matrix protein present in bone, plays a central role in bone mineralization.[29] Using real-time RT-PCR we were able to reproducibly quantify the expression of these genes induced in response to extracts of coatings (preconditioned in SBF) and of control materials. We found that coating extracts induced a two fold increase in the expression of Runx-2 compared to uncoated Ti6Al4V and TCPS. Col 1 expression induced by the extracts of either coating or Ti6Al4V, was about 80% of the expression induced by TCPS extract. Thus, in our simplified *in vitro* model, preconditioned coatings dissolution products did alter expression of selected genes important to osteoblast differentiation and function. The twofold induction of Runx-2 expression could be of clinical importance. *In vivo* implants are in contact with a variety of cells present in bone including mesenchymal stem cells.[30] These innovative coatings may promote the differentiation of mesenchymal stem cells towards the osteoblastic lineage by stimulating Runx-2 expression, thereby favorably affecting osteointegration. The coating composition may be modified to simultaneously promote mineralization by the induction of genes involved in the process such as Col 1.

Conclusions

In this thesis for the first time novel bioactive glasses and their functionally graded coatings on Ti6Al4V were studied with an *in vitro* bone model. The results indicated that the novel bioactive glasses are cytocompatible and no compositional change is required. The fabrication process is reproducible, introduces a small (average 6 vol%) amount of crystallization, which does not significantly affect bioactivity in SBF as tested. The coatings were cytocompatible, but should be preconditioned in SBF prior to their use.

Preconditioning stabilizes the coatings, eliminates possible contaminants introduced during processing and handling, and yields dissolution products capable of inducing specific gene expression (e.g. Runx-2). Future research will involve identification of such dissolution products as well as *in vivo* testing.

Future Research

The general hypothesis tested in this thesis is that the reaction products released from bioactive glasses exposed to buffered proteinaceous solutions and the resulting surface modifications significantly alter osteoblast behavior (e.g. adhesion and proliferation) and consequently determine the osteoconductive properties of the material.

The following aims tap into the same general hypothesis and address specific basic science questions.

Aim 1 To identify the ions released from bioactive glasses in tissue culture medium and their role on osteoblast gene expression.

Rationale: Few papers addressed the response of osteoblasts to bioactive glass reaction products at the molecular level. Ionic products from dissolution of Bioglass® particles altered human osteoblast cell metabolism [31] and caused up-regulation of genes involved in cell proliferation and differentiation, identified by microarray analysis. [25,32] The effect of singular ionic species, possible dose responses and synergies have not been investigated. This information may be necessary for the development of implant surfaces that have a pharmacological effect on bone before transforming into calcium phosphate.

Preconditioning the implant coating stabilized it (Chapter 6) but it is still unclear whether the same treatment might be advantageous to osteoblast differentiation and

mineralization. The results of Chapter 6 indicated that specific gene expression can be induced by the dissolution products of preconditioned bioactive glass coatings.

Aim 2 To determine the role of preconditioned bioactive glasses' products of dissolution, in modulating expression of genes involved in osteoblastic differentiation.

It is clinically desirable to minimize motion-induced damage at the implant site, which may be obtained by the rapid deposition of mineralized matrix on the implant surface by osteoblasts, supplying mechanical stability.[33] *In vivo* studies of various bioactive glass-ceramics reached one common result: bone bonded with the materials through an intervening layer of calcium phosphates.[34] It has been reported that the level of mineralization of the extracellular matrix affects bone-implant bonding.[35] More recent *in vitro* studies suggested that hydroxyapatite may exert a stimulatory effect on marrow stromal stem cells differentiation[36] and osteoblast-like cell mineralization.[37] The mechanism is unknown: the calcium phosphate's topography might have an effect, as well as the adsorbed proteins and the products of dissolution. Some *in vivo* experiments indicated that primary calcification during bone healing is significantly affected by the surface properties of the implant and the effect was apparent also in the contralateral limb.[38,39] This indicates a systemic effect, again underlying the importance of products of dissolution on bone metabolism. A biomaterial engineered to enhance osteoblastic mineral deposition could be of significant clinical use.

Background

Ions and bone

Silicon

It has been reported that silicon is required for proper extracellular matrix cross-linking during bone growth and it acts independently of vitamin D_1. In particular, silicon is required for synthesis of collagen and glycosaminoglycans, and it affects the mechanical properties of bone and other mineralized tissues.[40] *In vivo* experiments showed that silicon ingestion, in the form of silanols, caused increased bone formation in mature ovariectomized rats when bone loss was expected.[41] Evidence from different animal models suggested that silicon in trace amounts is involved in bone mineralization.[42-44]. Silicon induced increased proliferation, differentiation, expression of TGF-β mRNA and osteocalcin production in human primary osteoblasts.[45] No cellular silicon receptor has been identified and the precise effect of bioactive glass-derived silicon on human osteoblasts remains unclear.

Calcium, magnesium, potassium, and phosphorus

Bone mineral contains about 26-36 wt% Ca, and 11-16 wt% P in the form of apatite with incorporation of significant amounts of carbonate, sodium, magnesium, potassium and other ions.[46,47] In the body, extracellular free calcium concentration is tightly regulated and maintained within a narrow physiological range. The integrated actions of hormones (e.g. parathyroid hormone (PTH), calcitonin (CT), 1,25-dihydroxyvitamin D_3 ($1,25(OH)_2D_3$)) regulate renal and intestinal absorption of Ca^{2+} as well as skeletal Ca^{2+} mobilization to maintain systemic calcium homeostasis.[48] Osteoblasts sense changes of extracellular calcium through ion channels and through a recently identified extracellular calcium receptor (CaR).[49] The role of CaR, a G protein coupled receptor, in bone is not clear. During bone resorption the concentration of extracellular calcium can increase locally as high as 40 mM. Such a high concentration can be a signal affecting osteoblast

physiological response. In fact, it has been reported that extracellular calcium can induce DNA synthesis and act as a chemoattractant on mouse osteoblastic cells.[50] A biomaterial leaching calcium ions might have a similar effect.

Magnesium acts as an agonist on calcium channels in osteoblasts, and is able to affect cellular metabolism.[47] Physiological levels of magnesium, the fourth highest concentrated cation in the human body, promote bone mineralization influencing biological apatite crystal formation.[51-54] It seems that Mg ions form surface bound ionic complexes on hydroxyapatite and their incorporation in the lattice is limited.[55] The content of Mg in a bioactive glass should be carefully monitored because high concentrations showed a toxic effect on bone cells.[47] Other ions present in bioactive glasses, such as potassium and phosphates might have an effect on osteoblast metabolism. For example it has been reported that potassium and calcium channels are involved in the regulation of secretion of osteocalcin.[56] Phosphorus in the form of organic or inorganic phosphates directly increased osteoblast expression of osteopontin, while sodium had no effect.[57]

Experimental

ICP-MS and/or atomic absorption (AA) analysis of extracts will allow the identification and quantification of glass dissolution products.

Test solutions can be prepared by the addition of single or combination of ions, in various concentrations, to tissue culture medium.

The effect on the expression of specific genes can be assessed by treating osteoblast-like cells (or primary human osteoblasts) with test and control solutions (without added ions) followed by real time RT-PCR analysis.

References

1. http://www.aahks.org.
2. Long M, Rack HJ. Titanium alloys in total joint replacement--a materials science perspective. Biomaterials 1998;19(18):1621-39.
3. Hulbert SF. The use of alumina and zirconia in surgical implants. In: Hench LL, Wilson J, editor. An introduction to bioceramics. Singapore ; River Edge, N.J.: World Scientific; 1993. p c, 386 p.
4. Kèuhn KD. PMMAs as bone cements. In: Kèuhn KD, editor. Bone cements : up-to-date comparison of physical and chemical properties of commercial materials. Berlin ; New York: Springer; 2000. p 21-34.
5. Klein C, Wolke J, de Groot K. Stability of calcium phosphate ceramics and plasma sprayed coating. In: Hench LL, Wilson J, editor. An Introduction to bioceramics. Singapore ; River Edge, N.J.: World Scientific; 1993. p c, 386 p.
6. Brink M, Turunen T, Happonen RP, Yli-Urpo A. Compositional dependence of bioactivity of glasses in the system Na_2O- K_2O-MgO-CaO-B_2O_3-P_2O_5-SiO_2. J Biomed Mater Res 1997;37(1):114-21.
7. Gomez-Vega JM, Saiz E, Tomsia AP. Glass-based coatings for titanium implant alloys. J Biomed Mater Res 1999;46(4):549-59.
8. Gomez-Vega JM, Saiz E, Tomsia AP, Marshall GW, Marshall SJ. Bioactive glass coatings with hydroxyapatite and Bioglass particles on Ti-based implants. 1. Processing. Biomaterials 2000;21(2):105-11.
9. Forman G. A study of color centers produced in quartz by x-radiation. J Opt Soc Am 1951;41(6):377-80.
10. Ezz-Eldin FM, Abdel-Rehim F, Abdel-Azim AA, Ahmed AA. Soda-lime-silica glass for radiation dosimetry. Med Phys 1994;21(7):1085-9.
11. McKellop H, Shen FW, Lu B, Campbell P, Salovey R. Effect of sterilization method and other modifications on the wear resistance of acetabular cups made of ultra-high molecular weight polyethylene. A hip-simulator study. J Bone Joint Surg Am 2000;82-A(12):1708-25.
12. Thierry B, Tabrizian M, Trepanier C, Savadogo O, Yahia L. Effect of surface treatment and sterilization processes on the corrosion behavior of NiTi shape memory alloy. J Biomed Mater Res 2000;51(4):685-93.
13. Keller JC, Draughn RA, Wightman JP, Dougherty WJ, Meletiou SD. Characterization of sterilized CP titanium implant surfaces. Int J Oral Maxillofac Implants 1990;5(4):360-7.
14. Ferreira SD, Dernell WS, Powers BE, Schochet RA, Kuntz CA, Withrow SJ, Wilkins RM. Effect of gas-plasma sterilization on the osteoinductive capacity of demineralized bone matrix. Clin Orthop 2001(388):233-9.
15. Davies JE, Matsuda T. Extracellular matrix production by osteoblasts on bioactive substrata in vitro. Scanning Microsc 1988;2(3):1445-52.
16. Saiz E, Goldman M, Gomez-Vega JM, Tomsia AP, Marshall GW, Marshall SJ. In vitro behavior of silicate glass coatings on Ti6A14V. Biomaterials 2002;23(17):3749-56.
17. Sepulveda P, Jones JR, Hench LL. In vitro dissolution of melt-derived 45S5 and sol-gel derived 58S bioactive glasses. J Biomed Mater Res 2002;61(2):301-11.

18. Radin S, Ducheyne P, Rothman B, Conti A. The effect of in vitro modeling conditions on the surface reactions of bioactive glass. J Biomed Mater Res 1997;37(3):363-75.
19. Radin S, Ducheyne P, Falaize S, Hammond A. In vitro transformation of bioactive glass granules into Ca-P shells. J Biomed Mater Res 2000;49(2):264-72.
20. Morais S, Dias N, Sousa JP, Fernandes MH, Carvalho GS. In vitro osteoblastic differentiation of human bone marrow cells in the presence of metal ions. J Biomed Mater Res 1999;44(2):176-90.
21. Hallab NJ, Vermes C, Messina C, Roebuck KA, Glant TT, Jacobs JJ. Concentration- and composition-dependent effects of metal ions on human MG-63 osteoblasts. J Biomed Mater Res 2002;60(3):420-33.
22. Kasemo B, Lausmaa J. Biomaterial and implant surfaces: on the role of cleanliness, contamination, and preparation procedures. J Biomed Mater Res 1988;22(A2 Suppl):145-58.
23. Smith D. Surface characterization of implant materials: biological implications. In: Davies J, editor. The bone-biomaterial interface. Toronto: Univeristy of Toronto Press; 1991. p 3-18.
24. Xynos ID, Edgar AJ, Buttery LD, Hench LL, Polak JM. Ionic products of bioactive glass dissolution increase proliferation of human osteoblasts and induce insulin-like growth factor II mRNA expression and protein synthesis. Biochem Biophys Res Commun 2000;276(2):461-5.
25. Xynos ID, Edgar AJ, Buttery LD, Hench LL, Polak JM. Gene-expression profiling of human osteoblasts following treatment with the ionic products of Bioglass 45S5 dissolution. J Biomed Mater Res 2001;55(2):151-7.
26. Hench LL, Polak JM. Third-generation biomedical materials. Science 2002;295(5557):1014-7.
27. Komori T, Yagi H, Nomura S, Yamaguchi A, Sasaki K, Deguchi K, Shimizu Y, Bronson RT, Gao YH, Inada M, Sato M, Okamoto R. Targeted disruption of Cbfa1 results in a complete lack of bone formation owing to maturational arrest of osteoblasts. Cell 1997;89(5):755-64.
28. Karsenty G. The genetic transformation of bone biology. Genes Dev 1999;13(23):3037-51.
29. Owen TA, Aronow M, Shalhoub V, Barone LM, Wilming L, Tassinari MS, Kennedy MB, Pockwinse S, Lian JB, Stein GS. Progressive development of the rat osteoblast phenotype in vitro: reciprocal relationships in expression of genes associated with osteoblast proliferation and differentiation during formation of the bone extracellular matrix. J Cell Physiol 1990;143(3):420-30.
30. Bianco P, Robey PG. Stem cells in tissue engineering. Nature 2001;414(6859):118-21.
31. Silver IA, Deas J, Erecinska M. Interactions of bioactive glasses with osteoblasts in vitro: effects of 45S5 Bioglass, and 58S and 77S bioactive glasses on metabolism, intracellular ion concentrations and cell viability. Biomaterials 2001;22(2):175-85.
32. Xynos ID, Hukkanen MV, Batten JJ, Buttery LD, Hench LL, Polak JM. Bioglass 45S5 stimulates osteoblast turnover and enhances bone formation In vitro: implications and applications for bone tissue engineering. Calcif Tissue Int 2000;67(4):321-9.

33. Dee KC, Rueger DC, Andersen TT, Bizios R. Conditions which promote mineralization at the bone-implant interface: a model in vitro study. Biomaterials 1996;17(2):209-15.
34. Hench LL. Bioceramics: from concept to clinic. J Am Ceram Soc 1991;74:1487-1510.
35. Gross U, Brandes J, Strunz V, Bab I, Sela J. The ultrastructure of the interface between a glass ceramic and bone. J Biomed Mater Res 1981;15(3):291-305.
36. Ohgushi H, Dohi Y, Yoshikawa T, Tamai S, Tabata S, Okunaga K, Shibuya T. Osteogenic differentiation of cultured marrow stromal stem cells on the surface of bioactive glass ceramics. J Biomed Mater Res 1996;32(3):341-8.
37. Chang YL, Stanford CM, Keller JC. Calcium and phosphate supplementation promotes bone cell mineralization: implications for hydroxyapatite (HA)-enhanced bone formation. J Biomed Mater Res 2000;52(2):270-8.
38. Schwartz Z, Amir D, Boyan BD, Cochavy D, Mai CM, Swain LD, Gross U, Sela J. Effect of glass ceramic and titanium implants on primary calcification during rat tibial bone healing. Calcif Tissue Int 1991;49(5):359-64.
39. Schwartz Z, Swain LD, Marshall T, Sela J, Gross U, Amir D, Muller-Mai C, Boyan BD. Modulation of matrix vesicle enzyme activity and phosphatidylserine content by ceramic implant materials during endosteal bone healing. Calcif Tissue Int 1992;51(6):429-37.
40. Carlisle EM. Silicon: a requirement in bone formation independent of vitamin D1. Calcif Tissue Int 1981;33(1):27-34.
41. Hott M, de Pollak C, Modrowski D, Marie PJ. Short-term effects of organic silicon on trabecular bone in mature ovariectomized rats. Calcif Tissue Int 1993;53(3):174-9.
42. Carlisle EM. Silicon: a possible factor in bone calcification. Science 1970;167(916):279-80.
43. Carlisle EM. Silicon: an essential element for the chick. Science 1972;178(61):619-21.
44. Landis WJ, Lee DD, Brenna JT, Chandra S, Morrison GH. Detection and localization of silicon and associated elements in vertebrate bone tissue by imaging ion microscopy. Calcif Tissue Int 1986;38(1):52-9.
45. Keeting PE, Oursler MJ, Wiegand KE, Bonde SK, Spelsberg TC, Riggs BL. Zeolite A increases proliferation, differentiation, and transforming growth factor beta production in normal adult human osteoblast-like cells in vitro. J Bone Miner Res 1992;7(11):1281-9.
46. Akesson K, Grynpas MD, Hancock RG, Odselius R, Obrant KJ. Energy-dispersive x-ray microanalysis of the bone mineral content in human trabecular bone: a comparison with ICPES and neutron activation analysis. Calcif Tissue Int 1994;55(3):236-9.
47. Serre CM, Papillard M, Chavassieux P, Voegel JC, Boivin G. Influence of magnesium substitution on a collagen-apatite biomaterial on the production of a calcifying matrix by human osteoblasts. J Biomed Mater Res 1998;42(4):626-33.
48. Chattopadhyay N, Brown EM. Cellular "sensing" of extracellular calcium (Ca(2+)(o)): emerging roles in regulating diverse physiological functions. Cell Signal 2000;12(6):361-6.

49. House MG, Kohlmeier L, Chattopadhyay N, Kifor O, Yamaguchi T, Leboff MS, Glowacki J, Brown EM. Expression of an extracellular calcium-sensing receptor in human and mouse bone marrow cells. J Bone Miner Res 1997;12(12):1959-70.
50. Yamaguchi T, Chattopadhyay N, Kifor O, Butters RR, Jr., Sugimoto T, Brown EM. Mouse osteoblastic cell line (MC3T3-E1) expresses extracellular calcium (Ca2+o)-sensing receptor and its agonists stimulate chemotaxis and proliferation of MC3T3-E1 cells. J Bone Miner Res 1998;13(10):1530-8.
51. Wuthier RE. Zonal analysis of electrolytes in epiphyseal cartilage and bone of normal and rachitic chickens and pigs. Calcif Tissue Res 1971;8(1):24-35.
52. Jones JE, Schwartz R, Krook L. Calcium homeostasis and bone pathology in magnesium deficient rats. Calcif Tissue Int 1980;31(3):231-8.
53. Marie PJ, Travers R, Delvin EE. Influence of magnesium supplementation on bone turnover in the normal young mouse. Calcif Tissue Int 1983;35(6):755-61.
54. Wiesmann HP, Tkotz T, Joos U, Zierold K, Stratmann U, Szuwart T, Plate U, Hohling HJ. Magnesium in newly formed dentin mineral of rat incisor. J Bone Miner Res 1997;12(3):380-3.
55. Posner AS. Crystal chemistry of bone mineral. Physiol Rev 1969;49(4):760-92.
56. Moreau R, Aubin R, Lapointe JY, Lajeunesse D. Pharmacological and biochemical evidence for the regulation of osteocalcin secretion by potassium channels in human osteoblast-like MG- 63 cells. J Bone Miner Res 1997;12(12):1984-92.
57. Beck GR, Jr., Zerler B, Moran E. Phosphate is a specific signal for induction of osteopontin gene expression. Proc Natl Acad Sci U S A 2000;97(15):8352-7.

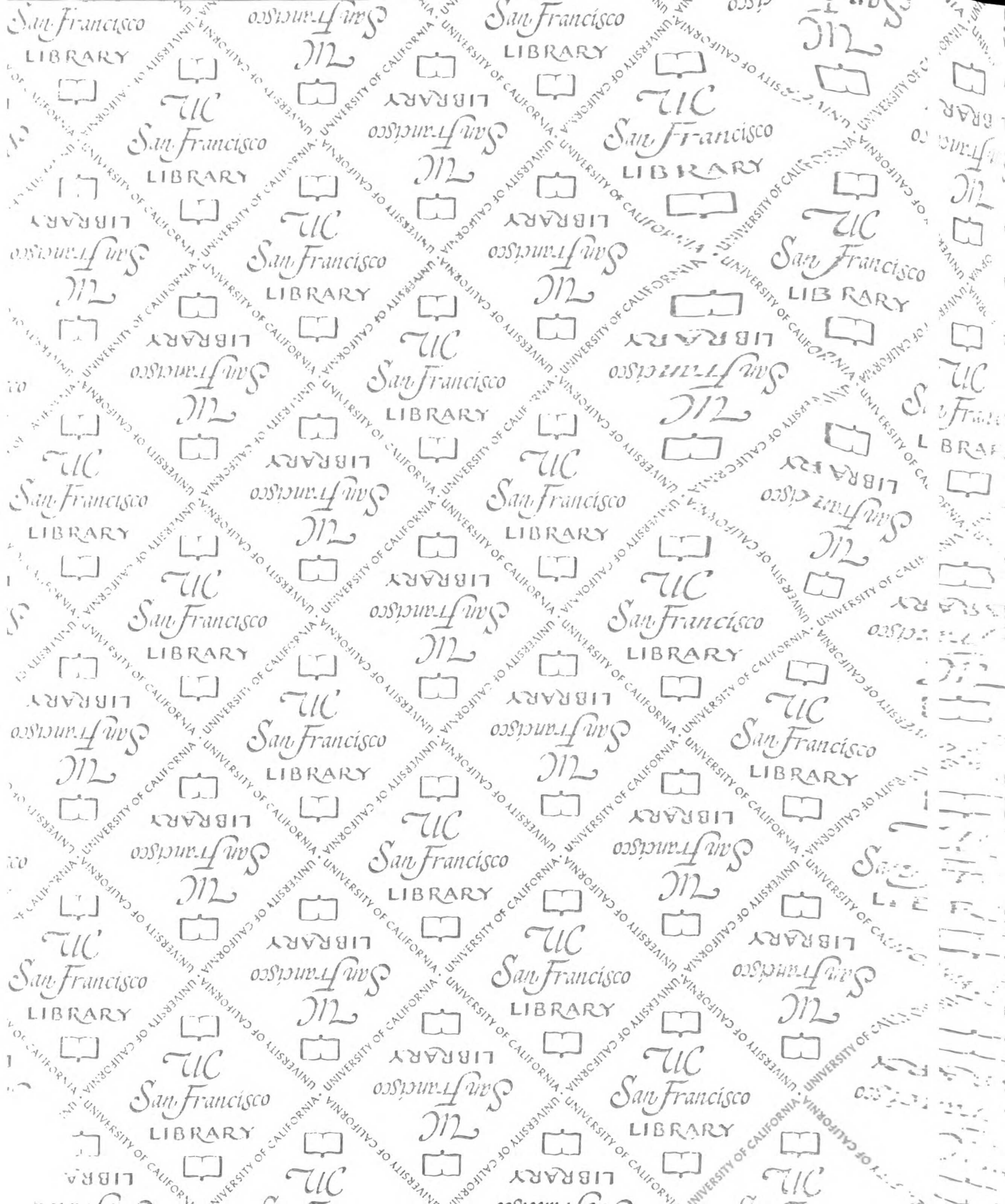
UC
San Francisco
LIBRARY
UNIVERSITY OF CALIFORNIA · UNIVERSITY OF CALIFORNIA

7434288
3 1378 00743 4288
For reference
Not to be taken from the room.